



UNIVERSITÀ
DEGLI STUDI
DI PADOVA

Università degli Studi di Padova

Dipartimento di Scienze Biomediche

CORSO DI DOTTORATO DI RICERCA IN SCIENZE BIOMEDICHE

31° CICLO

The odorant receptor expressed at the axon terminal of olfactory sensory neurons: mechanism of activation and function

Coordinatore: Ch.mo Prof. Paolo Bernardi

Supervisore: Ch.ma Dr. Claudia Lodovichi

Co-Supervisore: Ch.ma Prof. Daniela Pietrobon

Dottoranda: Franca Simona

Anno Accademico 2018-2019

Index

SUMMARY	4
SOMMARIO	9
1. INTRODUCTION	14
1.1 The olfactory system	14
1.1.1 The main olfactory epithelium.....	18
1.1.2 The olfactory bulb: organization and circuitry.....	21
1.1.3 Olfactory bulb connections to the brain.....	31
1.2 The odorant receptors	32
1.2.1 Signaling transduction cascade at the cilia of olfactory sensory neuron.....	36
1.2.2 The combinatorial receptors code for odors	40
1.2.3 Deorphanization of the odorant receptor	41
1.3 The topographic map	45
1.3.1 Organization of the main olfactory epithelium.....	45
1.3.2 From the main olfactory epithelium to the olfactory bulb	47
1.3.3 Visualizing the olfactory map.....	50
1.3.4 Functional map.....	52
1.3.5 Instructive role of the odorant receptor in sensory map formation	54
1.3.6 The odorant receptor is also expressed at the axon terminal of OSN.....	58
1.3.7 The growth cone	59
1.4 The development of the sensory map	69
1.4.1 Axon guidance molecules in the formation of the sensory map	74
1.4.2 Role of the electrical activity in the development of the topographic map ...	79
1.5 A brief summary of a previous work: the odorant receptor expressed at the axon terminal of olfactory sensory neurons is activated by molecules expressed in the olfactory bulb	82
1.6 Phosphatidylethanolamine binding-protein family (PEBP)	88
1.6.1 PEBP1 role in the brain.....	90
1.6.2 Hypocampal cholinergic neurostimulating peptide (HCNP)	91
2 AIM	92
3 MATERIAL AND METHODS	94
3.1 Animal Models	94
3.1.1 PEBP1 ^{-/-} mice (RKIP1 ^{Gt(pGT01xrBetageo)1Jkl}).....	94
3.2 Isolation of olfactory bulb products	95
3.3 Identification of the eluted material from HPLC	96
3.4 Primary culture of rat and mouse olfactory sensory neurons	97
3.5 HEK 293T cell culture	98
3.6 Ca²⁺ imaging in olfactory sensory neurons (OSN) and HEK293T cells	98

3.7	Cyclic AMP imaging in olfactory sensory neurons	100
3.8	Stimuli	100
3.9	Time-lapse imaging of axon turning of olfactory sensory neurons.....	101
3.10	Expression and purification of pGEX-RKIP-1 fusion protein	102
3.11	RT-PCR.....	103
3.12	Western blot.....	104
3.13	Immunohistochemistry	104
3.14	Whole mount analysis.....	105
3.15	Habituation and dishabituation test in mice.....	106
3.16	Statistical analysis	107
3.17	Key resources table	108
4	RESULTS	112
4.1	Identification of a ligand of axonal odorant receptor: a phosphatidyletanolamine-binding-protein-1 (PEBP1)	112
4.2	PEBP1 activates odorant receptors expressed at the axon terminal of olfactory sensory neurons.	113
4.3	PEBP1 modulates axon turning behavior of olfactory sensory neurons	117
4.4	PEBP1 expression in the rat and mouse olfactory bulb	120
4.5	PEBP1 ^{-/-} mice show a deeply perturbed sensory map organization	131
4.6	Altered P2-glomeruli position in PEBP1 mutant mice.....	140
4.7	Olfactory deficit in PEBP1 ^{-/-} mice	145
5	DISCUSSION.....	147
6	APPENDIX.....	152
7	BIBLIOGRAPHY.....	155
8	ACKNOWLEDGEMENTS	173

SUMMARY

A unique feature in the topographic organization of the olfactory bulb (OB) is the dual role of the odorant receptor (OR). It detects odors but it also plays an instructive role in the convergence of olfactory sensory neuron axons expressing the same odorant receptor to form glomeruli in specific loci of each olfactory bulb. This segregation of sensory afferents gives rise to the olfactory map, that has a critical role in encoding odors. How the OR could accomplish such different roles has remained enigmatic for more than 20 years.

If the OR can determine axon convergence, it should act as an axon guidance molecule. The demonstration that the OR is expressed not only at the cilia, but also at the axon terminal, a suitable location for an axon guidance molecule, corroborated this hypothesis. However the mechanism of activation and the function of the OR at the axon terminal has remained unknown for all these years.

The odorant receptors (OR) expressed at the cilia, is a G-protein-coupled receptor, that upon binding odorant molecules, activates a specific G-protein, G_{olf} , that stimulates adenylyl cyclase type III (ACIII) to produce cyclic AMP (cAMP). cAMP, in turn, opens olfactory specific nucleotide-gated (CNG) channels, driving an influx of Ca^{2+} and Na^+ within the cell. The rise of intracellular calcium concentration opens Ca^{2+} activated Cl channels, leading to a Cl^- efflux, that further depolarizes the membrane potential.

More recently, Lodovichi's group demonstrated for the first time that the odorant receptor expressed at the axon terminus-growth cone of the olfactory sensory neurons is functional and coupled to local increase of cAMP and Ca^{2+} . These second messengers play a key role in axon elongation and turning in several systems, including the olfactory system, where it has been shown that the OR-derived cAMP contributes to the location of the glomeruli in the olfactory bulb.

The open critical question that remained to be addressed was the mechanism of activation and function of the odorant receptor at the axon terminal. In particular,

what are natural ligands of the odorant receptor expressed at the axon terminal? A few molecules expressed in the olfactory bulb could bind and activate the odorant receptors expressed at the axon terminal.

To verify this hypothesis, Lodovichi's group purified several groups of molecules (by chromatographic procedures) from the embryonic rat olfactory bulb and tested their ability to activate the OR at the axon terminal. Performing real time Ca^{2+} imaging in olfactory sensory neurons, they observed that a pool of molecules from the olfactory bulb, locally applied, was able to elicit a prompt Ca^{2+} rise at the axon terminal.

By mass spectrometry of the active pool of molecules, phosphatidylethanolamine-binding protein-1 (PEBP1), also known as Raf kinase inhibitory protein (RKIP), was identified as a putative ligand of the axonal OR. PEBP1 is a ~21 KDa protein that belongs to a highly conserved family of proteins, expressed in numerous tissues and cell types in a variety of species. In rodents, PEBP1 is expressed in several brain areas, both in neurons and in non-neuronal cells. The physiological function of PEBP1 in the brain has remained obscure. Its low molecular weight, its ability to be secreted, to modulate G-protein coupled receptor (GPCR) and the presence of olfactory deficits in mice carrying a null mutation for PEBP1 (PEBP1^{-/-} mice), make PEBP1 a putative OR ligand.

During my PhD work, I have studied whether PEBP1 could activate the OR and its contribution in the formation of the sensory map.

First, we studied Ca^{2+} dynamics in response to PEBP1, in rat and mouse olfactory sensory neurons (OSN) loaded with the calcium indicator, fura-2, and transfected with a specific odorant receptors (OREG, P2, ORS6, Olfr62 and M72)

We found that rat embryonic olfactory sensory neurons exhibited a prompt Ca^{2+} rise in response to PEBP1 locally applied at the axon terminal with a glass pipette. Noteworthy, PEBP1 extracted from rat bulb elicited a prompt Ca^{2+} rise also at axon terminus of mouse olfactory sensory neurons, suggesting that this response is highly conserved between species.

To ascertain that the Ca^{2+} rise in response to PEBP1 observed in OSN was due to OR receptor activation, we performed Ca^{2+} imaging in Human embryonic kidney 293 cells (HEK293Tcells) transfected with specific odorant receptors (OREG, P2, S6, Olfr62, M72), loaded with the calcium indicator fura-2 and challenged with PEBP1 and with the specific odor ligand (used as control). HEK293Tcells transfected with a specific odorant receptor exhibited a prompt Ca^{2+} rise in response to PEBP1 and to the cognate odor for the specific odor receptor HEK293Tcells transfected with the odorant receptor M72 did not exhibit Ca^{2+} rise in response to PEBP1 but only to the M72 cognate-odor ligand methylsalicylate. This result indicates that there are likely a few other ligands that can activate the OR.

Indeed, HEK293Tcells transfected only with the empty-vector (pCI, not expressing any odorant receptors) did not exhibit Ca^{2+} rise in response to PEBP1, nor to the cognate odor ligand. These data demonstrated that PEBP1 elicits Ca^{2+} response via odorant receptor activation.

HEK293T cells loaded with fura-2 and transfected with specific OR, did not present a Ca^{2+} response when challenged with PEBP1 denatured by higher temperature or with proteinase K. To exclude that possible contaminants in the purification procedure, could trigger Ca^{2+} responses, HEK cells expressing specific OR and loaded with fura-2, were challenged with a cyclin-dependent kinase 2 (CDK2), a protein isolated with the same purification procedure of PEBP1. No calcium rise was observed in response to CDK-2, confirming the specificity of PEBP1 response.

Axon guidance molecules steer the direction of axon elongation. To explore whether that was the case for PEBP1, we performed time-lapse imaging of single olfactory sensory neuron axon behaviour in response to a gradient of molecules able to modulate cAMP and Ca^{2+} signaling at the axon terminal (i.e forskolin). We found that PEBP1 regulates the turning behaviour of sensory axons with a similar effect of forskolin (FRSK) or odors able to modulate the level of cAMP and Ca^{2+} at

the growth-cone of OSN. The turning behaviour of OSN was not affected by Ringer' solution, used as a negative control.

Where is PEBP1 expressed in the olfactory bulb? By immunofluorescence on embryonic, postnatal rat and mouse olfactory bulb (OB) sections, we found that PEBP1 is expressed in periglomerular cells, a suitable location to act on incoming axons. PEBP1 is expressed with a patchy pattern mostly in the anterior (A), medial (M) and lateral (L) side of the bulb while in the posterior (P) side is hardly detected.

By immunofluorescence, RT-PCR and western blot we observed that PEBP1 was not expressed in olfactory sensory neurons (OSNs) located in the main olfactory epithelium (MOE) of embryonic, postnatal rats. Accordingly, no staining for PEBP1 was observed in the core of the glomeruli. For all these techniques, we used as a negative control tissues from mice carrying a null mutant of PEBP1 (PEBP1^{-/-} mice).

If PEBP1 plays an important role in the 1). organization and 2). location of glomeruli in the OB, then PEBP1 mutant mice (PEBP1^{-/-} mice), should exhibit a disrupted sensory map.

To verify this hypothesis PEBP1 mutant mice (PEBP1^{-/-} mice), were crossed with mice in which specific OR is co-expressed with GFP (such P2-GFP , M72-YFP mice) and we analyze the convergence of GFP positive fibers to form glomeruli in the bulb. We found that in PEBP1^{-/-} mice the convergence of sensory neurons expressing P2-OR were disrupted by the presence of several additional heterogeneous glomeruli while sensory neurons expressing M72 (not responsive to PEBP1 *in vitro*) were not affected. Noteworthy, the alteration in the topographic organization of the sensory map in PEBP1^{-/-} mice crossed with P2-GFP mice was stronger in homozygous than in heterozygous mice, showing a dosage dependent effect.

We then evaluated the location of specific glomeruli in the OB, a crucial aspect of the topographic map.

We computed the position of the main P2 and M72-homogeneous glomeruli (i.e. formed exclusively by sensory axons expressing the same OR) in whole-mount bulbs along the antero-posterior (A-P) and dorso-ventral axis (D-V). We found that the position of the P2-glomeruli was significantly shifted along the antero-posterior axis (A-P) in PEBP1 mutant mice compared to controls. The defect was stronger in homozygous than in heterozygous PEBP1^{-/-} mice crossed with P2-GFP mice, showing a dosage dependent effect.

No defects were reported along the D-V axis, in agreement with the presence of specific molecules that dictate the location of glomeruli along the D-V axis.

The location of M72-glomeruli was similar in control and PEBP1^{-/-}, in agreement with the unaltered organization of the M72 glomeruli and with our *in vitro* data, in which the odorant receptor P2, but no M72, was responsive to PEBP1.

To explore the functional outcome of the altered sensory map, we analyzed the olfactory behaviour in PEBP1^{-/-} mice. We performed an olfactory habituation-dishabituation test that showed an olfactory deficit in the detection and discrimination of a new odor in PEBP1^{-/-} mice compared to control mice.

The data obtained in my PhD thesis suggested that the OR at the axon terminal can act as an axon guidance molecule activated by the natural ligand identified, PEBP1.

SOMMARIO

Una caratteristica peculiare dell'organizzazione topografica del bulbo olfattivo (OB) è il "duplice ruolo" dei recettori olfattivi (OR). Esso, infatti, non è unicamente coinvolto nella percezione degli odori, ma svolge anche un ruolo cruciale nella convergenza assonale di neuroni sensoriali olfattivi (OSN) esprimenti lo stesso OR, nella formazione di glomeruli in specifiche regioni del OB. Tale organizzazione delle afferenze sensoriali dà origine alla mappa sensoriale. Ciò nonostante, il meccanismo attraverso cui l'OR svolga queste due distinte funzioni è rimasto sconosciuto per più di 20 anni.

Se l'OR svolgesse una funzione nella convergenza assonale, potrebbe agire come "axon guidance", molecole guida, per gli assoni stessi. A sostegno di questa ipotesi, è stato dimostrato che l'OR è espresso non solo alle ciglia del neurone sensoriale olfattivo, ma anche nell'assone terminale, assumendo quindi una posizione ottimale per guidarne il movimento. Il loro meccanismo di attivazione, così come la loro funzione all'assone terminale, rimane però sconosciuta.

I recettori olfattivi (OR) espressi nelle ciglia, sono recettori accoppiati a proteine G che, in seguito al legame con molecole odorose, attivano una specifica proteina G, G_{olf} , che stimola l'adenilato ciclasi di tipo III (ACIII) a produrre AMP ciclico (cAMP). Quest'ultimo induce l'apertura di specifici canali regolati da nucleotidi ciclici chiamati "cyclic nucleotide-gated (CNG)", con conseguente influsso di ioni Ca^{2+} e Na^+ nel citoplasma della cellula. Tale aumento intracellulare di Ca^{2+} attiva canali di Cl^- che, permettendo l'uscita di ioni Cl^- dal citoplasma, depolarizzando la cellula. Recentemente, il gruppo della Dott.ssa Lodovichi ha dimostrato per la prima volta che il recettore olfattivo espresso all'assone terminale (cono di crescita) dei OSN è funzionale e accoppiato ad un locale incremento di cAMP e Ca^{2+} . Ca^{2+} e cAMP sono due secondi messaggeri che svolgono un ruolo chiave nell'allungamento e nel "turning" movimento assonale in diversi sistemi, compreso il sistema olfattivo, in cui è stato dimostrato che cAMP che si produce in

seguito all'attivazione del recettore olfattivo contribuisca a formare i glomeruli in una specifica posizione nell' OB.

Il punto critico che rimane da affrontare e definire è il meccanismo di attivazione e la funzione del recettore olfattivo espresso all'assone terminale dei OSN.

In particolare: Quali siano i ligandi naturali espressi all'assone terminale? Un gruppo ristretto di molecole espresse nel bulbo potrebbero legare e attivare il recettore olfattivo espresso all'assone terminale. Al fine di verificare questa ipotesi il gruppo della Dottoressa Lodovichi è stato in grado di identificare un gruppo di molecole (mediante tecniche cromatografiche) estratte da bulbi olfatti di ratti embrionali e ne ha testato la capacità di attivare l'OR all'assone terminale. Attraverso la tecnica dell'imaging del calcio in neuroni sensoriali olfattivi, il gruppo della Dott.ssa Lodovichi ha osservato che un gruppo di molecole applicate localmente, è in grado di attivare i neuroni sensoriali olfattivi, determinando una risposta di calcio all'assone terminale. Mediante spettrometria di massa delle molecole in grado di attivare l'OR è stato identificato un possibile ligando dell'OR espresso all'assone terminale dei OSN. Si tratta di una proteina, apparentemente alla famiglia delle etanolammine, chiamato phosphatidylethanolamine-binding protein-1 (PEBP1) o inibitore delle Raf chinasi (RKIP).

PEBP1 è una proteina di circa ~21 KDa che appartiene ad una famiglia di proteine molto conservata espressa in diversi tessuti di diverse specie. Nei roditori PEBP1 è espressa in diverse aree cerebrali, sia in neuroni che in cellule non neuronali. La funzione fisiologica di PEBP1 nel cervello rimane tuttavia non nota . Il suo basso peso molecolare, il fatto che venga secreta, che moduli i recettori accoppiati a proteine G, nonché la presenza di deficit olfattivi in linee di topo che possiedono mutazioni di PEBP1 (topi PEBP1^{-/-}), rendono PEBP1 un possibile ligando del recettore olfattivo.

Durante il mio lavoro di tesi di dottorato ho investigato se e in che modo PEBP1 potesse attivare l'OR e il suo contributo nella formazione della mappa sensoriale olfattiva.

Come primo step, sono state studiate le dinamiche del calcio in risposta a PEBP1 sia nei neuroni sensoriali di ratto che di topo, caricati con l'indicatore di calcio, fura-2.

Questi esperimenti hanno permesso di identificare risposte calcio in seguito all'applicazione di PEBP1 all'assone terminale di OSN di ratto embrionale mediante una pipetta di vetro. Degno di nota è che PEBP1, estratto dal bulbo olfattivo di ratto è in grado di indurre risposte calcio anche in OSN di topo. Questa evidenza suggerisce che l'aumento di calcio in risposta all'applicazione di PEBP1 è altamente conservata tra le specie.

Al fine di verificare che l'aumento di calcio in risposta di PEBP1 osservato in OSN fosse dovuto all'attivazione di OR, esperimenti di calcium imaging sono stati effettuati in linee cellulari derivate da cellule endoteliali di rene embrionale umano (HEK293T). Alle linee cellulari HEK, trasfettate con uno specifico OR (OREG, P2, S6, Olfr62, M72) caricate con l'indicatore per il calcio fura-2, è stato applicato PEBP1 e il corrispondente odore del OR trasfettato. Nelle linee cellulari HEK293T trasfettate con specifici OR (OREG, P2, S6, Olfr62) è stata osservata un'immediata risposta di calcio intracellulare in seguito sia all'applicazione di PEBP1 che dell'odore specifico del OR trasfettato (usato come controllo); Un'eccezione è stata riscontrata in HEK293T esperimenti il recettore M72 che sono responsive soltanto per l'odore specifico di M72 (Methylsalicilate) ma non a PEBP1. Questo risultato suggerisce la presenza di altre molecole, oltre che a PEBP1, che possano attivare l'OR.

Inoltre, in HEK293T trasfettate con il solo vettore pCI, non esprimente l'OR, non è stato osservato alcun aumento di calcio intracellulare né in risposta a PEBP1, né all'odore specifico del OR trasfettato, ma solamente in risposta al carbacolo, usato come test di vitalità cellulare. Questi risultati mettono in evidenza che l'aumento di calcio intracellulare in seguito all'applicazione di PEBP1 è dovuto all'attivazione del OR.

Tuttavia, PEBP1 denaturato mediante alte temperature o con proteinase K non determina alcuna risposta di calcio intracellulare in HEK293T trasfettate con OR

specifico. Al fine di escludere che la presenza di contaminanti nella procedura di purificazione, possa indurre una risposta calcio nelle linee cellulari HEK esprimenti uno specifico OR è stata applicata un'altra proteina chinasi 2 ciclina-dipendente (CDK2), purificata con lo stesso protocollo di PEBP1. Nessuna risposta di calcio intracellulare è stata osservata confermando la specificità di risposta di PEBP1.

Molecole guida "axon guidance" dirigono l'allungamento assonale. Al fine di investigare se PEBP1 fosse in grado di modulare il movimento assonale, è stato valutato il comportamento del cono di crescita mediante la tecnica di "time-lapse imaging" sul singolo assone in risposta a gradienti di molecole in grado di modulare il signaling dei secondi messaggeri cAMP e Ca^{2+} all'assone terminale (es. foscolina). Abbiamo osservato che PEBP1 regola il movimento dell'assone di OSN con un simile effetto della foscolina o degli odori, capaci di modulare i livelli di cAMP e Ca^{2+} al cono di crescita del neurone sensoriale olfattivo.

Dov'è espresso PEBP1 nel bulbo olfattivo? Mediante la tecnica di immunofluorescenza su sezioni di OB di ratto embrionale, postnatale e di topo, è stata osservata l'espressione di PEBP1 nelle cellule periglomerulari, un'ottima posizione per guidare gli assoni degli OSN. PEBP1 è espresso con un pattern discontinuo, maggiormente nella regione anteriore (A), mediale (M) e laterale (L) dell'OB mentre è difficile osservare cellule positive per PEBP1 nella zona posteriore (P).

Mediante immunofluorescenza, RT-PCR e western blot è stata osservata l'assenza di espressione di PEBP1 nei OSN localizzati nell'epitelio olfattivo (MOE) di ratti embrionali, postnatali e di topo.

In accordo con queste evidenze, PEBP1 non è espresso nel "cuore" dei glomeruli. Per tutte queste tecniche, tessuti provenienti da una linea di topo con mutazioni per PEBP1 (topi PEBP1^{-/-}) sono stati utilizzati come controlli negativi.

Se PEBP1 giocasse un ruolo importante nell'organizzazione e nella posizione dei glomeruli nel bulbo olfattivo (OB), linee di topi che presentano mutazioni per questa proteina (topi PEBP1^{-/-}), dovrebbero mostrare alterazioni nella mappa sensoriale.

Al fine di verificare questa ipotesi, i topi che presentano mutazioni per PEBP1 (topi PEBP1^{-/-}) sono stati incrociati per linee di topi in cui uno specifico OR è co-espresso con una proteina fluorescente, GFP (es. come le linee di topi P2-GFP , M72-YFP). In queste linee di topi è stata studiata la convergenza delle fibre positive per la proteina fluorescente (GFP) nella formazione dei glomeruli nell'OB. La convergenza assonale dei OSN esprimenti il recettore P2-OR è distrutta dalla presenza di numerosi glomeruli eterogenei, mentre quella delle fibre esprimenti il recettore M72 (non responsivo a PEBP1 *in vitro*) non è alterata. Degno di nota è che l'alterazione nell'organizzazione topografica della mappa sensoriale è maggiormente evidente nei topi omozigoti per la mutazione di PEBP1 rispetto ai topi eterozigoti, suggerendo un meccanismo dosaggio dipendente.

Successivamente, è stata valutata la posizione di specifici glomeruli nel OB, un punto cruciale della mappa topografica.

Nessun difetto è stato riportato lungo l'asse dorso-ventrale (D-V) del bulbo, in accordo con la presenza di altre molecole che guidano le afferenze assionali dei OSN nella formazione dei glomeruli in una specifica posizione lungo l'asse dorso-ventrale del OB.

La posizione del glomerulo M72 non differisce tra i topi PEBP1^{-/-} e controlli. Questo dato è in accordo con una normale organizzazione dei glomeruli in cui convergono le fibre-M72 e con i dati *in vitro* in cui il recettore P2 ma non M72 è responsivo per PEBP1.

Al fine di investigare l'effetto funzionale dell'alterazione della mappa sensoriale è stato effettuato un test olfattivo (habituation-dishabituation test) nei topi PEBP1^{-/-}. E' stato riscontrato un deficit olfattivo nel riconoscimento e discriminazione degli odori nei topi PEBP1^{-/-} rispetto ai controlli.

Tutti i dati raccolti in questa tesi di Dottorato suggeriscono che OR espresso all'assone terminale può agire come molecola guida attivate dal ligando naturale del OR identificato PEBP1.

1. INTRODUCTION

1.1 The olfactory system

Olfaction is the most ancient and still the most mysterious sensory modality, that represents the sense of smell (*Firestein, 2001*).

The olfactory system (OS) is a very sophisticated and highly conserved system from fly to mammals, able to detect and discriminate thousands of odorant molecules (odors) presents in the environment even at very low concentration. Odors are small molecules, less than 400 Da, that could be organic (airbone molecules) or, less frequently, inorganic. Odors are mostly represented by a wide variety of different organic compounds that exhibit a carbon chain of different length and distinct functional groups such as aldehydes, alcohols, amines, thiols, carboxylic acids, ketones, esters, nitriles, thiols. The odor molecules therefore differ based on the length of the carbon chain, shape and size of the functional groups and charge. The perception of odors depends on the structure and also on the concentration of the odorant molecules and on individual variability. Actually, it does not exist a precise estimation of the number of odors that could be detected by a given species (*Firestein, 2001; Lledo et al., 2005*).

The OS is also able to detect another class of compounds: pheromones. Pheromones are molecules secreted or excreted in urine and/or other body fluids that influence the hormonal and sexual behaviors of con-specifics, member of the same species.

The variety of sensory stimuli detected by the OS, makes this modality important not only in detecting and discriminating odorant molecules (odors), but also in identifying food, recognizing con-specifics or predators, regulating the maternal and sexual behaviors (*Firestein, 2001; Tirindelli et al., 2009*).

I will describe the organization of the OS in mammals, that are the object of my thesis. In particular I will focus on mouse and rat OS, that are described below.

The mouse olfactory system includes different subsystems (**Figure 1.1**), anatomically separated within the nasal cavity, and specialized in distinct functions thanks to the different receptors they express, to the chemosensory selectivity and transduction of chemosensory information to specific areas of the brain (**Table 1**).

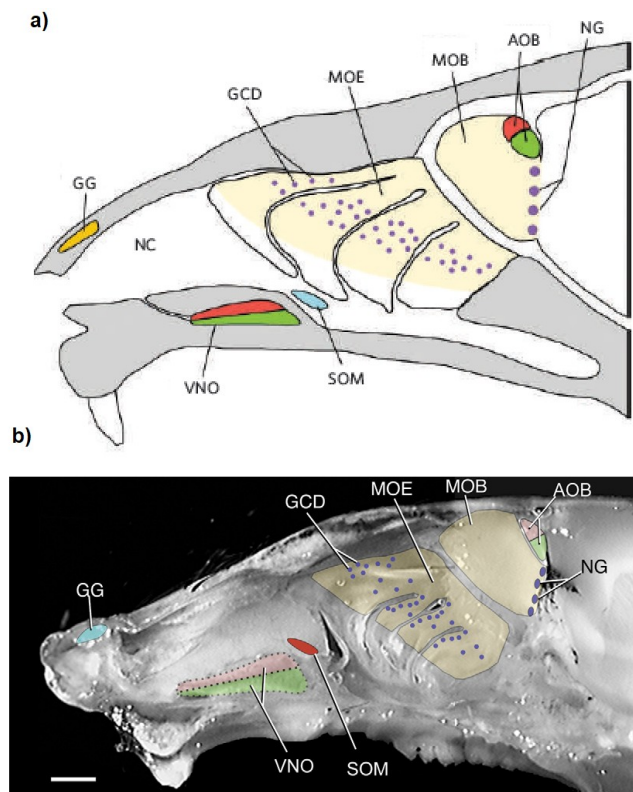


Figure 1.1. The mouse olfactory system. a) A cartoon of the organization of the olfactory system in the mouse. **b)** Sagittal view of the mouse olfactory systems within the nasal cavity and the forebrain. Modified from (Zufall & Leinders-Zufall, 2007). *AOB*=accessory olfactory bulb, *GCD*= guanylylcyclase type D system, *GG*=Gruneberg ganglion, *MOB*=main olfactory bulb, *MOE*=main olfactory epithelium, *NC*=nasal cavity, *NG*=necklace glomeruli, *SOM*=septal organ of Maserati, *VNO*=vomeronasal organ (Brennan & Zufall, 2006).

The olfactory system is divided in:

- **The main olfactory system (MOS)** includes the main olfactory epithelium (MOE), the main olfactory bulb (MOB) and higher olfactory brain areas that receives direct information from the MOB. The MOS is involved in detecting volatile molecules (odors) although it was reported that it can smell also pheromones (*Luo et al., 2003*).
- **Accessory olfactory system (AOS)** is formed by the vomeronasal organ (VNO), the accessory olfactory bulb (AOB) and higher olfactory brain areas that receives direct information from the AOB. The AOS detect pheromones (*Dulac & Torello, 2003; Brennan & Zufall, 2006; Zufall & Leinders-Zufall, 2007; Tirindelli et al., 2009*).
- **Septal organ of Masera (SOM)** is considered an "island of sensory tissues within the nasal mucosa", located posterior to the nasal-palatine duct which connect the nose to the oral cavity. This location suggested the possible role in the initial detection of molecules (i.e. cues from licking behaviour) (*Masera, 1947; Breer et al., 2006*)
- **Gruneberg Ganglion (GG)** located in the antero-dorsal area of the nasal cavity, it has been rediscovered (*Fuss et al., 2005*). The hypothesis that GG could detect alarm pheromones has been revised. GG cells may detect volatile molecules (i.e. gaseous stimuli) released by animals to alert members of the same species in danger situations. Actually, the function of Gruneberg Ganglion remains unclear (*Brennan & Zufall, 2006; Munger et al., 2009*)


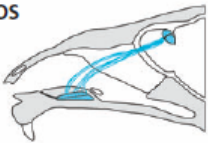
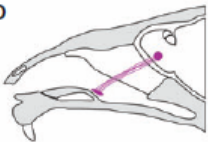

System	Principal target	Signal transduction components	Stimuli	
MOS  Canonical OSNs	Glomeruli in general MOB	ORs, ACIII, G α_{olf} , PDE1C2, PDE4A, CNGA2, CNGA4, CNGB1b	Volatile and nonvolatile (?) odor ligands	
	TAAR-expressing neurons	N.D.	TAARs, G α_{olf}	Volatile amines
	GC-D ⁺ neurons	Necklace glomeruli (dark circles, above)	GC-D, PDE2, CNGA3, CAII	Uroguanylin, guanylin, cues in urine, CO ₂
	TRP-expressing cells	TRPM5: glomeruli in medial, ventral, and lateral MOB TRPC2: N.D. TRPC6: restricted to MOE	TRPM5, G γ 13, CNGA2, PLC β 2 TRPC2 TRPC6, IP ₃ R3, PLC β 2	TRPM5: 2,5-dimethylpyrazine, 2-heptanone TRPC2: N.D. TRPC6: liliac, volatile odor ligands
	V1R-expressing cells	N.D.	V1Rs	N.D.
AOS  V1R-expressing VSNs	Rostral AOB	V1Rs, G α_{12} , TRPC2, PDE4A	Volatile pheromones	
	V2R-expressing VSNs: H2-Mv ⁻ H2-Mv ⁺	Anterior part of caudal AOB Posterior part of caudal AOB	V2Rs, G α_o , TRPC2 V2Rs, G α_o , TRPC2, H2-Mv	Genetically encoded ligands (peptides, proteins)
	OR-expressing VSNs	Rostral AOB	ORs, G α_{12} , TRPC2	General odor ligands (?)
SO  Canonical OSNs	Posterior part of the ventromedial MOB	ORs, ACIII, G α_{olf} , CNGA2	Volatile odors	
	GC-D ⁺ neurons	Necklace glomeruli (?)	GC-D, PDE2	N.D.
GG  Dorsocaudal MOB, near AOB and necklace glomeruli	Dorsocaudal MOB, near AOB and necklace glomeruli	TAARs V2R83, G α_o , G α_{12} , ORs, G α_{olf}	Alarm signal	

Table 1. Chemosensory subsystems in the mouse. Abbreviations used: ACIII, adenylyl cyclase type III; AOB, accessory olfactory bulb; AOS, accessory olfactory system; CAII, carbonic anhydrase type II; CNG, cyclic nucleotide-gated channel; GG, Grueneberg ganglion; IP₃R₃, inositol 1,4,5-trisphosphate receptor 3; MOB, main olfactory bulb; MOS, main olfactory system; N.D., not determined; OR, odor receptor; OSN, olfactory sensory neuron; PDE, phosphodiesterase; PLC, phospholipase C; TAAR, trace amine-associated receptor; V1R, type 1 vomeronasal receptor; V2R, type-2 vomeronasal receptor; TRPC2/6, transient receptor potential channel types C2 and C6; TRPM5, transient receptor potential channel type M5; VSN vomeronasal sensory neuron. For the signaling pathway coupled to the odorant receptor see paragraphs 1.2-1.3 (Munger *et al.*, 2009).

1.1.1 The main olfactory epithelium

The initial event of odor detection occurs in the main olfactory epithelium (MOE). The odors enter in the nasal cavity and reach the turbinates, cartilaginous lamellae covered by the olfactory epithelium. These structures are considered the sensory neuroepithelium, in which olfactory sensory neurons detect odors in the environment. The main olfactory epithelium is a specialized pseudostratified epithelium that covers the turbinates located in the posterior nasal cavity (Firestein, 2001) (Figure 1.2). The MOE is composed by three main cells types: olfactory sensory neurons (OSNs), supporting or sustentacular cells and basal cells, including the olfactory stem cells. In the MOE are located also the Bowmann glands, involved in the secretion of the mucus that plays a key role to allow the entrance of the odorant molecules into the neuroepithelium (Shepherd 2004).

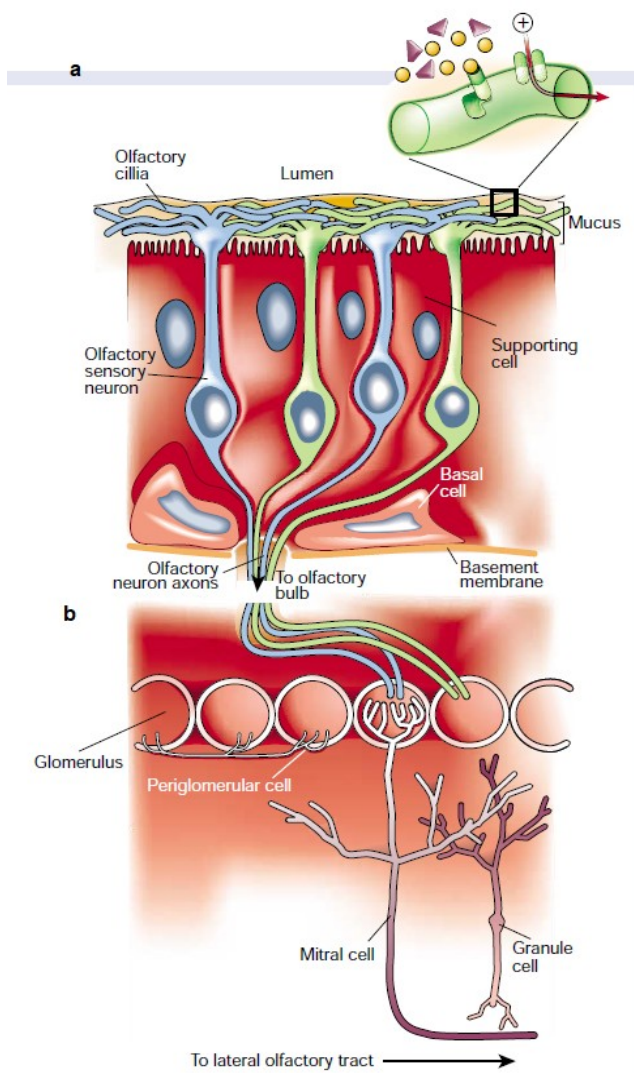


Figure 1.2. A schematic representation of the main olfactory epithelium and the main olfactory bulb. a) Main olfactory epithelium (MOE) formed by olfactory sensory neurons, sustentacular (supporting) cells and basal cells (neuron stem cells). **b)** Olfactory sensory neurons send their axons into glomeruli in the olfactory bulb. Glomeruli are spheric structures of neuropil formed by the incoming axons of the OSNs that form synapses with the apical dendrites of the postsynaptic cells, namely mitral and tufted cells and the periglomerular cells. Olfactory information is conveyed to higher brain regions by the lateral olfactory tract, formed by axon of the mitral and tufted cells, the output neurons of the olfactory bulb (Firestein, 2001).

Olfactory sensory neurons (OSNs)

Olfactory sensory neurons (OSNs) represent about the 70-80% of the entire cells population of the MOE. They constantly regenerate during the entire life of an individual, with an hemi-life of 60-90 days (*Mori et al., 1999; Gogos et al., 2000; Firestein, 2001*)(*Shepherd 2004*).

OSNs are bipolar neurons. From the apical pole of the OSN cell body, a single and unbranched dendrite is extended to the surface of the MOE. It ends in a swelling-like structure, named knob, from which emerge several thin and long cilia that protrude in the nasal cavity (*Firestein, 2001*)(**Figure 1.3**).

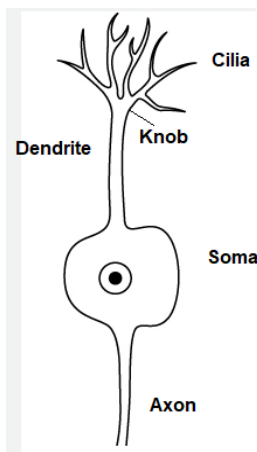


Figure 1.3 A schematic of a bipolar olfactory sensory neuron.

From the soma of the olfactory sensory neuron (OSN), an unbranched dendrite ends in a swelling-structure (knob) with protruding cilia in the apical side. A single thin axon is present on the opposite side.

Within the epithelium, each olfactory sensory neuron expressed only one type in a repertoire of more than one thousand odorant receptor genes, following the rule "one-neuron-one receptor"(*Chess et al., 1994; Serizawa et al., 2004; Lomvardas et al., 2006*).

The odorant receptors are expressed on the cilia of OSN, that are the location of the odorant signals transduction. It was discovered that also pheromones could be detected by the main olfactory epithelium (*Luo et al., 2003*).

From the proximal pole of OSN emerges a thin unmyelinated, unramified axon that projects directly to the olfactory bulb (**Figure 1.3**) where it forms synapses with the postsynaptic cells of the OB, in specific locations, named glomeruli.

The sustentacular (supporting) cells

The sustentacular cells act as the glia of the MOE, stabilizing and supporting the neuroepithelium. Indeed, they separate and electrically isolate OSNs, and release components of the mucus and growth factors essential for the development of OSNs.

Bowman glands

Bowman's glands distributed throughout the olfactory epithelium, produced the mucus in which cilia of olfactory sensory neurons are immersed. The mucus protects the neuroepithelium and creates the optimal environment for the odor perception. It contains mucopolysaccharides, salt, enzymes and olfactory binding proteins (OBP). OBPs are low-molecular weight soluble proteins, secreted in the nasal mucosa by the nasal glands that convey the transport of hydrophobic odorant molecules through the aqueous nasal mucus allowing their binding to the odorant receptors at the cilia level of OSN (*Pelosi, 1998*).

The basal cells (olfactory stem cells)

The basal cells (including the olfactory stem cells) are the precursor of the olfactory sensory neurons located in the basal lamina of the MOE. It is reported two different types of basal cells: 1. the dark/horizontal basal cells, that contact the basal lamina, and 2. the light/ globose basal cells (GBC) situated more superficially (*Huard & Schwob, 1995*). The first type are a quiescent population of basal cells with an adhesion receptor expression profile similar to non-neural stem cells.

On the contrary, GBCs are neurogenic showing a conserved multipotent progenitor phenotype. Indeed their differentiation is regulated by bone morphogenetic protein 4 and FGF2 (*Carter et al., 2004*).

1.1.2 The olfactory bulb: organization and circuitry

The olfactory bulbs (OB) are part of the vertebrate forebrain and consist of two symmetrical ovoid structures located bilaterally above the nasal cavity. The OB is a well layered structure. From the outer to the inner layer, are observed: the olfactory nerve layer (ONL), the glomerular layer (GL), the external plexiform layer (EPL), the mitral cells layer (MCL), internal plexiform layer (IPL) and the granule cell layer (GCL) (Figure 1.4) .

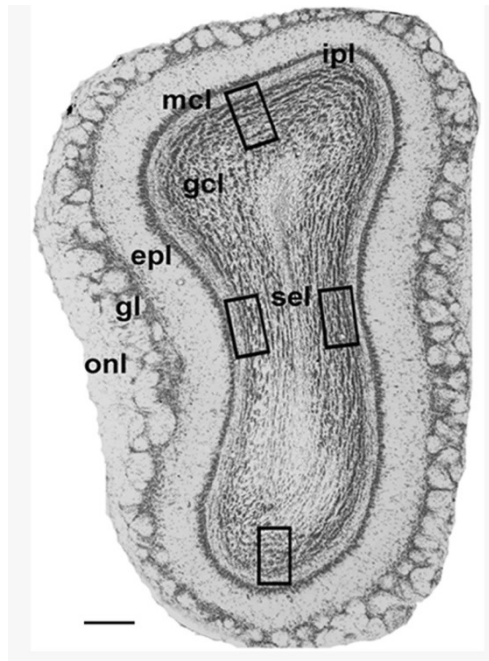


Figure 1.4: Organization in layers of the olfactory bulb. Sagittal section of the mouse olfactory bulb, stained with neutral red staining. Olfactory nerve layer (ONL), glomerular layer (GL), external plexiform layer (EPL), mitral cells layer (MCL), internal plexiform layer (IPL), granule cell layer (GCL) subependymal layer (SEL) Scale bar=200 μ m (Smail et al., 2016).

The neuronal elements of the olfactory bulb are classified in three categories: input, output and intrinsic (Shepherd 2004) (Figure 1.5).

a) Inputs (Afferent neurons).

Olfactory sensory neurons (OSNs) extend their axons through the basal lamina within the epithelium and then reach the olfactory nerve layer (ONL) in the olfactory bulb. Then, the axons of olfactory sensory neurons (OSN) converge in the glomerular layer (GL) to form spherical structures of neuropil, named glomeruli, in specific loci (medial and lateral side) of each olfactory bulb (Mombaerts, 1996; Mombaerts et al., 1996). OSN constantly regenerate with an hemi-life of 60-90 days (Gogos et al., 2000; Firestein, 2001)

The olfactory glomerulus. Glomeruli, spherical structure of neuropil with a diameter of 50-100µm in the mouse, are located in the glomerular layer (GL) of each OB. In the glomerular layer the axons of OSNs form excitatory synapses with the dendrites of the postsynaptic cells (mitral, tufted and periglomerular cells). These connections form the glomeruli in the OB.

Each glomerulus is a functional unit that processes sensory information related to a given odorant receptor (one neuron-one glomerulus) (**Figure 1.5**). This spatial segregation of the sensory afferents gives rise to the sensory map that plays a key role in encoding odorant molecules (*Imai et al., 2010; Mori & Sakano, 2011*).

In each glomerulus, OSN expressing the same odorant receptor form synapses with the postsynaptic cells of the OB: mitral cells, tufted cells and periglomerular cells. In this way, each glomeruli defines a functional unit, so called an "odor column", that consist of mitral, tufted cells and periglomerular cells receiving input from a specific group of OSNs along with the granule cells connected to them (*Schepherd 2004*) (**Figure 1.5**).

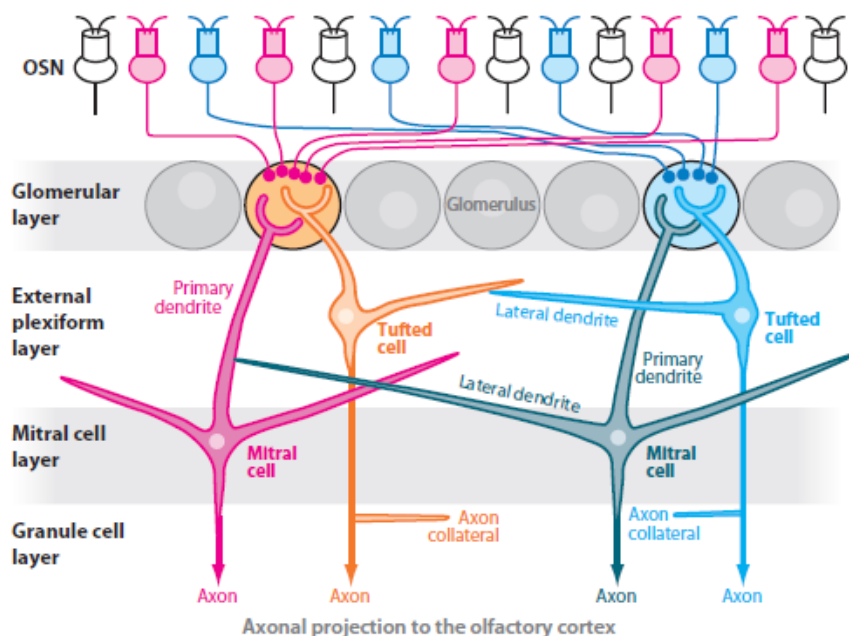


Figure 1.5: Schematic representation of the olfactory bulb (OB) circuitry. OB layers including the different neurons are shown. OSN = olfactory sensory neuron (*Mori & Sakano, 2011*).

Centrifugal inputs: There are several types of central inputs from higher brain regions to the olfactory bulb. Centrifugal inputs can be subdivided in two groups. Centrifugal afferents that release neuromodulators, such as serotonin, acetylcholine and noradrenaline. A second group of afferents that originate in the olfactory cortex (*Schepherd 2004*).

b) Outputs (Efferent neurons) consist of mitral cells (MC) and tufted (T) cells. MC and T cells represent the efferent pathway forming the lateral olfactory tract (LOT). MC are excitatory glutamatergic neurons that lie in the mitral cell layer (MCL), 200-400µm deep to the glomerular layer (GL). T cells are located more superficially in the EPL and are considered as a small type of MC (**Figure 1.5**).

MC have a cell bodies diameter of 15-30 µm and constitute the major output of the OB. A single primary apical dendrite (2-10 µm in diameter and 200-800 µm in length) projects in the EPL and ends in a tuft of branches (30-150µm in diameter) in a specific glomerulus. Each mitral cell gives rise to multiple lateral secondary dendrites that extend in the external plexiform layer (EPL) and create dendro-dendritic synapses with the granule cells (*Schepherd 2004*) (**Figure 1.5**).

Based on the depth of their second dendrites MC are subdivided in type 1 and type 2. MC axons forms the lateral olfactory tract (LOT) through which the connections from the bulb are send to the olfactory cortex (*Nagayama et al., 2014*) (**Figure 1.5; Figure1.6**).

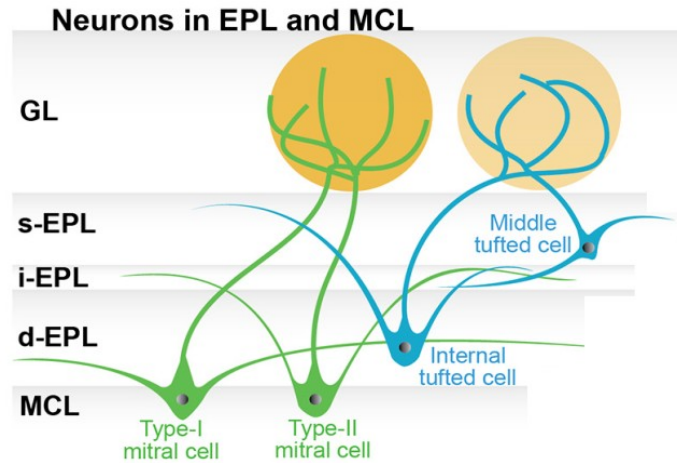


Figure 1.6. Subtypes of neurons in the external plexiform layer (EPL) and in mitral cell layer (MCL). Description of subtypes of tufted cells (blue) and mitral cells (green). GL = Glomerular layer; EPL = external plexiform layer; MCL =mitral cell layer. Modified from (Nagayama *et al.*, 2014).

Tufted cell (T) are cells similar to the MC but located more superficially in the external plexiform layer (EPL). Within the external plexiform layer, the lateral dendrites of the M/T cells make synapse with the dendrites of the granule cells, located in the layer below (**Figure 1.5**).

According to the position of their cell body (15-20 μm) they are subdivided in: middle tufted cells (T_m), the external tufted cells (T_e) and internal tufted cells (T_i).

T_m represent the main population of tufted cells that lies in the middle EPL. They have a cell body diameter of 15-20 μm , several basal dendrites of 300-600 μm and a primary dendrite of 200 μm that ends in a relatively confined tuft of branches in a glomerulus. Their axons form the olfactory tract and project to the olfactory cortex. T_e cells body lies into the glomeruli and their axons are connected with a specific loci in the internal plexiform layer (IPL) (Schepherd 2004) (**Figure 1.6**).

In the IPL, the ETC form a topographically ordered intrabulbar connections between isofunctional glomeruli, i.e. glomeruli that receive OSN expressing the same OR (Schoenfeld *et al.*, 1985; Belluscio *et al.*, 2002; Lodovichi *et al.*, 2003) (Figure 1.7)

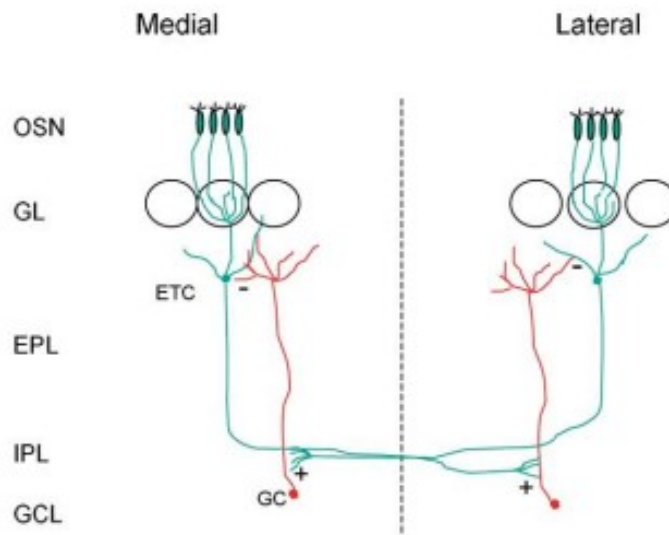


Figure 1.7. Intrabulbar connection between the medial and lateral olfactory bulb. External tufted cells (ETC) axons are connected with a specific glomerulus (one glomerulus-one receptor) and form excitatory synapses (+) with the dendrites of the granule cells (GC) in a restricted region of the internal plexiform layer (IPL) on the opposite side of the bulb. In turn, the GC make inhibitory synapses (-) on the ETC connected to a specific glomerulus (Lodovichi *et al.*, 2003).

c) Intrinsic neurons

The intrinsic neurons are located in three different layers: Glomerular layer (GL), external plexiform layer (EPL) and granule cells layer (GCL) (Figure 1.4).

Intrinsic neurons in the glomerular layer (GL)

Glomeruli are enwrapped by a heterogeneous population of cells.

PGC with a small soma of 6-8 μm in diameter. They possess a short dendrite that it is extended within a glomerulus for about 50-100 μm , while their axons is extended laterally in the extraglomerular part of the bulb for about 5 adjacent glomeruli. Some PGC are axonless. PGC form synapse with the axons of OSNs and with the dendrites of mitral and tufted cells (**Figure 1.5- 1.6**).

PGC are divided in: 1. short axon glutamatergic (SA) cells (Juxtaglomerular cells) with axons that reach glomeruli further away than the periglomerular classical short axons. Their dendrites branch the interglomerular spaces (**Figure 1.18**).

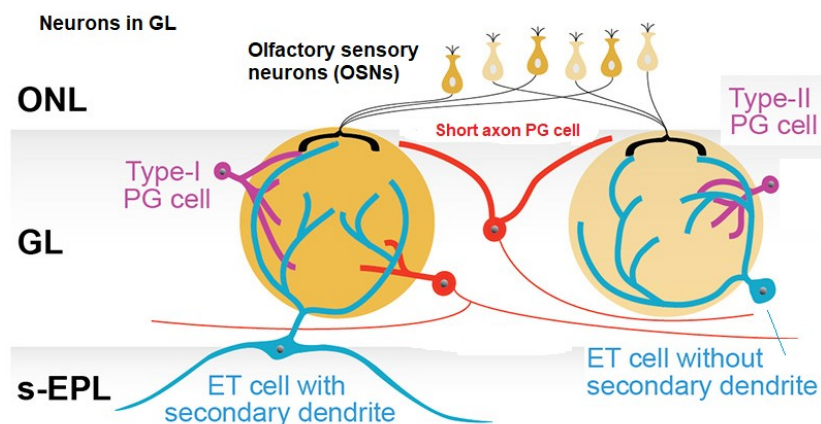


Figure 1.8. Subtypes of periglomerular cells (PGC) in glomerular layer (GL). Schematic representation of the of periglomerular cells (PG cells; purple), superficial short-axon PG cells (red), and external tufted cells (ET cells; blue). Modified from (*Nagayama et al., 2014*).

Indeed, based on the different neurotransmitters released, subpopulations of PGC are observed (*Kosaka & Kosaka, 2007; Batista-Brito et al., 2008*) (**Figure 1.9**):

- Type 1 PGC dopaminergic neurons that expressed tyrosine hydroxylase (TH). and make connections with the olfactory nerves;
- Type 2 PGC expressing the two calcium binding protein calretinin (CR) and calbindin (CB) positive neurons (*Toida 2000*)(*Kosaka et al., 2001*);

It is reported that in periglomerular cells tyrosine hydroxylase (TH), calretinin (CR) and Calbindin (CB) are co-expressed with glutamic acid decarboxylase (GAD) isoforms (GAD65/GAD67) (Kosaka & Kosaka, 2007). Some periglomerular cells express GAD65, while dopaminergic PGC the isoform GAD67 (Parrish-Aungst *et al.*, 2007).

PGC release different transmitters, such as λ -amino-butyric acid (GABA), glycine, neuropeptide Y, dopamine, NADPH or nitric oxide (NO) (Maher & Westbrook, 2008).

Intrinsic neurons in the external plexiform layer (EPL)

The external plexiform layer (EPL) lies immediately below the glomerular layer where glomeruli are located. It contains mitral (M)/ Tufted (T) cells dendrites and GABAergic granule cells dendrites. Parvalbumin (PV) positive interneurons reside primarily in the EPL, are GABAergic and make connections to mitral and tufted cells (Hamilton *et al.*, 2005).

Intrinsic neurons in the granule cell layer (GCL)

The granule cell layer (GCL) contains the cellular bodies (6-8 μ m in diameter) of granule cells that represent the core of the olfactory bulb. The granule cells are axonless while possess a basal and apical dendrites with several spines. The granule cells extend processes radially toward the surface and laterally in the EPL. They establish dendro-dendritic connections with the output neurons (Price & Powell, 1970).

According to the position of their soma (Mori *et al.*, 1983) (Schepherd 2004) are divided in:

1. Superficial (s) that extend the peripheral dendrites mostly in the EPL where MC and T cells are located.
2. Intermediate granule cells (i), whose dendrites branch in all EPL levels;
3. Deep (d), (Type I-V) (**Figure 1.9**) extend their dendrites mostly in the deep EPL

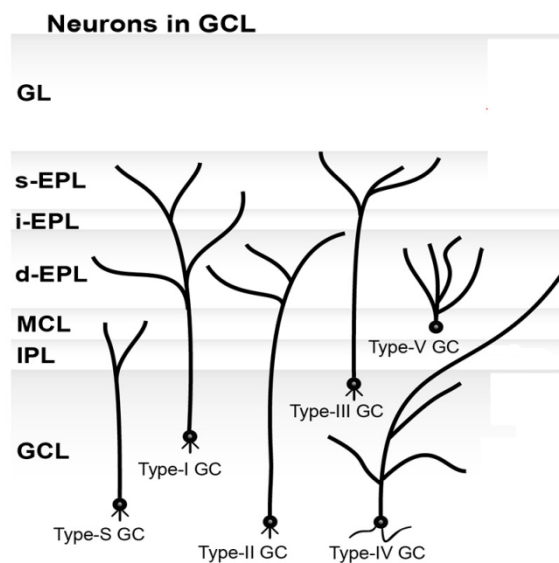


Figure 1.9. Subtypes of granule cells in the granule cells layer (GCL). Schematic representation of the different subtypes of granule cells based on the distribution of their dendrites in the external plexiform layer (EPL) s=superficial; i=intermediate; d=deep. Modified from (Nagayama *et al.*, 2014).

Granule cells are the major population of GABAergic inhibitory interneurons in the OB. They formed synapses on lateral dendrites of mitral and external tufted cells (Shiple & Ennis, 1996) (Figure 1.5)(Figure 1.8-1.9).

Noteworthy, granule cells play several important roles in the OB circuitry. They shape neural firing (Yokoi *et al.*, 1995; Fantana *et al.*, 2008) balance the excitation-inhibition in OB neuronal network, and are involved in odor learning processes (Lepousez & Lledo, 2013), including form of LTP within the OB (Nissant *et al.*, 2009). GC coordinate activity of ensembles of neurons, that result in OB oscillations. In particular gamma oscillations (40-100Hz) originate at the dendrodendritic synapses between GC and output neurons (Lepousez & Lledo, 2013).

Deep short axon cells are located mostly in the granule cells layer (GCL) and rarely in the glomerular layer (GL)(Burton *et al.*, 2017) whose dendrites branch in the EPL or GCL.

Blanes cells are cells intermixed together with the granule cells in the GCL. They represent a new mechanism of OB circuitry in the GCL.(Schoppa, 2006).

OB interneurons comprise several type of cells, different both in morphology and immunochemically.

Brito and colleagues (*Batista-Brito et al., 2008*) characterized with different markers (tyrosine hydroxylase (TH), calretinin (CR), Calbindin (CB) and parvalbumin (PV) the interneurons subtypes in the OB and investigate the temporal profile by which they are produced (**Figure 1.10**). TH-positive interneurons surround the glomeruli and are characterized by a fairly large soma (11-12 μ m). They receive synapses from the axons of OSNs (*Kosaka & Kosaka, 2016*). CR positive granule cells are mostly located in the external region of the GCL. Although CR and CB-positive cells make synapses with mitral and tufted cells, CB-positive cells occasionally make connections with other interneurons. PV-interneurons are located mostly in EPL and form synapses with the primary dendrite and soma of MC and T cells. (*Batista-Brito et al., 2008*). Brito and coauthors observed that in the glomerular layer different subtypes of interneurons (TH, CR and CB-positive interneurons) possess a distinct temporal production profile (i.e. the embryonic stage E.15.5 for TH-positive interneurons while E.15.5-E17.7 for CB-positive interneurons. (*Batista-Brito et al., 2008*). CB interneurons reach the maximal percentage in the late phase of embryogenesis but decrease postnatally, while CR-positive interneurons show the opposite behaviour. In fact during the postnatal stage, CR-positive-interneurons represent the highest number of cells while during embryogenesis forms a small percentage of cells (*Batista-Brito et al., 2008*). PV-positive interneurons are GABAergic and are produced only perinatally (**Figure 1.10**).

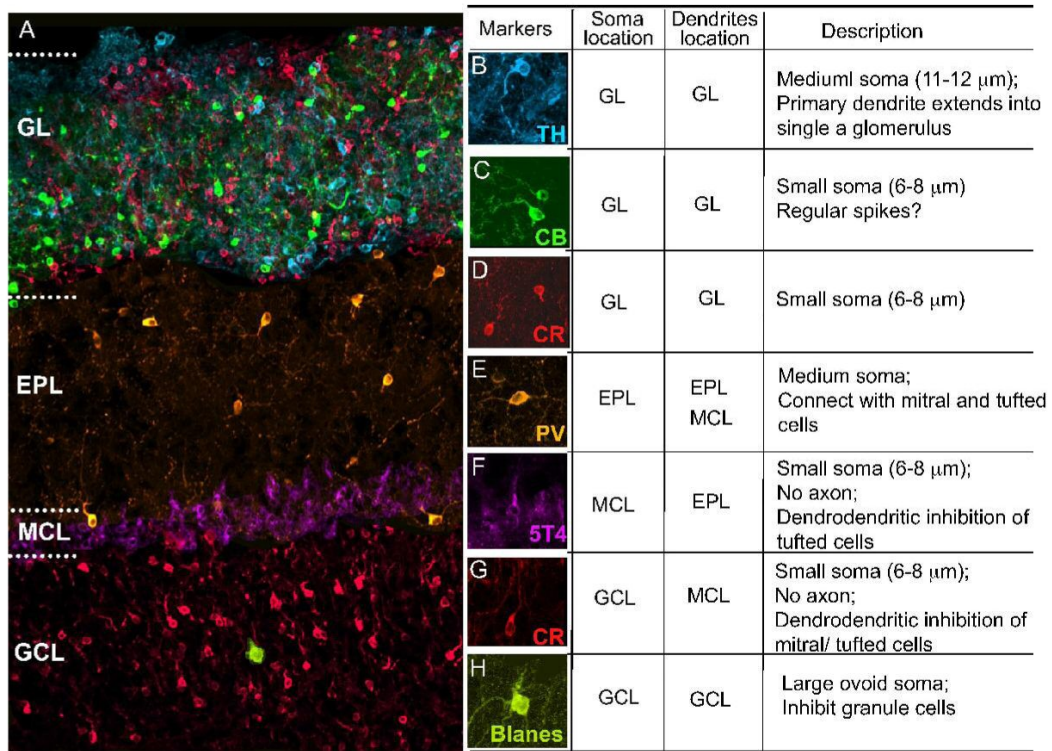


Figure 1.10. Interneuron population of the olfactory bulb. Interneurons are identified by the expression of specific markers: TH=Tyrosine hydroxylase; CB=Calbindin (green); PV=Parvalbumin (orange); 5T4 (purple); CR=Calretinin (red) modified from (Batista-Brito et al., 2008).

1.1.3 Olfactory bulb connections to the brain

The olfactory cortex comprehends the brain regions that receive direct projections from the mitral and tufted cells of olfactory bulb. In humans and most mammals the olfactory cortex comprises: the anterior olfactory nucleus, the olfactory tubercle, the piriform cortex, the lateral entorhinal cortex, the anterior cortical nucleus of the amygdala. The piriform cortex receives substantial projections from the ventral tegmental area, the substantia nigra, the locus coeruleus (*Imai, 2014*).

The olfactory cortex is reciprocally connected to the orbito-frontal cortex, insular cortex, the hippocampus and amygdala. Reaching several forebrain regions, odor information can affect cognitive, emotional and visceral behaviours.

The OB is the first retransmission station of the olfactory system. Olfactory sensory neurons project their axons to the OB, where the chemosensory information is first elaborated and then conveyed to higher brain areas by the lateral olfactory tract, formed by the axons of the output neurons of the OB (*Schepherd 2004*) (**Figure 1.11**).

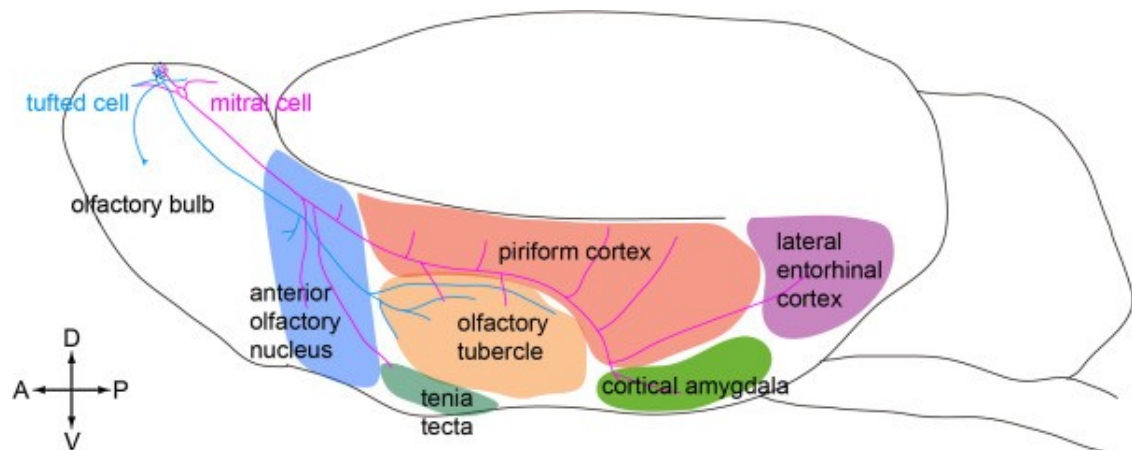


Figure 1.11. Sagittal view of the olfactory bulb and the connected brain areas, that form the olfactory cortex. A=anterior; P=Posterior; D=dorsal; V=ventral (*Imai, 2014*).

1.2 The odorant receptors

The detection of odors is mediated by the odorant receptor (OR), a G-protein coupled receptors that belong to the highly conserved family of seven-transmembrane-domain receptors (7-TMR), i.e. the G-protein-coupled receptor (GPCRs) (*Mombaerts, 1999b; Firestein, 2001; Zhang & Firestein, 2002*) (**Figure 1.12**).

GPCRs, according to the latest version of the GPCR database (Version 9.9.1, September 2009) are divided in 5 families or classes based on sequence homology and functional similarity: Class A (Rhodopsin like); Class B (secretin receptor like), Class C (Metabotropic glutamate/pheromone), Class D (vomeronasal receptors V1R/V3R); Class E (Taste receptor T2R) (*Peng et al., 2010; Weis & Kobilka, 2018*). GPCRs family plays a key role in many physiological processes such as secretion, neurotransmission, cellular differentiation and metabolism transmitting extracellular signals across the plasma membrane .

In mammals, the repertoire of odorant receptors (ORs) consists of more than 1000 genes and is one of the biggest gene family in the genome.

In 1991, for the first time Linda Buck and Richard Axel cloned the large family of the odorant receptor, in rodents (*Buck & Axel, 1991*).

Molecular structure of the odorant receptor (OR)

The odorant receptors share many motifs with the other GPCRs.

The OR is characterized by a coding region that lacks introns and by a hydrophobic seven α -helical transmembrane domains (7-TMR) connected to variable domains: an extracellular N-terminus and intracellular C-terminus (*Mombaerts, 1999b; Firestein, 2001; Spehr & Munger, 2009; de March et al., 2015*).

Noteworthy, the OR has not been crystallized yet. To predict the structure- function of the OR, several studies based on different computational approaches, sequences analysis, docking interactions, simulations with structural models, targeted

mutagenesis have been employed (*de Castro, 2009; Baud et al., 2015; Geithe et al., 2017*).

In the majority of these studies, in the absence of the crystal structure of the OR, crystal structure of other, better characterized, GPCRs, were exploited. To this end, the X-ray structure of the β_2 -adrenergic receptor offers a useful tool to investigate and predict the structure of odorant molecules (*Salom et al., 2013; Omura et al., 2014*). For instance, it is reported that the three dimensional model of the odorant receptor (mOREG) is based on the alignment of sequences and the structure of a β_2 -adrenergic receptor (β_2 AR)(*Kosaka & Kosaka, 2005; Kato et al., 2008; Kato & Touhara, 2009; de March et al., 2015; Ahmed et al., 2018; Bushdid et al., 2018*) (**Figure 1.12**).

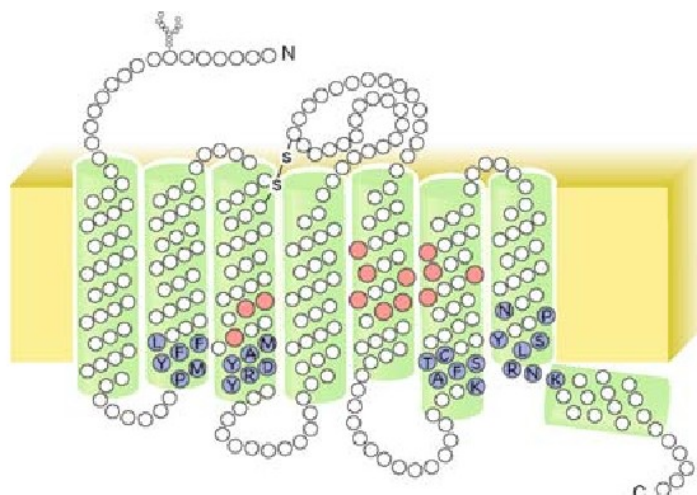


Figure 1.12: Molecular structure of the odorant receptor. Odorant receptors exhibit the canonical structure of seven- α -helical membrane-spanning domains (7-TMR). In red, the most variable amino acid motifs, that are supposed to be involved in the binding of odors. In blue, the most highly conserved sequences of the OR. DRY (aspartate-arginine-tyrosine) motif. A=Ala; C=Cys; D=Asp; F=Phe; K=Lys; L=Leu; M=Met; N=Asn; P=Pro; R=Arg; S=Ser; T=Thr; Y=Tyr; (*Kato & Touhara, 2009*).

To monitor protein-protein interactions with high sensibility and selectivity, Barnea and colleagues developed a new experimental tool named Tango assay. This strategy was developed for three different receptors classes: the tyrosine kinase, GPCRs and steroid hormone receptors. After receptor's activation, the recruitment of a signaling protein fused to a protease cuts and releases a transcription factor bind to the receptor. Then, the transcription factor activates the nuclear gene reporter, whose signals are amplified and used to monitor and to record the receptor's activation (*Barnea et al., 2008*).

The size of the OR is around 1000bp. Different OR share sequence homology in the range from 40 to 96%. The sequence of each OR exhibits highly conserved regions interleaved to highly variable strands. Several studies demonstrated that highly variable GPCRs motifs are important in the olfactory signals transduction (*Menini, 1999; Bradley et al., 2005; Pifferi et al., 2009; Pifferi et al., 2010*). In particular, several molecular modeling and mutagenesis studies suggested that the odorant binding-site is located in a 9 amino acid pocket located in TM3, TM5 and TM7 (*Katada et al., 2005; Abaffy et al., 2007; Kato et al., 2008*). However no direct binding evidence between the OR and the odors has never been provided.

The binding site of G protein is a conserved aspartate-arginine-tyrosine amino acid motif (DRY) (aspartate-arginine-tyrosine) located at the cytoplasmic side of the III domain (*Kato & Touhara, 2009; Munger et al., 2009; de March et al., 2015*) (**Figure 1.12**). Indeed, mutations in the DRY motif, hampers the coupling between the OR and G-protein (*Imai et al., 2006*). Furthermore, Kato and colleagues provided evidence that the truncation of C-terminal of the OR impairs the odorant responsiveness, suggesting the crucial role of this domain in the G-protein coupling of ORs (*Kato et al., 2008*).

Odorant receptor repertoire

The OR sequences have been identified in different invertebrates (nematode and fruit fly) and vertebrates (amphibians, lizards, fish, birds and mammals) (*Mombaerts, 1999b; Zhang & Firestein, 2002; Hallem & Carlson, 2006; Oh, 2018*).

In vertebrates, ORs genes are phylogenetically classified based on their sequences homology in: Class I (vertebrate marine heritage) activated by water-soluble ligands (i.e. aliphatic acids, aldehydes and alcohols) and Class II (mammalian terrestrial heritage) that bind airborne (volatile) odorants ligand (*Zhang et al., 2004*).

GPCRs can assume two different conformations, active or inactive in absence of a ligand. Activation of GPCRs occurs physiologically upon binding agonist (*Kobilka, 2013*)

Mammals ORs genes are distributed in clusters on all chromosomes with the exception of chromosome 12 and Y. The largest odorant receptor sequences are located in the chromosome 7 (252 ORs sequences) and then in the chromosome 11 (190 ORs sequences) and chromosome 9 (131 ORs sequences). Only 2 and 4 ORs sequences are located in the chromosome 3, 8 and X respectively (*Fuchs et al., 2001; Glusman et al., 2001; Zozulya et al., 2001; Zhang et al., 2007*)

It is reported that OR genes from the same family tended to form “subclusters”, meaning they are located near each other. Non-OR genes are present within the OR clusters.

In mouse and rat, the OR repertoire include ~1000 OR sequences and ~about 20% are pseudogenes. In humans, nearly 60% are pseudogenes giving mice over 3 times as many intact genes as humans. The OR is one of the largest family genes, that occupy more than 2%, of our genome (*Zhang & Firestein, 2002*).

Human ORs account for more than 4% of our proteome and represent the largest subfamily of class A (or Rhodopsin like) G-protein coupled receptors (GPCRs) (*Mombaerts, 1999b; a*).

Each olfactory sensory neuron expresses only one type of OR. The odorant receptor choice follows the monogenic and monoallelic mode and is known as “one-neuron-one receptor rule” (*Chess et al., 1994; Serizawa et al., 2004*).

It is known that a combination of positive or negative regulations direct the expression of the odorant receptor (*Eggan et al., 2004; Li et al., 2004*). Furthermore, it is reported the monoallelic mechanism allows the expression of only one functional OR gene and prevent that of all other ORs, including the allelic OR expressed from the opposite chromosome. The monoallelic expression is thought to ensure that a single type of OR is expressed in each OSN.

1.2.1 Signaling transduction cascade at the cilia of olfactory sensory neuron

Once the odorant molecules enter in the nasal cavity, dissolve in the mucus of the main olfactory epithelium and there bind the odorant receptors expressed at the cilia of the olfactory sensory neuron (OSN).

The OR, a G-protein coupled receptor (GPCR), upon binding odorant ligands, activates a specific G-protein, G_{olf} , that stimulates adenylyl cyclase type III (ACIII) to produce cyclic adenosine monophosphate AMP (cAMP). cAMP, in turn, opens olfactory specific nucleotide-gated (CNG) channels that drives an influx of Ca^{2+} and Na^{+} within the cell. The increase in Ca^{2+} concentration induces the opening of Ca^{2+} -activated Cl^{-} -channel, allowing an outflow of Cl^{-} that leads to further depolarization of membrane potentials in the neuron. Then, the action potentials are conducted along the axon of OSN to the olfactory bulb (*Boekhoff et al., 1990; Breer et al., 1990; Kato et al., 2008; Kato & Touhara, 2009; Pifferi et al., 2009; Kaupp, 2010*)(**Figure 1.13**).

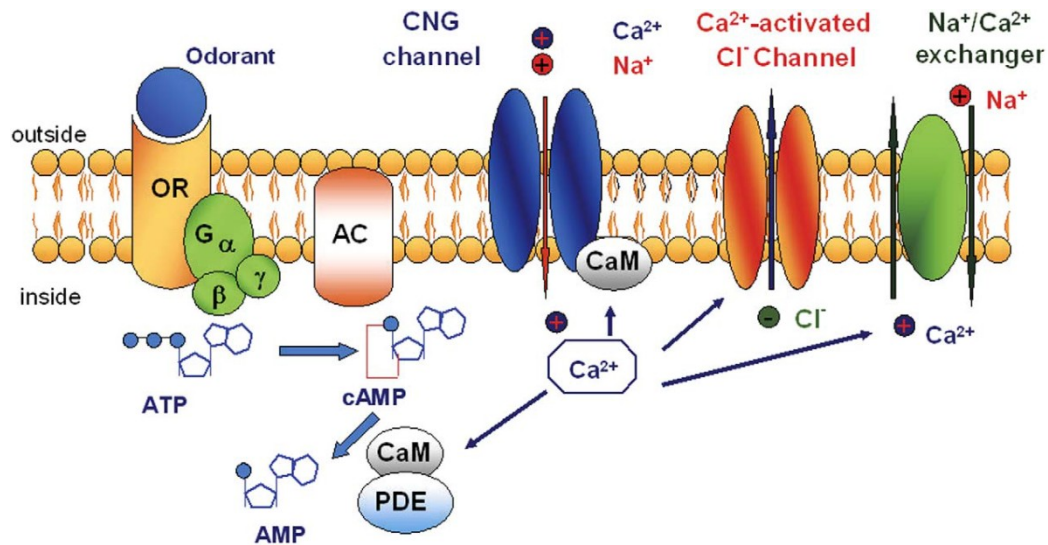


Figure 1.13. Odorants activate a cAMP and Ca^{2+} -mediated signaling pathway at the cilia of olfactory sensory neurons. Upon binding odors, the OR activates the olfactory specific G-protein, G_{olf} that stimulates in turn the adenylyl cyclase type III (ACIII) to produce cAMP. cAMP, in turn, opens olfactory specific nucleotide-gated (CNG) channels, driving an influx of Ca^{2+} and Na^{+} within the cell. The rise of intracellular calcium concentration opens Ca^{2+} activated Cl^{-} channels, leading to a Cl^{-} efflux, that further depolarizes the membrane potential (Pifferi et al., 2006).

Following the excitation, an Na^{+} - Ca^{2+} exchanger (Figure 1.13) restores the intracellular level of Ca^{2+} to the pre-stimulus condition. Upon binding odors, the increased concentration of Ca^{2+} at the cilia level, mediates not only the activation but also the desensitization of the olfactory sensory neurons (Pifferi et al., 2006)..

The high concentration of Ca^{2+} reduces the sensitivity of the CNG channel to cAMP through a direct interaction with the complex Ca^{2+} -calmodulin (Matthews et al., 1994). Then, together with the inhibition of the ACIII and the blocking of cAMP synthesis, calcium/CaM-dependent kinase II (CaMKII) activates a type 1C2 phosphodiesterase (PDE1C2) that hydrolyzes cAMP and generates a negative feedback on the CNG channel, mediating the olfactory adaptation (Menini, 1999).

Thus, the odor perception depends not only to the chemical structure, the concentration of odorants but also to the odor adaptation of OSNs. The adaptation is a form of neural plasticity that prevents the cellular transduction saturation. OSNs have the ability to adjust their sensitivity during a continuous odor stimulation through a negative feedback regulation (Kato & Touhara, 2009).

Channels in OSNs

In olfactory sensory neurons there are three different subunits of CNG channels: CNGA2, CNGA4 and CNGB1b (Pifferi et al., 2006)(Munger et al., 2009). CNGA4 and CNGB1b mediates the feedback inhibition Ca^{2+} -Calmodulin and increase the sensitivity to cAMP. CNG channels are formed by six transmembrane domains (TMDs), an intracellular N-terminal and C-terminal, similar to the voltage-gated ion channels family (Pifferi et al., 2006) (Figure 1.14).

In olfactory sensory neurons, CNG channels showed an higher affinity for cGMP rather than cAMP. Noteworthy cyclic nucleotides do not lead to the desensitization or inactivation of CNG channel.

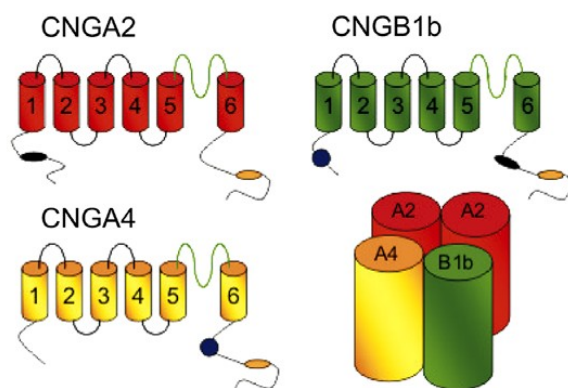


Figure 1.14. Structure of CNG channel in olfactory sensory neurons. Subunits and stochiometry of CNG channels subunits: CNGA2, CNGB1b and CNGA4. It is shown 6 transmembrane domains (TMDs) and cAMP binding site (blue) and CaM binding site (Yellow) (Pifferi et al., 2006).

Murthy's group, recently, provided evidence of the function of the calcium-activated chloride channel anoctamin-2 (Ano2) in the olfaction transduction (Zak et al., 2018) by investigating the firing activity in $Ano2^{-/-}$ mice. $Ano2^{-/-}$ mice display a reduced transduction current in $Ano2^{-/-}$ OSN, however their firing activity in

response to odors may be higher. As a consequence of a perturbed OR signaling transduction, $Ano^{2-/-}$ mice are slower to identify and reach an odor source in respect to controls, revealing an olfactory behavioral deficits.

In the last years, it has been shown that bestrofinins, Cl calcium activated chloride channels and anoctamin/transmembrane 16 (TMEM16) protein family are the molecular component of the Ca^{2+} -activated Cl^- channel (Pifferi *et al.*, 2009) (Schroeder *et al.* 2008). Several study demonstrate that the TMEM16B/Anoctamin2, a member of the TMEM16B (Anoctamin) gene family (Pedemonte & Galiotta, 2014) highly expressed at the cilia level of OSNs, is involved in the Ca^{2+} -activated Cl^- currents. (Pifferi *et al.*, 2009; Pifferi *et al.*, 2012) (Billig *et al.*, 2011). However, its role in olfaction is still debated. It is reported by Billig and coauthors (Billig *et al.*, 2011) that the disruption of TMEM16b/Ano2 gene in mice abolish the Ca^{2+} -activated Cl^- currents in OSNs but mice do not exhibit an olfactory deficit.

On the contrary, Pietra and colleagues (Pietra *et al.*, 2016) suggested an involvement of TMEM16b in olfaction using TMEM16b KO mice crossed with I7-IRES-tauGFP (Bozza *et al.*, 2002) as a model. By studying spontaneous and odor-evoked activity in I7 expressing OR, they observed a change in OSNs firing in response to the cognate-ligand of I7-OR (heptanal) in respect to wild-type mice. Indeed, in TMEM16B KO mice, spontaneous firing activity decreased while the odor-evoked response to heptanal was prolonged that lead to an high number of action potentials for response in I7-OSNs. TMEM16b KO mice exhibit an altered segregation of OSN expressing I7-OR that form an increased number of I7-GFP glomeruli and is reflected in olfactory deficit. All this data suggest a role of the TMEM16bAno2 channels in OSN activity and wiring.

1.2.2 The combinatorial receptors code for odors

Each OR is able to recognize specific structure features of the odorant molecules (odotopes), that are classified based on their size, shape, charge and functional groups.

Each OSN expresses only one type of OR gene that define the identity of the OSN.

There are two main features that characterize the odorant molecules: the length of the hydrocarbon chain and the functional group of the chemicals. Each odor contains several odotopes that can bind to different OR. Moreover, each odorant receptor could recognize several odors carrying the same odotope. This pattern of OR -odor interaction was defined “the combinatorial code” according to which, one odor can be recognized by different OR, and each OR can binds several odors. However each odor is identified by a specific combination of activated odorant receptors. This specific pattern of activated OR provides the specificity of the odor percept (*Malnic et al., 1999; Mori et al., 1999; Saraiva et al., 2016*) (**Figure 1.15**).

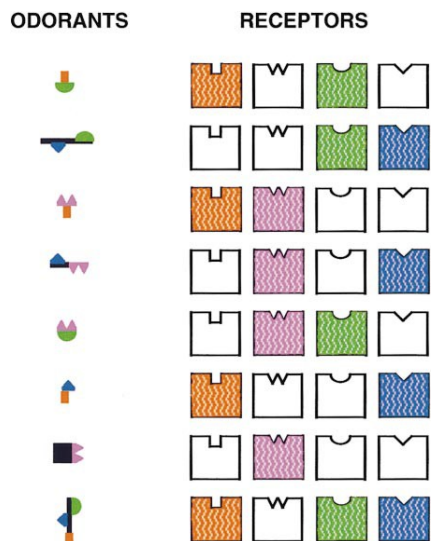


Figure 1.15. Combinatorial receptor codes for odorant molecules. This scheme shows the identities of different odorant molecules (left) that are encoded by multiple combinations of receptors (right). Each odorant receptor (OR) can be considered as a component of the combinatorial receptor code for several odors. The number of the ORs possible combinations is shown in colors on the right column and recognize the unlimited variety of different odorant molecules on the left (*Saraiva et al., 2016*).

1.2.3 Deorphanization of the odorant receptor

For long time, it has been difficult to deorphanize the OR, i.e. connect the OR to specific odor ligand. The majority of the OR are semi-orphan receptors, meaning that is not still proved the specificity of each receptor to the corresponding cognate odorants. The biggest obstacle in deorphanizing OR was related to the impossibility to express functional OR in heterologous systems, possibly due to the retention of the OR in the endoplasmic reticulum, and subsequent degradation of the OR in the proteasome.

This limitation eventually was bypassed by Firestein group who discovered that OR could be over expressed in OSNs. By infecting the MOE with AAV expressing a given OR, I7, and performing electrophysiological recording from the MOE, they found that a given I7 responded to a small subset of odors, in particular to optanal. This method allowed to define the molecular receptive range of a given OR

A major breakthrough in deorphanizing OR came from the work of Matsunami and colleagues. They identified accessory proteins that act as chaperons proteins and that co-transfected with the OR sequences allowed the expression of functional OR on the plasma membrane in heterologous system, such as HEK cells (*Zhuang & Matsunami, 2007*) (*Saito et al., 2004; Zhuang & Matsunami, 2008*)(**Figure 1.16**).

In order to identify possible molecules that can enhance the targeting of the OR to the cell-surface, Saito and colleagues screened several genes involved in the OR trafficking. They found that RTP1, receptor transporting protein (RTP) 1 (RTP1) and 2 (RTP2), are expressed in OSNs and are able to enhance the response of the OR to the odorants when they are co-transfected with the ORs in HEK293T cells.

They further demonstrated that the short form of receptor transporting protein 1 (RTP1s) and RTP2 promote the cell surface expression of OR, enhancing the response to odorants when co-expressed with the ORs sequences (*Saito et al., 2004*) (**Figure 1.16-1.17**).

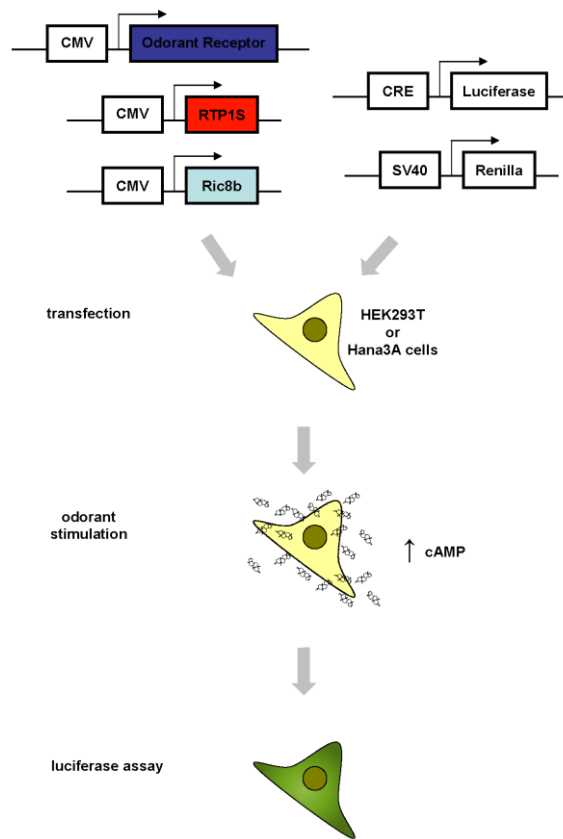


Figure 1.16. Activation of the odorant receptor in an heterologous system.

Transfection: A mammalian odorant receptor, RTP1s and Ric8b were cloned in pCI vector and transfected in an heterologous system (HEK293T cells or Hana3A cells) together with a luciferase reporter gene driven by CRE (cAMP responsive element) promoter and Renilla luciferase plasmid under SV40 promoter. Odorant stimulation: One day after transfection, odorant molecules were challenged to cells that lead to an increase of cyclic AMP (cAMP). Luciferase assay: Increase of cAMP levels turns on the expression of the luciferase reporter gene (Zhuang & Matsunami, 2008).

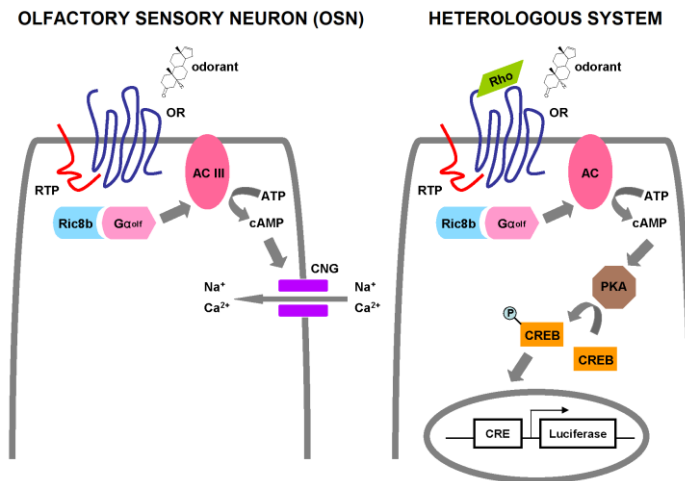


Figure 1.17. The endogenous and heterologous odorant receptor signal transduction pathways in endogeneous and in heterologous system. The endogenous odorant receptor signal transduction pathway in an olfactory sensory neuron (on the left) and in the heterologous system (Hana3A cells/HEK293T cells) (on the right). G_{olf} =Olfactory neuron specific G-protein; OR,=odorant receptor. RTP= receptor-transporting protein. PKA=protein kinase A. CREB=cAMP response element binding protein. CRE= cAMP response element. (Zhuang & Matsunami, 2008).

The genetic strategy designed by Matsunami to express functional OR in heterogeneous systems requires several steps (**Figure 1.16**):

1. The addition of the first 20 amino acids of the Rhodopsin (Rho tag) to the N-terminal of the specific OR transfected promote its cell-surface expression. It still unclear how this tag can enhance the OR expression on the membrane. Noteworthy, it is known that the modification at the N-terminal of the OR do not affect the recognition of its cognate odor ligand.
2. Co-Transfection of different accessory proteins, named receptor transporting protein (RTP) 1 (RTP1) and 2 (RTP2), that improve the OR-trafficking to the cell-

surface membrane in an heterologous system and enhance the response to odors (*Saito et al., 2004*).

The heterologous system developed by Matsunami and colleagues provided a powerful tool for the "deorphanization" of the odorant receptors that could be finally expressed *in vitro*. This approach leads to the identification of several cognate ligands of the odorant receptors (*Saito et al., 2004; Zhuang & Matsunami, 2007; 2008*).

Before Matsunami work, only few odors were identified as cognate ligand of specific OR. For example the receptor I7 is activated by Octanal, the receptor M71 is activated by acetophenone and OR23 by lylal.

Matsunami approach allowed to deorphanize a significant number of *OR* .

To better understand the role of single OR in odor perception a similar approach was performed with the human OR repertoire against several combination of odorant molecules. Since only 10% of human ~400 intact human ORs have a identified cognate-ligand, Mainland and colleagues used an heterogeneous system coupled to Luciferase assay to screen a cloned library of human ORs in response to odors. They screened about 73 types of odorant molecules against 511 human ORs and they identified new agonists for 27 human ORs, deorphanizing 18 human ORs (*Mainland et al., 2015*).

1.3 The topographic map

A topographic map is a spatially ordered segregation of sensory afferents to higher brain regions, that translates sensory stimuli in an internal representation. Topographic maps encode the quality, the intensity and the location of sensory stimuli.

The term "topographic" was referred for the first time to the topographic map of the visual system (i.e. retinotopic map), and then was extended to other sensory modalities such as auditory system and the somatosensory (Luo & Flanagan, 2007).

How do 1000 OR provide odor percept?

1.3.1 Organization of the main olfactory epithelium

Sensory systems are the interface between the external and the internal world.

In most sensory systems, sensory neurons in the most peripheral region, such as the retina for the visual system, cochlea for the auditory system, are spatially distributed according to the physical features of the stimulus they detect.

The spatial distribution of sensory neurons is maintained in more central brain regions. Namely, peripheral sensory neurons project their axon in specific loci in the brain, such that neighbor spatial relation in the periphery is maintained in the brain, giving rise to a topographic map.

How the repertoire of more than 1000 OR is organized in the MOE?

The olfactory system differs in several ways from the classic organization of sensory systems (see above). In the OS, segregation of sensory afferents reflects the identity rather than the spatial distribution of sensory neurons, giving rise to a sensory map (Ressler et al., 1993; Vassar et al., 1993; Luo & Flanagan, 2007) (**Figure 1.18**).

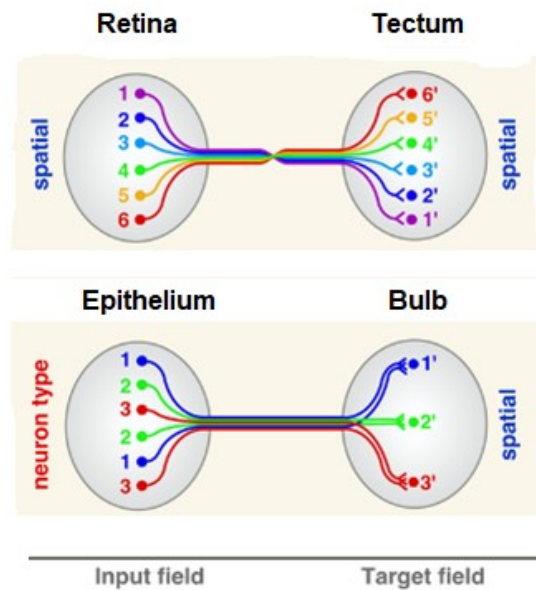


Figure 1.18. Schematic representation of topographic map in sensory systems. Visual map (top) while the olfactory system (Bottom). Top: In the visual map, neighbor spatial relation of sensory neurons in the retina (input field) is maintained in the tectum (target field). Bottom: The topographic organization in the bulb (target field) reflects the identity of the OR rather than the spatial location of olfactory sensory neurons. Each color indicates OSN expressing one OR targeting a specific glomerulus. Modified from (Luo & Flanagan, 2007).

To explore the distribution of OSN expressing different OR in the MOE, Axel's group (Vassar *et al.*, 1993) performed *in situ* hybridization assay with 11 different ORs cDNA probes to investigate the ORs pattern expression in the rat olfactory epithelium.

Using different OR probes, they found that OSN expressing the same OR are located within a broad but circumscribed area of the epithelium. Within a given area of the epithelium, however, sensory neurons expressing different OR are randomly intermixed.

The OR expression was symmetric for the MOE of the two nostrils.

In the same year, Buck's group (Ressler *et al.*, 1993) ,using a similar experimental approach, found a similar organization of the MOE. Based on the OR

expression, the MOE was subdivided in 4 zones along the dorso-ventral (D-V) axis (Ressler *et al.*, 1993; Vassar *et al.*, 1993).

More recent studies (Miyamichi *et al.*, 2005), using a wider arrays of probes against the OR, identified a higher number of zones in the epithelium. The organization of the MOE in distinct areas along the DV, was however confirmed.

In mouse, OSNs located in the dorsal area of the main olfactory epithelium (MOE) express Class I ORs that consist of ~10% of intact OR genes. In contrast, in the dorsal and ventral area of the MOE are expressed the ORs Class I (Miyamichi *et al.*, 2005; Niimura & Nei, 2007; Bozza *et al.*, 2009)

Axel and Buck, independently demonstrated that, the olfactory epithelium exhibits only a coarse topographic organization (Vassar *et al.*, 1993).

1.3.2 From the main olfactory epithelium to the olfactory bulb

How a random distribution of OSN project to higher brain areas?

To decipher the spatial organization of the axonal projections of OSN to the OB, Axel and colleagues performed *in situ* hybridization with cDNA probes for OR in the olfactory bulb. Surprisingly, they found that probes for a given OR hybridized in specific location of each OB. They conclude that, OSN axons expressing the same OR converge to form glomeruli in specific location on the medial and the lateral side of each olfactory bulb to provide the topographic map (Ressler *et al.*, 1994; Vassar *et al.*, 1994) (Figure 1.21-1.22).

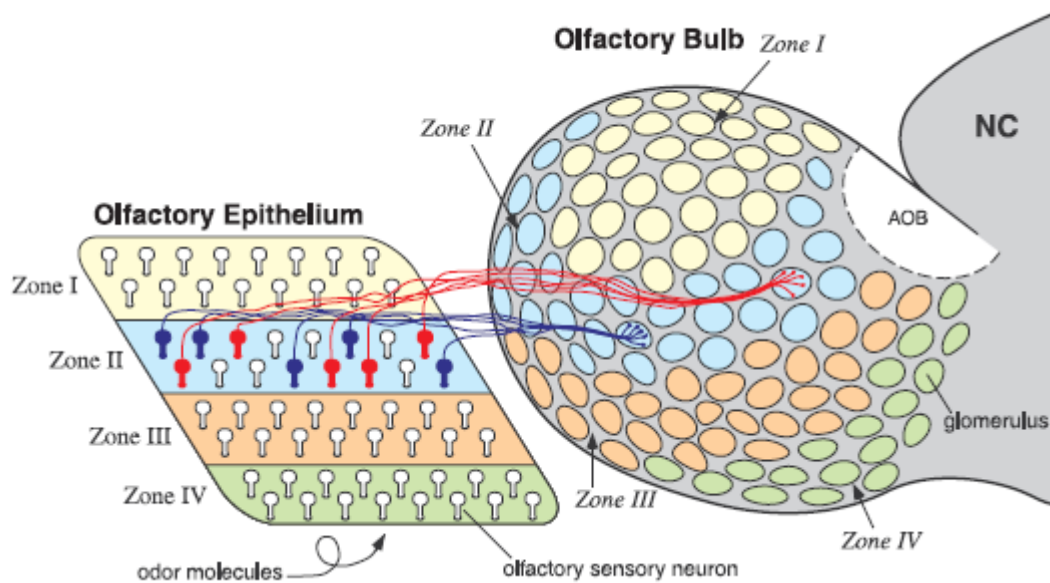


Figure 1.19. A cartoon of the axonal connectivity pattern between the olfactory epithelium (OE) and the olfactory bulb (OB). The olfactory epithelium is divided in four zones (I-IV)(indicated by different colors) are defined by a specific expression of the odorant receptors. OSNs expressing the same OR (blue and red colors) located in a precise and circumscribed zone of the OE project their axons to the corresponding zone in the OB, forming a main homogeneous glomerulus in a specific location in the medial and lateral side. NC=neocortex; AOB=Accessory olfactory bulb; (Mori *et al.*, 1999).

Furthermore, they observed that OSN located in the most ventral part of the MOE tend to project their axon in the most ventral part of the bulb while neurons located in the most dorsal region of the MOE project to the most dorsal area of the OB (Mori *et al.*, 1999; Tsuboi *et al.*, 2006) (**Figure 1.20**).

These observations lead to the conclusion that exists a coarse correspondence between the zones of the MOE and the projections of OSN to distinct areas of the OB, along the dorso-ventral axis.

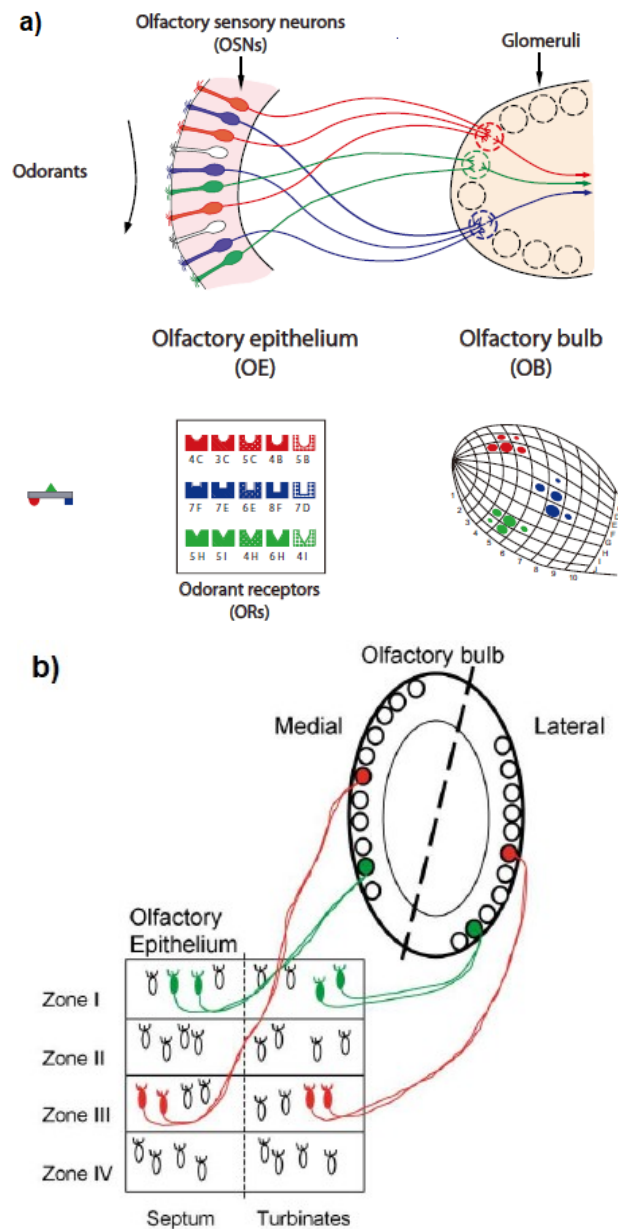


Figure 1.20. Axonal convergence from the epithelium to the olfactory bulb. a) OSN expressing the same OR target a specific homogeneous glomerulus located in the medial and lateral side of each OB (top). Following the combinatorial code each odor can be detected by a multiple combination of ORs and a given OR responds to several odorant molecules (bottom, left). Odors signals are represented by a topographic map of activated glomeruli (bottom, right) (*Sakano, 2010*). **b)** The olfactory epithelium is subdivided in four zones (I-IV) where OSNs expressing the same OR (green and red) converge to form glomeruli in specific loci, on the medial and lateral side of each OB. Dashed lines indicate the separation between the “two mirror symmetric map” in horizontal sections (*Lodovichi et al., 2003*).

1.3.3 Visualizing the olfactory map

In 1996, Mombaerts and coauthors developed an elegant genetic strategy that allowed to visualize individual axons of olfactory sensory neurons expressing a given receptor (*Mombaerts et al., 1996; Mombaerts, 2001; Bozza et al., 2004*).

They obtained genetically modified line of mice (P2-IRES-Tau-LacZ mice) that carry the endogenous P2 odorant receptor gene modified by targeted mutagenesis (**Figure 1.21**). After the transcription termination, P2-OR allele was modified by adding an internal ribosome entry site (IRES). Olfactory sensory neurons transcribed the modified P2-OR together with the tau-LacZ, a fusion of the microtubule-associated protein tau with β -galactosidase. Thus, these populations of OSNs showed a blue color, after the X-gal staining that revealed the β - galactosidase activity allowing the visualization of the axonal projections. Thanks to this genetic strategy, in P2-IRES-tau-LacZ mice, P2-expressing OSNs are easily identified. It was therefore possible to “visualize” the convergence of P2 expressing axons to form glomeruli on the medial and lateral side of each olfactory bulb. In other words, it was possible to “visualize the olfactory map” (*Mombaerts et al., 1996*).

Later, the tau-LacZ reporter gene was replaced with the green fluorescent protein (GFP), that allows to identify the entire OSN, from cilia to axon terminal, and the corresponding glomeruli, *in vivo* (*Gogos et al., 2000*).

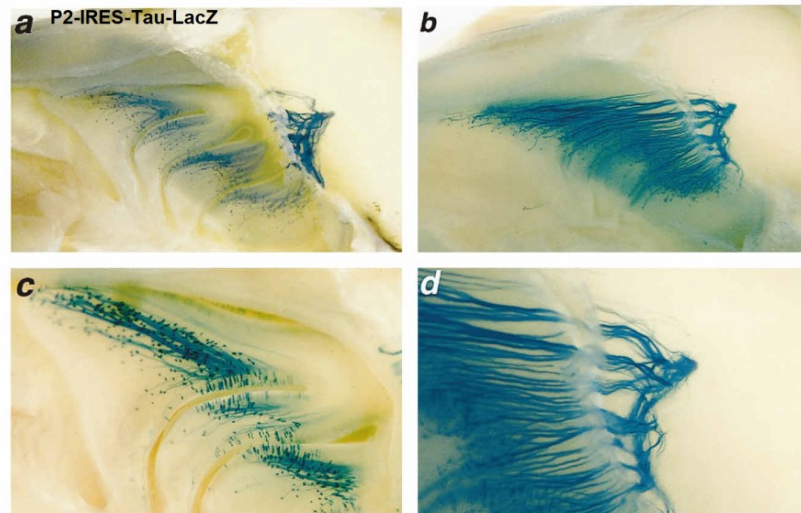


Figure 1.21. Visualizing the sensory map in the olfactory system. a-d) Whole mount view of turbinates in the MOE and medial side of the olfactory bulb in P2-IRES-tau-LacZ mice. X-Gal staining revealed the β -galactosidase activity. P2 expressing fibers located in the antero-posterior side of the epithelium target a P2 glomerulus in the medial part of the bulb. In P2-IRES-tau-LacZ mice, OSNs expressing P2-OR also expressed tau-LacZ are easy to identify thanks for the blue coloration (*Mombaerts et al., 1996*).

The olfactory map in the OB results from the axonal convergence of OSN expressing the same OR to form glomeruli in specific loci on the medial and lateral side of each OB. Each OB, therefore presents two mirror symmetric maps of homologous (i.e. isofunctional) glomeruli. By targeting injection of fluorescent dye to a given glomerulus, it was found that the corresponding projection, related to external tufted cells (ETC), was exactly beyond the homologous glomerulus, on the opposite side of the OB. This connection is reciprocal. This intrabulbar link between homologous glomeruli provides a second level of topography in the OB (*Schoenfeld et al., 1985; Belluscio et al., 2002; Lodovichi et al., 2003*) (**Figure 1.7**).

1.3.4 Functional map

How is an odor represented in the sensory map?

Topographic maps provide the anatomical basis of the functional representation of sensory stimuli.

How are odors represented in the brain?

The first evidences that demonstrate how an odor is represented in the OB was conducted by Leon and colleagues by using the technique of [¹⁴C]-2-deoxyglucose (2-DG) autoradiography in fixed rat OB tissues. This technique was used to visualize the spatial pattern of increased metabolic activity in response to odors, through the uptake of [¹⁴C]-2-DC in glomeruli. The limitation of this approach was the inability to track the real-time changes in a functional sensory representation. However, in 1999 Rubin and Katz (*Rubin & Katz, 1999*) tracked, for the first time, functional odor representation, *in vivo*. Performing optical imaging of intrinsic signals they visualized how odorant are represented in the rat OB. Intrinsic signal imaging are based on the activity-dependent changes in hemoglobin absorption, blood volume, light scattering of OB tissues (*Frostig et al., 1990*). Since active neurons reflect light in a different way from the non-active neurons, the optical properties of the active tissues resulted to be different to the surrounding non-active tissues allowing the visualization of the active pattern of activated glomeruli. These data indicated that the an odor is encoded by a spatial pattern of activated glomeruli. Single spot observed in their experiments were interpreted as be single glomeruli, based on the size and morphology.

Direct evidence that activate spots in functional odor maps correspond to glomeruli was provided by Belluscio and coauthors (*Belluscio et al., 2002*). Optical imaging of intrinsic signal was performed in a genetically modified line of mice expressing a given receptor (i.e. I7) with GFP. In response to the specific cognate-ligand of the I7-OR, the activated spot correspond to the GFP glomerulus. Since GFP labeled exclusively the OSN axon, the I7-GFP glomerulus diameter was slightly smaller

than the spot of activity record with optical imaging of intrinsic signal. The signal in the functional odor map is evoked mostly from the sensory afferents, although the post synaptic cells, mostly the periglomerular cells, provide a contribution to the active spot. This account for the slightly (about 20%) larger spot of the active zone in functional maps in respect to GFP labeled glomeruli.

Uchida and coauthor (*Uchida et al., 2000*) performed optical imaging of intrinsic signal to investigate how the odorant molecules are spatially represented in the olfactory bulb. By recording the intrinsic signal evoked by several distinct classes of organic compounds in the dorsal area of the bulb, they found that odors with a specific functional group activated glomeruli located in specific domains in the bulb. They observed that fatty acids (R-COOH) and aliphatic aldehydes (R-CHO) activated glomeruli in the antero-medial area, although aldehydes with more C-chain and primary alcohols (R-OH) evoked several glomeruli also in the later part of the OB. They, therefore, suggested that the OB exhibits a “chemotopy”, i.e. distinct functional odor groups are represented in specific OB regions.

The functional response to odors was also studied with calcium imaging (*Wachowiak & Cohen, 2001*). In response to odors, the activation of OSN converging in a specific glomerulus was revealed by the fluorescence increase after loading OSN with a calcium dye (*Wachowiak & Cohen, 2001*). In addition, odor evoked responses in OSNs, were revealed with genetic strategy. Namely, Bozza and colleagues designed a gene targeting strategy that leads to the expression of a fluorescent protein, Synapto-pHluorin in OSN axon terminals. Synapto-pHluorin is a pH sensitive protein that reports the synaptic vesicle fusion allowing the investigation of activated neurons (*Bozza et al., 2004*).

1.3.5 Instructive role of the odorant receptor in sensory map formation

The association between the identity of the OR and the glomeruli in the olfactory bulb circuitry suggested that the OR could have an important role in the formation of the sensory map

Evidence that the OR can impact the wiring of OSN in the OB were provided by a series of elegant genetic experiments by Wang and colleagues.

Wang and colleagues (*Wang et al., 1998*) performed several genetic experiments in which they replaced the sequence of P2-OR gene with that of several other ORs in order to observe how the organization of the topographic map could be affected after these substitutions.

These genetic experiments showed that the substitution of a given receptor sequence such as the odorant receptor P2, with another one, such the odorant receptor M71, located in a different zone of epithelium and in distinct chromosomal locus from P2, resulted to form a glomerulus in an ectopic position. The ectopic glomerulus is not located in the original P2-glomerulus position nor M71 but in an intermediate location along the antero-posterior axis, perturbing the sensory map (**Figure 1.22 A, a'-a''**) (**Figure 1.23 a-b**). Thus an altered OR sequence resulted in an mistargeting of sensory neurons that coalesce in a glomerulus located in an ectopic position.

The location of the ectopic glomerulus could be influenced by the homology between the zone of epithelium where OSN expressing the original OR is located, and the swapped OR sequences itself. Moreover, the shift of the swapped glomerulus depends on the chromosomal loci where the original and swapped OR genes are located. These evidence highlight the link between the OR identity and the olfactory bulb region where OSN expressing the swapped OR converge.

Furthermore, Wang and colleagues substitute the P2-OR sequences with another of a closely related-OR expressed in the same zone of the epithelium and same

chromosomal locus, such that P3-OR sequence. The swap of P2 in P3 sequence lead to a formation of a glomerulus closed to the original P3-glomerulus but not located in the same position (**Figure 1.22 B**).

Other substitutions consists of the replacement of P2-OR with other OR sequences present in the same chromosomal locus but expressed in the different zone of the epithelium, such as M50, or in different chromosomal locus such as M12 (**Figure 1.22 A-B**) In all these examples, the swapped OR glomerulus are located in a distant position in respect to the wild-type P2-glomerulus.

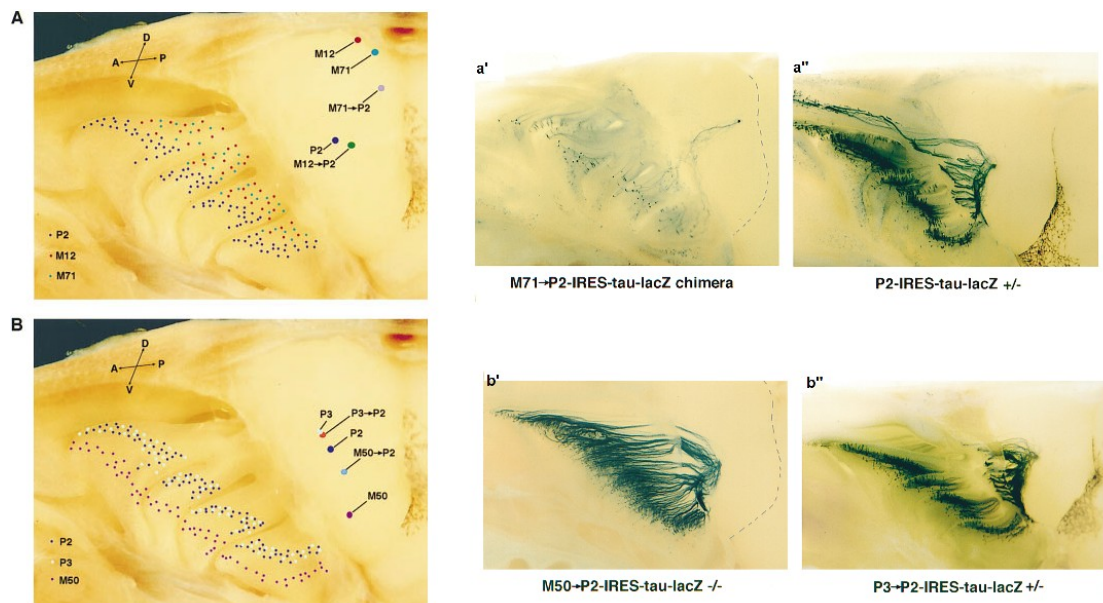


Figure 1.22. Swap of distinct OR in the olfactory bulb. A-B). Different OR expression pattern in the epithelium and schematic representation of the mutations in the sequence of distinct ORs (M71, P2, M12 in A; P2, P3 and M50 in B) and the position of the corresponding glomeruli. A=anterior; P=posterior; D=dorsal; V=ventral. a'-a'': Whole-mount view of the olfactory epithelium and the olfactory bulb in M71-P2-IRES-tau-lacZ chimera (a'-a'') and in P2-IRES-tau-lacZ +/- (a''-a''). β -galactosidase activity was revealed by X-gal staining. Modified from (Wang *et al.*, 1998)

Similar studies were conducted by Feinstein and Mombaerts (*Feinstein & Mombaerts, 2004*). They substituted the sequence of two closely related ORs, such as M71 and M72 and demonstrated the presence of a “core sequence” that is necessary for a proper OSN targeting.

A deletion in the OR sequences of M71 and P2 cause a mistargeting of OSN axons that failed to coalesce in a specific glomerulus but targeted a circumscribed area near the wild type glomerular position (*Feinstein et al., 2004; Feinstein & Mombaerts, 2004*) (**Figure 1.23C**).

Other experiments show that substitution of the β -adrenergic receptor (β_2 AR) with the M71-OR sequence determines the formation of distinct glomeruli shifted along the anterior and ventral axis compared to the position of wild type M71 homogeneous glomerulus (*Feinstein et al., 2004*). This shift was due to the absence of specific OR. On the contrary, the replacement of the OR sequences with another G-protein receptor, such as the vomeronasal receptor V1R (i.e. V1rb2), perturbed the axonal convergence to form a specific glomerulus. Thus, β_2 AR are coupled to the G-protein G_s while V1rb2 cannot.

All this data showed that alterations in the sequence encoding the OR lead to an abnormal and altered convergence of olfactory sensory axons that form glomeruli located in an ectopic position in the olfactory bulb in respect to controls.

These experiments demonstrate that the OR plays an instructive role in the axon convergence to form glomeruli in specific location in the OB.

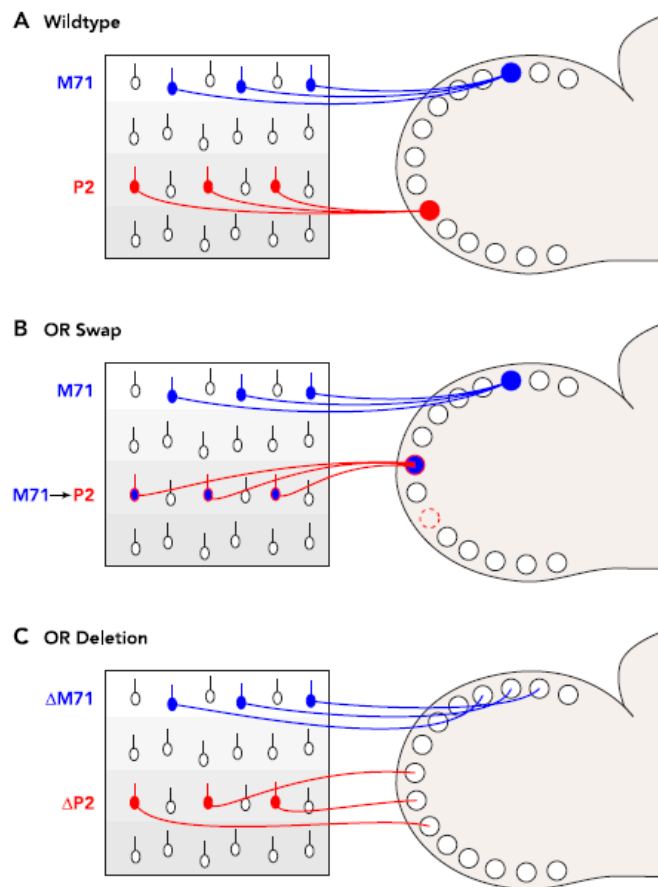


Figure 1.23. Examples of OR swap experiments demonstrate the instructive role of the OR in the sensory map formation. Different substitutions of the coding sequence of ORs. Rectangles on the left represent the epithelium where axons of OSN project to the OB, represented on the right. M71 wild-type expressing fibers and the corresponding M71 glomerulus are shown in blue color in A, B, while in red are indicated the swapped OR fibers that target an ectopic glomeruli in b (colored in blue with the border in red) or do not coalesce in a specific glomerulus as is shown in c after the deletion of M71 or P2 genes. **A)** M71-expressing fibers target a homogeneous glomerulus in the bulb. **B)** Substitution of P2 sequences with M71 lead to the formation of an ectopic glomerulus, located in a region closed to the original and swapped OR. **C)** Deletion of the OR sequences of M71 or P2, failed to converge in a specific glomerulus but target a circumscribed region closed to the endogenous OR (Lodovichi & Belluscio, 2012).

1.3.6 The odorant receptor is also expressed at the axon terminal of OSN

In the discussion of their work Wang and colleagues (1998) suggested that the instructive role of the OR in the formation of the sensory map confers to the OR the role of an axon guidance molecule. They further speculated that in order to direct the targeting and the convergence of sensory axons, the OR should be expressed at the axon terminal (*Wang et al., 1998*).

This hypothesis was confirmed in 2004 again in the Axel group, by Barnea (*Barnea et al., 2004*) and concomitantly in a different laboratory, by Strotmann (*Strotmann et al., 2004*). They both found that the OR is not only expressed at the cilia level of OSN playing a role in the odors transduction but also in the most distal part of the axon: the axon terminal-growth-cone.

Furthermore, Barnea reported that the proximal axon and the soma of OSN do not express the OR (*Barnea et al., 2004*).

In 2009, Dubacq and colleagues using RT-qPCR assay together with an approach that divides the polysome-associated mRNA from untranslated mRNA, demonstrated that mRNA encoding OR is present at the axon terminal of OSN. This evidence suggested that the mRNA of the OR is locally translated in this location (*Dubacq et al., 2009*).

The expression (*Barnea et al., 2004; Strotmann et al., 2004*) and the local translation (*Dubacq et al., 2009*) of the OR at the axon terminal of olfactory sensory neurons strongly suggested that the axonal OR could act as an axon guidance molecules. However, the mechanism of activation and the function of the OR expressed at the axon terminal remained unknown.

Several evidence indicate that mRNA translation for molecules involved in axon guidance takes place locally at the axon terminal, that acts as an autonomous compartment. This allows to the axon terminal to promptly respond to axon guidance cues present in the environment (*Campbell & Holt, 2001; Lin & Holt, 2008*).

1.3.7 The growth cone

In the central nervous system the formation of neural circuits depends on the target recognition and sequentially to the correct pathfinding by the growing axons, named growth cone (*Huber et al., 2003*).

The growth cone is the neuron axon leading edge that undergoes to the process of growing toward the target cells. Extracellular cues guide the growing axons to reach their target (*Chilton & Hewetson, 2005*).

The growth cone is formed by two different regions (*Cioni et al., 2018*) (**Figure 1.24**):

1. P-region (Peripheral region) is formed by lamellopodia, a dense actin network located between filopodia, that is also associated with microtubules which transiently enter in the growth cone. Filopodia are the growth cone's fine extensions that contain bundles of F-actin filaments. They are bound to the membrane that contains receptors and cell adhesion molecules important for the axon growth and guidance process. Granule cells extends its filaments of actin in these structures (Filopodia and Lamellipodia) that allow the axon growth and pathfinding toward the target cells (*Huber et al., 2003*).

2. C-region (Central region) characterized by microtubules, also extended into the P-region, vesicles and organelles that guide the trafficking and the elongation of the neurite.

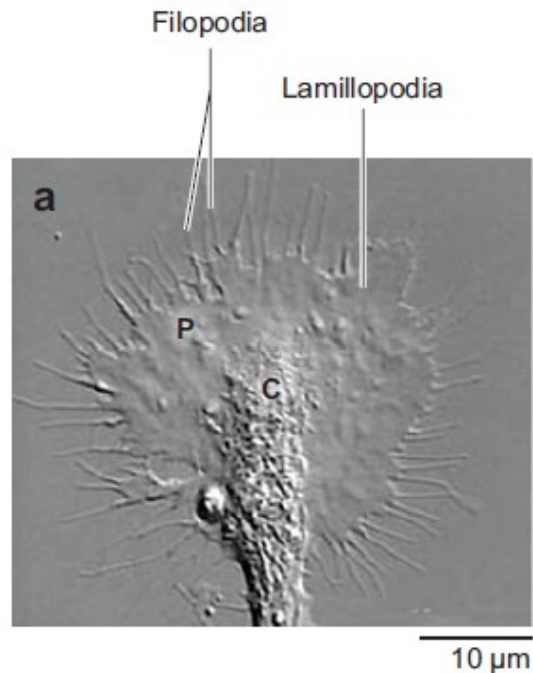


Figure 1.24. The growth cone morphology. Xenopus growth cone contrast image that show its regions: P=peripheral; C=Central. Lamellopodia and filopodia are shown. Scale bar=10 μ m (Zheng & Poo, 2007).

The growth cone as an semi-autonomous compartment of neurons

The GC represents an unique semi-autonomous compartment, including a complex molecular machineries able to local translate mRNA of protein that guide and direct the axon to the proper target. All growth cone machineries components are required to respond to extracellular cues (stimuli) and are necessary to chemotropic response of the growth cone (Cioni *et al.*, 2018). Since the growth cone is located from millimeters to centimeters from the soma of the cells, the mechanism involved in its movement towards the target are made autonomously from the soma (Lin & Holt, 2008). Several evidences suggested that the mRNA translation plays a key role in the axon guidance. The synthesis of protein that occurs locally is involved in several mechanisms that orchestrate chemotropic responses of the growth cone to the extracellular stimuli and allow the navigation toward the target (Shigeoka *et al.*, 2013). The growth cone motility is due to it continuous build-up through the extension of the plasma membrane and the actin-filaments, that continuously

polymerize and depolymerize within filopodia and lamellopodia. Actin polymerization of filopodia and lamellopodia is regulated by the RhoGTPase family, that drive the continuous changes in the cytoskeleton architecture. The RhoGTPase pathway components regulate cytoskeletal proteins and influence the direction of the growth cone extension (*Dontchev & Letourneau, 2002*).

Growth cones are characterized by high motility, which allows them to respond to the environment cues in an extremely dynamic process characterized by rapid changes in the direction and branching of the growth cone (*Huber et al., 2003; Chilton & Hewetson, 2005*).

Axon guidance molecules: attractive or repulsive

The neuronal environment changes constantly and is formed by cues (i.e. axon guidance molecules) dissolved in the extracellular matrix (soluble or substrate-bound molecules) that can be divided in attractive and repulsive axon guidance molecules, depending on the intracellular pathways they trigger. The attractive and repulsive axon guidance molecules belong to different families: netrins, semaphorins, ephrins and slits families (*Cioni et al., 2018*).

Campbel and colleagues, for the first time, showed that isolated axons are responsive to the axon guidance molecules Netrin-1 and Sema3A (*Campbell & Holt, 2001*). Indeed, this chemotropic response was blocked by inhibitors of the protein synthesis and is not necessary for the extension of the axon suggesting that it is required for the turning behavior of the axon. Thus, the local translocation play a specific role in the chemotropic response to extracellular cues (Campbell & Holt, 2001). Attractive molecules such as nerve growth factor (NGF) and Netrin-1 are involved in the cytoskeletal protein synthesis (*Leung et al., 2006*). Repulsive molecules such as Sema3A induces the local translation of a member of GTPase family, named RhoA, known to be involved in the neurite retraction, while slit-2 induces the translocation of an actin depolarizing protein, named cofilin (*Lin & Holt, 2008*).

Role of cAMP and Ca²⁺ in turning behaviour of the growth cone

Axon guidance signals steer the growth cone direction.

It is known that the two second messenger cAMP and Ca²⁺ play a critical role in axon elongation and turning behaviour in several systems (*Song et al., 1997; Nishiyama et al., 2003; Henley & Poo, 2004*) including the olfactory system (*Imai et al., 2006*).

It is reported that alteration in cAMP levels influence the growth cone motility and neurite outgrowth (*Rydel & Greene, 1988*).

In 1992, Poo's group (*Lohof et al., 1992*) developed a new strategy to study axon behaviour *in vitro*.

Briefly, the response of isolated growth cones to microscopic gradients of molecules created by repetitive pulsatile ejections, was recorded by time-lapse imaging. They observed that cAMP was involved in the turning behaviour process and mediates the extracellular cues acting as a second messenger (*Lohof et al., 1992*) suggesting a cAMP -dependent turning behaviour. Later, other studies, used this approach to applied microscopic gradients of several different molecules able to modulate the axon turning behaviour such as acetylcholine, BDNF and Forskolin (*Song et al., 1997*). Differences in the cAMP activity may result in opposite turning behaviour of the growth cone in response to the same axon guidance cue (*Song et al., 1997*).

Ca²⁺ plays also an important role in the elongation of the axon, that depends on several factors including the spatio-temporal dynamics of Ca²⁺, Ca²⁺ effectors (CaMKs and MAPKs) and Ca²⁺ channel activity. After the entrance into the cytosol Ca²⁺ interacts with different Ca²⁺-binding proteins and with effectors involved in the cytoskeletal rearrangement. Thus, Ca²⁺ mediates the organization and movement of F-actin filaments of the growth cone (*Woo & Gomez, 2006*).

Ca²⁺ signals generated spontaneously or induced by chemical molecules/cues act on the calcium effectors (CaMKs and MAPKs) that play a role in the regulation of the branching and axon growth. A calcium rise activates several target proteins such as

Ca^{2+} binding protein Calmodulin (CaM), that is expressed in the filopodia and binds Ca^{2+} at low concentration. It is reported that Ca^{2+} - CaM binding persists for about 1 minute in the neurons after an electrical activity (Henley & Poo, 2004). Calcium-calmodulin complex (Ca^{2+} - CaM) triggers different signalling cascades interacting with several targets such as kinases and phosphodiesterase. In particular this interaction leads to the activation of Ca^{2+} /calmodulin dependent kinase (CaMK). Among this family, CaMKII plays a role in the neural development and plasticity and most importantly in the growth cone and branching.

Signaling transduction cascade coupled to the odorant receptor at the axon terminal of olfactory sensory neurons

It is well established that cAMP and Ca^{2+} are the second messengers coupled to the activation of the OR at the cilia of OSNs. However, whether the OR expressed at the axon terminal is functional and, if yes, the signaling pathway coupled to the odorant receptor expressed at the axon terminal (growth-cone) has remained elusive for many years.

In 2009, Lodovichi and colleagues (Maritan *et al.*, 2009) demonstrated for the first time that the OR at the axon terminal is functional and coupled to local increases of cAMP and Ca^{2+} (**Figure 1.25; Figure 1.26**).

Single OSN were transfected with a sensor for cAMP (Epac-1) or loaded with a Ca^{2+} indicator Fura-2. Then, local application of a puff of an odor mix at the growth-cone of OSN produced an increase of both cAMP and Ca^{2+} only at the axon terminal but not at soma nor at dendrite level (**Figure 1.26 a-e**). The Ca^{2+} experiments were performed in presence of tetrodotoxin (TTX) to avoid the action potential contribution to the measured calcium signal. Furthermore, they demonstrated that the Ca^{2+} rise observed locally at the axon terminal of OSN is due to CNG channel activation (**Figure 1.26 f**). By studying the spatio-temporal dynamics of cAMP and Ca^{2+} on isolated OSN, Maritan and colleagues (Maritan *et al.*, 2009), demonstrated that the OR expressed at the axon terminal is capable of

eliciting a prompt cAMP and Ca²⁺ rise, in response to odor stimuli locally applied with a glass pipette.

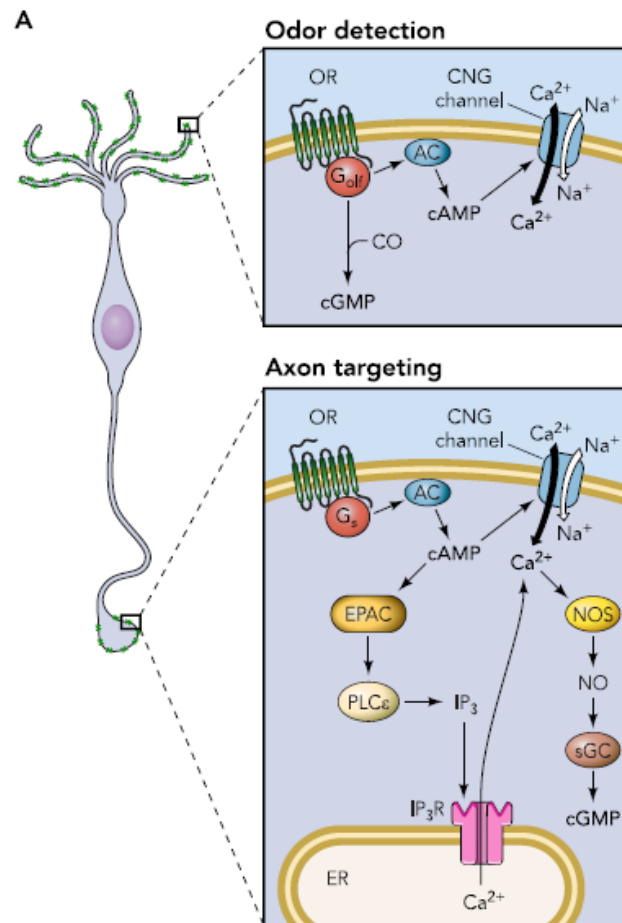


Figure 1.25. Odorant receptor signaling pathway at the cilia and at the axon terminal of OSNs. A schematic representation of a single neuron (OSN) on the left. Rectangles represent the cilia (up) and the axon terminal (bottom) of OSN. Signaling pathway coupled to OR at the cilia level (up) (Odor detection) and at the axon terminal (bottom) (Axon targeting). AC=adenylyl cyclase; CNG channel=cyclic nucleotide-gated channel; CO=carbon monoxide; EPAC=exchange protein directly activated by cAMP; G_{olf}=olfaction-specific G-protein; NO=nitric oxide; NOS= nitric oxide synthase; PLC=phospholipaseC PKA= protein kinase A; sGC= soluble guanylyl cyclase; (*Lodovichi & Belluscio, 2012*).

By blocking CNG channel with $MgCl_2$, or by the inhibition of cAMP production with an AC blocker (SQ22536) (tetrahydrofuryl-adenine, they observed that Ca^{2+} influx through CNG was abolished (**Figure 1.26 f**), clearly indicating that the Ca^{2+} influx was due to cAMP activation of CNG channels (*Maritan et al., 2009*).

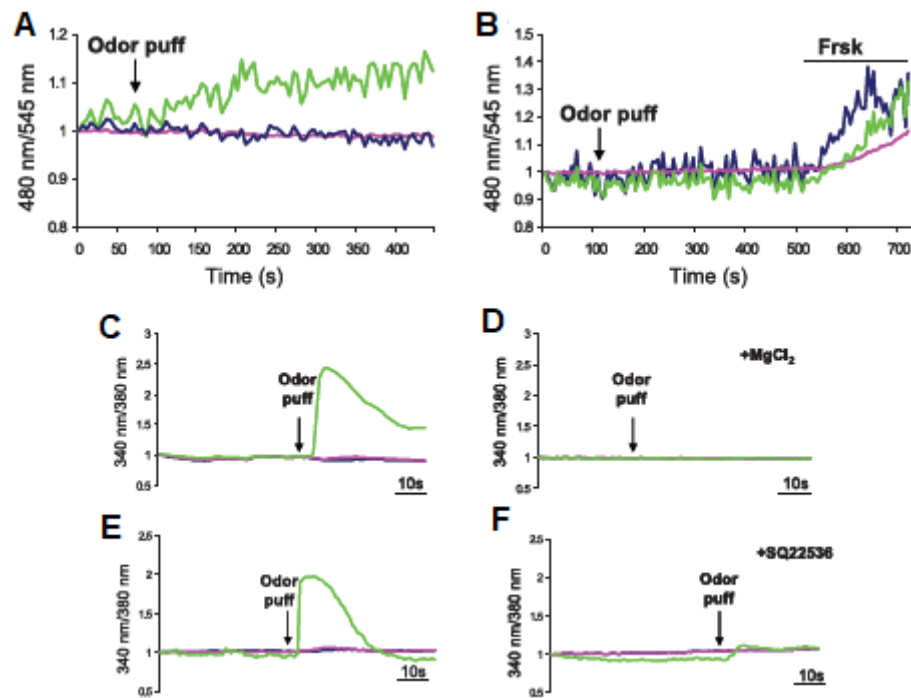


Figure 1.26. Dynamic of cAMP and Ca^{2+} in single olfactory sensory neuron (OSN). A-B) cAMP dynamics in OSN in response to odor mix locally applied at the axon terminal. Normalized fluorescent ratio changes (480nm/545nm). OSN in response to an odor mix (200uM) (A) and to forskolin (Frsk), a generic activator of AC, locally applied at the axon terminal (green) with a glass pipette. C-F) Ca^{2+} dynamics in OSN loaded with fura-2 and focally challenged with odors and different blockers. Normalized fluorescent ratio changes (340nm/380nm). Single OSN shown in c) and e) was re-challenged locally at the axon terminal with an odor mix + CNG channel blocker $MgCl_2$ (10 mM) in D) or AC blocker, SQ22536 (30uM) in f). Modified from (*Maritan et al., 2009*).

To ascertain whether the axonal OR-signaling pathway could act not only locally, at the axon terminal, but also at the nuclear level, likely modulating gene expression Maritan and coauthors transfected OSN with a genetically encoded sensor for cAMP, based on PKA (Zaccolo *et al.*, 2000) and they followed the PKA sensor catalytic subunits upon the axonal OR activation. They found that the selective odor activation of the axonal OR was followed by the nuclear translocation of the catalytic subunits of PKA. At nuclear level, PKA could modulate the expression of molecules involved in axon targeting via cAMP responsive element-binding protein (CREB) phosphorylation.

All these data, demonstrated that the odorant receptor expressed at the axon terminal of olfactory sensory neuron is functional and coupled to a local increase of cAMP and Ca^{2+} . Furthermore, they found that the axonal OR-derived cAMP can exert its action locally but also at the nuclear level, where it can modulate gene expression.

To verify that the pathway coupled to the axonal OR and its functional properties observed *in vitro* are reflected *in vivo*, Maritan and colleagues performed Ca^{2+} experiments in mouse hemi-head preparation, in which the connections from the epithelium, the OB and the brain were maintained. Forskolin, a generic activator of adenylyl cyclase (AC), used as a control, and odors were applied with a glass pipette to the hemi-head preparation. A prompt Ca^{2+} rise was observed in the presynaptic terminal in correspondence of specific glomeruli in the olfactory bulb, the calcium rise was abolished with the application of the AC blocker SQ22536 suggesting that this response was due cAMP-induced CNG channel.

The odorants binding leads not only an increase of cAMP and Ca^{2+} but also of another second messenger, cyclic GMP (cGMP) (Zufall & Munger, 2010)(Munger *et al.*, 2009).

In OSNs cGMP exhibits a slow kinetics, that suggests that cGMP is involved in long-term cellular responses rather than in the initial odor stimulus detection event (*Leinders-Zufall et al., 2007*). The mechanism underpinning the cGMP synthesis, regulation and its interaction with cAMP were poorly understood (**Figure 1.27**).

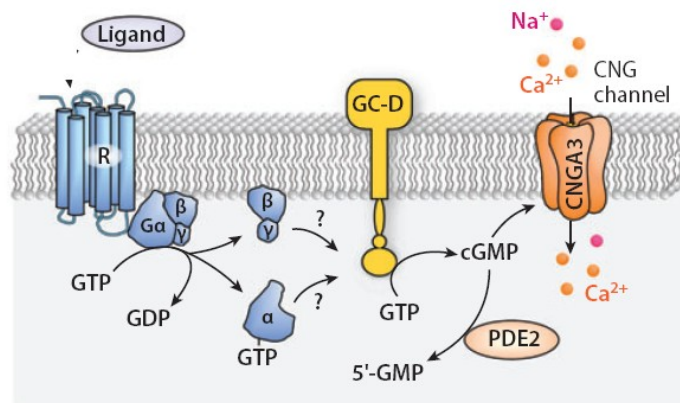


Figure 1.27. Signal transduction propose in GC-D⁺ neurons. The pathway show an unknown GPCR that could modulate the activity of GC-D. GC-D=guanylyl cyclase type D. CNGA3 channel= cyclic nucleotide-gated channel type A3; Gα,-β,-γ, unknown G protein α, β, and γ subunits; PDE2=phosphodiesterase type 2 (*Munger et al., 2009*).

In 2011, Pietrobon and coauthors investigated the mechanism underpinning the dynamics of cGMP in OSNs. They reported that the odor-induced increase of cGMP was due to activation of soluble guanylyl cyclase by nitric oxide (NO) and required cAMP. The link between cAMP and NO synthase appeared to be an increased in cytosolic Ca²⁺ concentration due to plasma membrane Ca²⁺ channel activity and release of Ca²⁺ from stores (*Pietrobon et al., 2011*).

All these data showed a strict interplay between the increase of cAMP, the intercellular Ca²⁺ and the synthesis of cGMP in OR signaling pathway.

Ectopic expression of the odorant receptor in non-olfactory tissues

The expression of mammals ORs, originally identified in rat olfactory epithelium (Buck and Axel 1991), is not limited to the olfactory system (*Feldmesser et al., 2006*). Several studies provided evidences of the expression of the odorant receptors in non-olfactory peripheral tissues such as blood, gut, colon, lung, kidney liver, skin, prostate, placenta, muscle and testis (*Mombaerts et al., 1999*)(*Spehr et al., 2003; Spehr et al., 2006*)

Kang and colleagues in 2015 used the olfactory marker protein (OMP) as a marker for OR-mediated chemoreception in non-olfactory systems (*Kang et al., 2015*).

Noteworthy, in testis the odorant receptor acts as a chemosensing receptors in the sperm-oocyte chemotaxis and sperm motility (*Vanderhaeghen et al., 1993; Milardi et al., 2017*) driven the spermatids to reach their target (oocyte). The odorant receptor, namely OR23, is expressed also in regenerating myocytes In regenerating myocytes the OR play a key role in migration and adhesion of muscle fibers. The OR expression in testis and in myocytes pointed out the chemotactic function of the OR in other tissues than the OS.

1.4 The development of the sensory map

How does the topographic map develop in the olfactory system?

In the sensory map, each glomerulus defines a functional unit that processes sensory information related to a given odorant receptor (one glomerulus-one receptor). The development of the sensory map results from the complex interplay between axon guidance molecules expressed in a specific spatio-temporal pattern and neuronal electrical activity.

A hallmark of a mature glomerulus is that is innervated exclusively by fibers of OSN expressing the same OR, indicated as homogeneous glomerulus. The development of a glomerulus in the mature form (homogeneous glomerulus) is a process that include different phases: 1.Regional targeting; 2.Glomerular formation; 3.Axonal refinement (*Royal & Key, 1999; Lodovichi & Belluscio, 2012*) (**Figure 1.28**).

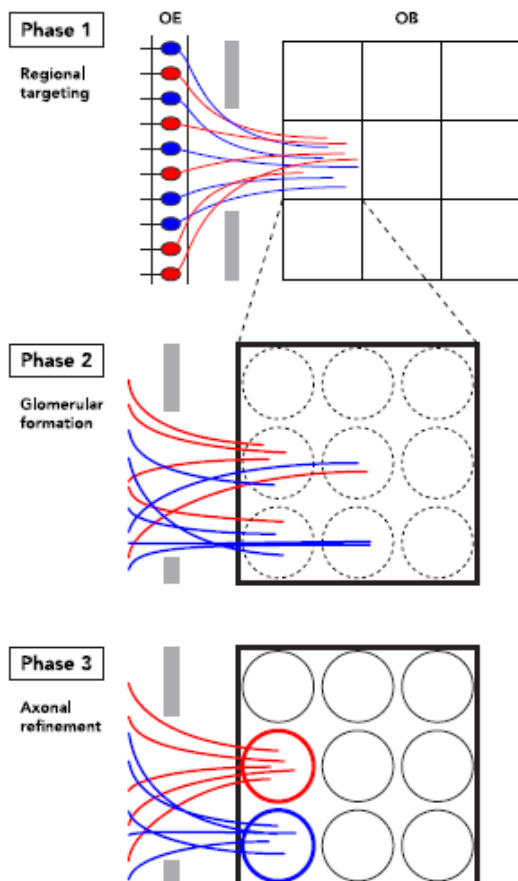


Figure 1.28. Developmental phases of the sensory map. Schematic representation of a model that includes three phases of the development of the sensory map. Regional targeting. Molecules triggers the OSN axons to a defined area of the bulb. Glomerular formation. The axonal OR acts as an axon guidance molecules playing a key role in the glomerular choice to coalesce in a specific glomerulus. Axonal refinement. OR-mediated signalling pathway together with the spontaneous activity triggers the OSN fibers to the refinement. OB=olfactory bulb; OE=olfactory epithelium (*Lodovichi & Belluscio, 2012*).

Initially, the targeting process of OSN expressing the same OR is characterized by axons that project to a circumscribed area of the bulb. Molecules/cues rather than the identity of the OR triggers the targeting of OSN axons. (Regional targeting). After the first phase, OSN fibers reorganize themselves to coalesce into specific glomeruli thanks to the role of the axonal OR as an axon guidance molecules (Glomerular formation). Finally, after the glomerular coalescence, the OSN fibers are directed by both spontaneous activity and OR-mediated signalling to glomerular refinement. During the final refinement process, thanks to the involvement of different homophilic adhesive molecules, a glomerulus reach the mature form (i.e. homogeneous glomerulus) in a specific location both in the medial and lateral side of each OB (*Lodovichi & Belluscio, 2012*) (**Figure 1.28**).

In the early stages of development, olfactory sensory neurons expressing the same OR project to a restrict area of the olfactory bulb where they target multiple glomeruli, that result formed by fibers expressing different OR (heterogeneous glomeruli). The subsequent refinement process, leads to the formation of homogeneous glomeruli.

Development of glomeruli

Development of glomeruli is not a uniform process. Glomeruli exhibit different time of maturation according to the OR they expressed. Some glomeruli complete their maturation at birth (such as P2 glomeruli), other acquire the mature organization at later stages of the postnatal life (such as M72).

P2-glomerulus development.

In embryonic stages (day 15.5, E15.5) olfactory sensory neurons expressing the P2 receptor project their axons to a confined area in the olfactory bulb. At this age, the P2 proto-glomeruli are formed by a mixed subpopulation of axons, expressing different OR. At E17.5, P2-axons begin to cluster and target a specific region in the glomerular layer, while at E18.5, the P2 fibers form two to three

rudimental glomeruli interconnected by axon bundles. By postnatal day 0.5 (PD 0.5) P2-glomeruli show the typical spherical morphology, although they could be still linked to each other by a bundle of axons. This connection is lost by PD 7.5, resulting in mature homogeneous glomeruli (*Royal & Key, 1999; Valle-Leija, 2015*).

The transgenic mice P2-IRES-tau-LacZ allow to visualize P2-expressing axons from the epithelium to the OB where they coalesce to form P2-homogeneous glomeruli in specific location of the OB (**Figure 1.21**).

M72-glomerulus development

M71 and M72 glomeruli are both located in the dorsal side of the OB but their development has a different timing. M71 glomeruli undergo a prolonged maturation than M72. Indeed, M71 and M72 present 96% homology of sequence. Initially, M71-expressing fibers can also innervate M72-glomeruli. The average number of M71 glomeruli per half-bulb did not reach the mature level until PD60. In contrast, the average number of M72 glomeruli per half-bulb rapidly decreased by PD20 (*Zou et al., 2004*).

At postnatal day 0 (PD 0), M72 expressing axons reach the posterior-dorsal areas in each bulb and are widely scattered. At this stage M71 and M72 glomeruli are not still visible. By PD10 M72 expressing axons coalesce to form multiple glomeruli, expressing different OR from M72. Between PD10 and PD40 a progressive removal of additional glomeruli is achieved.

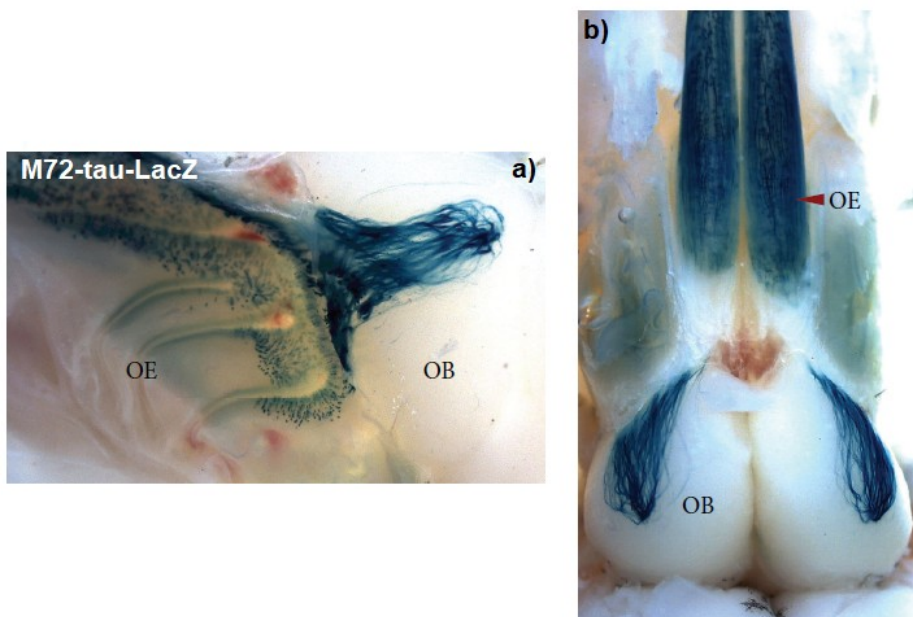


Figure 1.29. M72 expressing fibers and M72 glomeruli in M72-tau-LacZ. a-b). Beta galactosidase activity revealed by X-gal staining in the olfactory epithelium (OE) and in the olfactory bulb (OB) in M72-tau-lacZ mouse. a) M72 expressing fibers located in the dorso-posterior side of the epithelium target a M72 glomerulus in the dorsal part of the bulb (*Valle-Leija, 2015*).

Different olfactory stimuli can influence the formation and the plasticity of the glomerular map. An example is the chronic exposure to acetophenone (M72 cognate ligand) that influenced the formation of several number of additional M72 glomeruli in M72t-LacZ mice (*Valle-Leija, 2015*)(**Figure 1.30**).

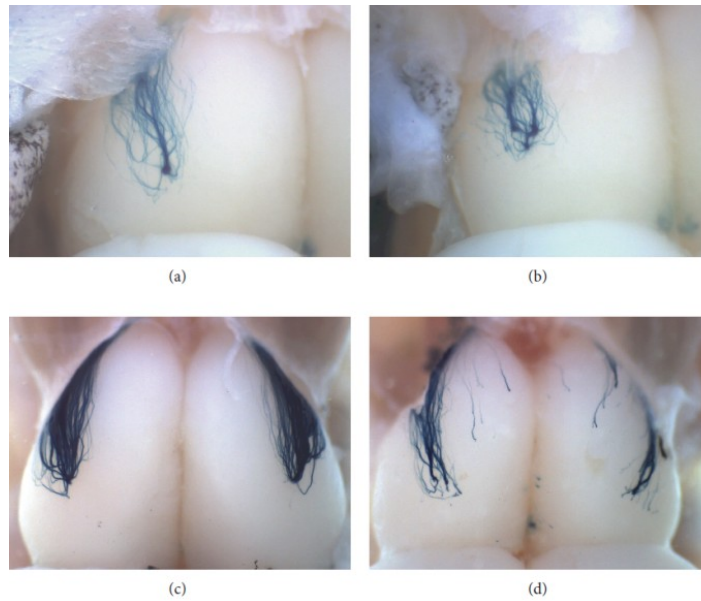


Figure 1.30. Specific olfactory stimuli influenced the formation of M72-glomeruli and the plasticity of the glomerular map. X-Gal staining. a) At PD20 formation only of a lateral M72 glomeruli (here the lateral M72 glomerulus is shown) in M72tLacZ mouse. **b-d)** Effects of the exposure to acetophenone in M72tLacZ mouse. **b)** At PD20 formation of several additional M72-glomeruli after 20 days of acetophenone exposure. **c)** Chronic exposure to acetophenone (methimazole treatment for 45 days) lead to a regeneration of the medial M72-glomeruli in M72tLacZ mouse. **d)** Mistargeting of M72-expressing fibers that do not converge in a specific glomerulus after 35 days of methimazole treatment (*Valle-Leija, 2015*).

1.4.1 Axon guidance molecules in the formation of the sensory map

Although the axonal OR plays an instructive role in the sensory map formation, it is not the only determinant. Several other molecules contribute to the proper location of glomeruli along the dorso-ventral (D/V), antero-posterior (A/P) and medio-lateral axis of the olfactory bulb.

Olfactory sensory neuron axon projections along the dorso-ventral (D-V) axis

Several studies suggested the tight correspondence between different zones of the epithelium and corresponding domains in the olfactory bulb, along the D-V axis (*Ressler et al., 1994; Miyamichi et al., 2005; Tsuboi et al., 2006*).

Two set of repulsive receptors/ligands, Robo 2/ Slit-1 and Neuropilin-2 (Nrp2)-/semaphorins3F (Sema3F) direct the OSN axonal convergence along the dorso-ventral axis of the olfactory bulb (*Cloutier et al., 2002; Cloutier et al., 2004*). Robo 2 is expressed in OSNs located in the dorsal zone (D-zone) of the epithelium and is influenced by the repulsive effects of its chemorepellents ligands, Slit-1 and Slit-3 expressed in the ventral zone (V-zone) (*Sakano, 2010*). In mutant mice for Robo-2 is observed a mistargeting of a subpopulation of axons in the ventral side of the bulb, normally projecting in the dorsal region. Indeed, a deletion of slit-1 determines similar defects observed in Robo-2 mutant mice.

In addition, loss of function and gain of function experiments demonstrate the role of Neuropilin-2 (Nrp-2) as an axon guidance molecules that guide the axonal convergence along the dorso-ventral axis of the olfactory bulb (*Takeuchi et al., 2010*).

The axon guidance molecules Neuropilin-2 (Nrp-2) and its repulsive ligand semaphorins 3F (Sema3F) are expressed in a complementary manner in OSNs. Sema3F is expressed in the dorsal -zone of the epithelium and secreted by-arrival OSN axons in the antero-dorsal domain in the bulb to repel the Nrp-2 positive axons that arrive, during development (*Takeuchi et al., 2010*). Sequential axonal

targeting of OSN occurs along the dorsomedial (DM)/ventrolateral (VL) axis. This process could maintain the topography of the map during development of axonal projections (**Figure 1.31**)

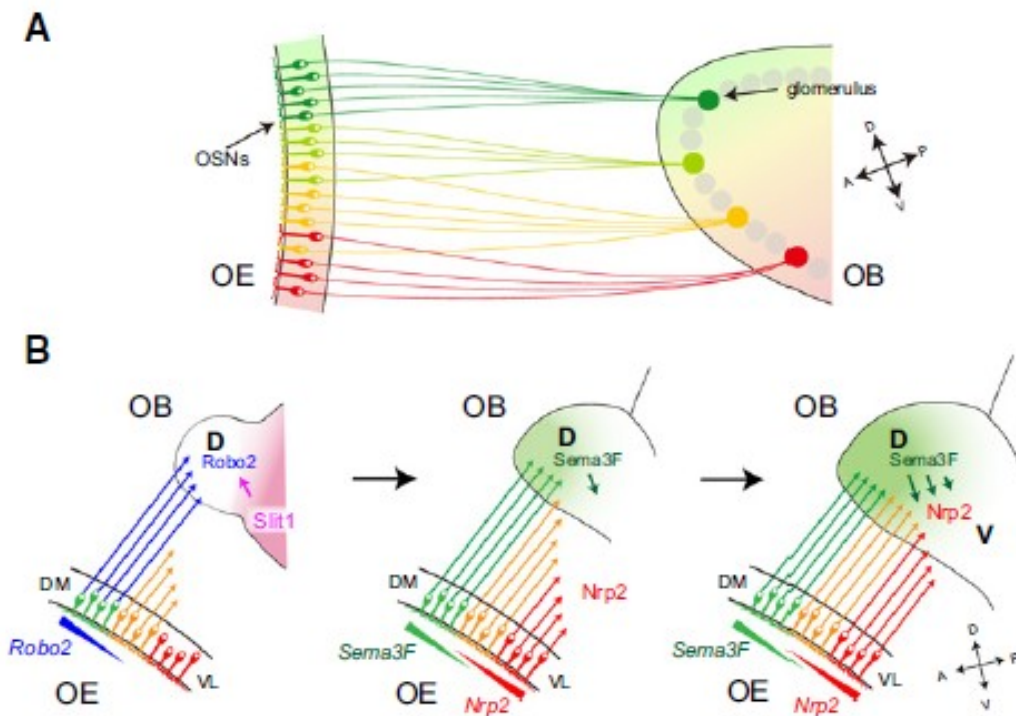


Figure 1.31. Axon guidance molecules along the dorso-ventral (D/V) axis. a) Schematic representation of the olfactory epithelium (OE) where axons of OSN project in specific location in the olfactory bulb (OB). **b)** Model of OSN axons projection along the dorsal-ventral axis of the OB. Involvement of the axon guidance molecules such as Robo2, that mature in the early stages (on the left). OSNs expressing Robo2 project axons in the corresponding dorsal region (D-zone) in the OB. Robo2 ligand named Slit-1, and Robo2 itself create repulsive interactions that guide the OSN projection in early development. Sema3F expressed in the antero-dorsal part of the OB and secreted by D-zone prevents the invading projections of Nrp-2 positive axons in this zone during the late development. In the three images is reported that the sequentially OSN axons projections along the dorsomedial (DM)-ventrolateral (VL) axis of the bulb. (DM=dorsomedial; VL=ventrolateral; D=dorsal; V=ventral; A=anterior;P=posterior)(Sakano, 2010).

Olfactory sensory neuron axon projections along the antero-posterior (A-P) axis

The location of glomeruli along the antero-posterior axis is regulated by the expression of axon guidance molecules such as ephrins family (Ephrin A3 and Ephrin A5) and their receptors Eph (Cutforth *et al.*, 2003). Eph receptors belong to the family of tyrosine kinase receptors that bind their ligands named ephrins, associated to the membrane. The over-expression or deletion of Ephrin A3 and A5 determine a shift in the glomerular formation along the antero-posterior axis (A/P) demonstrating their involvement in the axon targeting. In details, deletion of EphrinA5, Ephrin A3 caused a significant shift of glomeruli location toward the posterior side of the OB, in respect to the original locations. On the contrary, overexpression of Ephrin A5 and A3 caused an anterior shift of the same glomeruli (Cutforth *et al.*, 2003).

Moreover, the secreted chemorepellent semaphorin 3A (Sema3A) and its receptors neuropilin-1 (Nrp1) direct the axon convergence along the A/P axis of the bulb (Cloutier *et al.*, 2004; Imai *et al.*, 2006; Imai *et al.*, 2009). This evidence was demonstrated by investigating the sensory map formation in Sema3A mutant mice. This line of mice exhibit a mistargeting and small disrupted glomeruli together with the shift in glomerular position along the antero-medial and ventral region of the bulb (A/P axis). Sema 3A is expressed in the nerve layer, where OSN axons reach the OB, and in the mitral cells, while Sema3A receptor, Nrp1, is expressed in gradient in the OB and in OSNs (Assens *et al.*, 2016). Nrp-1 expressing fibers segregate to the medial or lateral side of the bulb, according to the target position along the A/P axis. Indeed, Nrp-1 and Sema3A are expressed in a complementary manner in OSNs, such that Nrp1^{LOW}-Sema3A^{HIGH} direct the sorting of axons to the center of axon bundles while Nrp1^{HIGH}-Sema3A^{LOW} to its outer-lateral part.

In contrast to the OSN axon projection along the dorso-ventral axis, the glomerular location along the antero-posterior axis of the bulb seems to be independent to the epithelium zones but dependent to identity of the OR (Mombaerts *et al.*, 1996; Wang *et al.*, 1998; Feinstein *et al.*, 2004).

Imai and colleagues demonstrated the OR-derived cAMP signals direct the target destination of OSN along the antero-posterior axis in the OB (*Imai et al., 2006*).

They performed a target genetic modification of the DRY motif the OR, that hampers the coupling between G-protein and the OR itself. As a consequence of this manipulation the OSN do not synthesized cAMP and are unable to project to the proper glomeruli in the OB (*Imai et al., 2006; Chesler et al., 2007*). According to Sakano and colleagues, each OSN produces distinct level of cAMP, that in turn stimulates the production of specific levels of cAMP, that modulates the level of Neuropilin 1 expression (*Sakano, 2010*). This hypothesis seemed unlikely, since it contemplates more than 1000 distinct stable levels of cAMP-Neuropilin.

More recently Sakano group itself revised this hypothesis and provided a possible different explanation for the origin of the OR derived-cAMP. They suggested that the spontaneous ligand-independent activation of the OR could produce the OR-derived cAMP. The OR has not been crystalized and in how many conformational states it could exist, it is not known. For these reasons, Sakano and colleagues used the β -adrenergic receptor, another G-protein receptor, that is known that can assume 3 conformational states, related to 3 different levels of cAMP, that in turn could dictate the level of Neuropilin and the location of glomeruli in 3 different domains of the OB along the AP axis (*Nakashima et al., 2013*).

Also this explanation, however, exhibits several controversial aspects. First, the OR is not the B receptor, and the absence of the crystal structure of the OR hampers to establish differences and similarities in the conformational changes of these receptors. The β -adrenergic receptor has been shown to promote the coalescence of sensory axons, but also to fail to dictate the proper location of glomeruli in the OB (*Feinstein & Mombaerts, 2004*). Furthermore, OSN were shown to exhibit spontaneous electrical activity related to the OR they express (*Connelly et al., 2013*). OSN expressing different OR have significant different rate of basal activity. However, also OSN expressing the same OR show considerable variation in their spontaneous firing. This high variability of basal activity in OSN is not reconcilable to the production of distinct and stable level of cAMP in specific subset of OR, as

proposed by Nakashiyama and coauthors in 2013. Last but not least, Sakano group never addressed the role and the function of the axonal OR. Altogether these results indicate that the enigma of the role of the OR in the map formation was far from being clear.

Olfactory sensory neuron projection along the medio-lateral (M-L) axis

In 2008, Scolnick and colleagues demonstrated that the location of glomeruli along the medial-lateral axis is dictated by the insulin-like growth factor 1 (IGF1). The disruption of IGF1 pathways by mutations causes the formation of glomeruli in an ectopic position, located in the ventro-medial side of each OB. In details, genetic ablation of IGF1 or its receptor IGF1R results in a reduced innervations of OSN axons in the lateral region of the OB (*Scolnick et al., 2008*). During the early stage of development, IGF1 is expressed in a gradient to low level (medial) to high levels (lateral) in the OB. Thus, IGF1 could be considered as an attractant that promote the axons growth in the lateral region of the bulb. It is also reported that IGF1 can attract OSN axon *in vitro*. The involvement of other axon guidance molecules that can act along the medial-lateral axis of the bulb remains poorly investigated.

Homophilic adhesive molecules in the refinement process

Homophilic adhesive molecules such as Kirrel 2 and Kirrel 3 contribute to the axonal refinement (*Serizawa et al., 2006; Lorenzon et al., 2015*). The gain of function of these homophilic adhesion molecules cause the additional number of heterogeneous glomeruli, expressing different OR, suggesting their role in the final refinement process. Other adhesion molecules involved in the refinement of the glomeruli are Ephrin A and Eph A, and Big 2 (*Cutforth et al., 2003; Serizawa et al., 2006; Kato et al., 2014*)

1.4.2 Role of the electrical activity in the development of the topographic map

The development of sensory maps results from the complex interplay between axon guidance molecules, expressed in specific spatio-temporal patterns, (see above), and neuronal electrical activity.

Neural electrical activity comprises spontaneous and odor-evoked activity, both involved in the development of neural circuits (*Zhang & Poo, 2001*).

However, the specific role of each type of activity in the olfactory system remained elusive for long time.

Odor-Evoked activity

The odor-evoked activity consists of action potentials generated in response to specific stimuli (i.e. in the case of the olfactory bulb are odor stimuli).

To ascertain the role of the evoked activity in circuit formation of the olfactory bulb, several genetic studies were performed by creating different KO lines of mice in which distinct component of the signaling pathway coupled to the OR were mutated to abolish their function. It is not possible to eliminate odor activity with more physiological manipulations such the ones used in the visual system (i.e. dark rearing, lid suture). Even in perfect isolation an animal can always smells its own scent. Hence the necessity of creating genetically engineered lines of mice carrying null mutation in distinct molecule involved in the signaling pathway coupled to the OR.

In 1998, Belluscio and colleagues demonstrated that mice homozygous for a null mutation for G_{olf} showed a reduction in the electrophysiological response of OSNs to a wide range of odors. However, G_{olf} KO mice exhibited a normal convergence of sensory axons to form glomeruli in a specific location in the OB. They hypothesized that in G_{olf} KO mice the presence of some electrophysiological responses together with normal OSN targeting, could be ascribed to the compensatory expression of another G-protein, G_{as} (*Belluscio et al., 1998*).

Mice lacking functional CNG channel, an essential component of the odors signaling pathway, display deficits in the odor-evoked response measured with electro-olfactogram (EOG). The convergence of sensory axons to form the glomerular map was again unaffected. A different study observed only a minor alteration in the convergence of M72-expressing axon to form M72-glomeruli in CNG KO mice (*Zheng et al., 2000*).

A completely different scenario was observed in adenylyl cyclase type III (ACIII) KO mice. These mice are anosmic and exhibit a deeply perturbed sensory map (*Trinh & Storm, 2003*). ACIII mutation hampers the production of cAMP. This mutation clarifies that the critical component of the OR signaling pathway for the convergence of sensory neurons is cAMP (*Trinh & Storm, 2003; Chesler et al., 2007; Col et al., 2007*).

Furthermore, *Zou et al 2007* observed a perturbation in the formation and organization of glomeruli in the bulb, together with a mistargeting of OSN axons in discrete glomeruli caused by the absence of the production of cAMP, in AC KO mice (*Col et al., 2007*).

All these genetic experiments indicated that odor evoked activity, per se, is not required for the sensory map formation and highlighted the importance of cAMP in this process.

Spontaneous activity

Spontaneous activity consists of action potentials generated in absence of sensory stimuli. In the visual system, the spontaneous activity plays a key role in the topographic organization of sensory afferents (*Galli & Maffei, 1988*). However the role of the spontaneous activity in the olfactory systems was poorly understood.

To investigate the role of spontaneous activity in the olfactory system, *Yu and colleagues* in 2004 generated a transgenic line of mice in which olfactory sensory neurons over-expressed the inwardly rectifying potassium channel (Kir2.1 mice). This genetic manipulation hyperpolarizes the OSN, decreasing the spontaneous firing. In Kir2.1 mice, the sensory map was perturbed by the presence

of several additional glomeruli. However, many critical aspects regarding the altered organization of the sensory map, the intrabulbar connections and olfactory behavior in Kir2.1 mice remained poorly understood.

Lodovichi's group (*Lorenzon et al., 2015*) examined in depth the role of spontaneous activity in the topographic organization of the OB. They demonstrated that the over-expression of Kir2.1 dramatically reduced basal activity in OSN, but did not affect odor evoked activity. Kir2.1 mice are therefore an ideal model to dissect specifically the role of spontaneous afferent activity in the topographic organization of the OB. The reduced basal neural activity leads to an unrefined connectivity in the map in the bulb and in the intrabulbar connections. By analyzing the organization of sensory map in Kir 2.1 mice, they observed the presence of an increase number of heterogeneous glomeruli (expressing different odorant receptors), a feature present in the early developmental stages of the topographic map. The intrabulbar link among homologous glomeruli was present, but it was larger than in controls. Even the intrabulbar link appeared to be unrefined, with the anatomical feature proper of early stages of development. The altered topography of the bulb affected the olfactory behaviour of Kir2.1 mice, that were unable to discriminate similar odors (i.e. enantiomers), although they maintained the capacity to differentiate very different odorants (*Lorenzon et al., 2015*).

1.5 A brief summary of a previous work: the odorant receptor expressed at the axon terminal of olfactory sensory neurons is activated by molecules expressed in the olfactory bulb

Here, a brief summary of the previous work performed by Lodovichi's group, that allowed the identification of a pool of molecules elaborated in the olfactory bulb, capable of activating the odorant receptor (OR) expressed at the axon terminal of olfactory sensory neurons. They obtained an olfactory bulb dialysate (from ~300 embryonic rat OB, see method sections) that was processed by different chromatographic techniques, such as size exclusion chromatography (SEC), that separates molecules according to their molecular weight, and the ionic exchange chromatography (IEC), that separates molecules according to their respective charge. Each peak obtained by these procedures was locally applied at the axon terminal of OSNs and in HEK293T cells transfected with a specific OR. By performing Ca^{2+} imaging experiments, they identified a pool of molecules able to elicit a prompt Ca^{2+} response at the axon terminal of sensory neurons (**Figure 1.32a-c**). In particular they found that the third peak of SEC (SEC-3) was the only one that elicited Ca^{2+} rises at the axon terminal (**Figure 1.32 a-c**). They further fractionated SEC-3 by ionic exchange chromatography (IEC) and they found two peaks (IEC-1 and IEC-2) that elicited a prompt Ca^{2+} rise at the axon terminal (**Figure 1.32 b-c**). Since they observed a Ca^{2+} rise in response to IEC-1 in HEK cells not expressing any OR (pCI vector), the peak IEC-1 was not further investigated (see appendix sections **supplementary Figure S1 a-c**). Peak IEC-2 was then further dissected and investigated first on olfactory sensory neuron (OSN) and in HEK293T cells transfected with specific OR (OREG, S6, olfr62 (**Figure 1.33 a-f**). The day of the experiment OSN and HEK293T cells were loaded with the Ca^{2+} indicator fura-2 for Ca^{2+} imaging experiments.

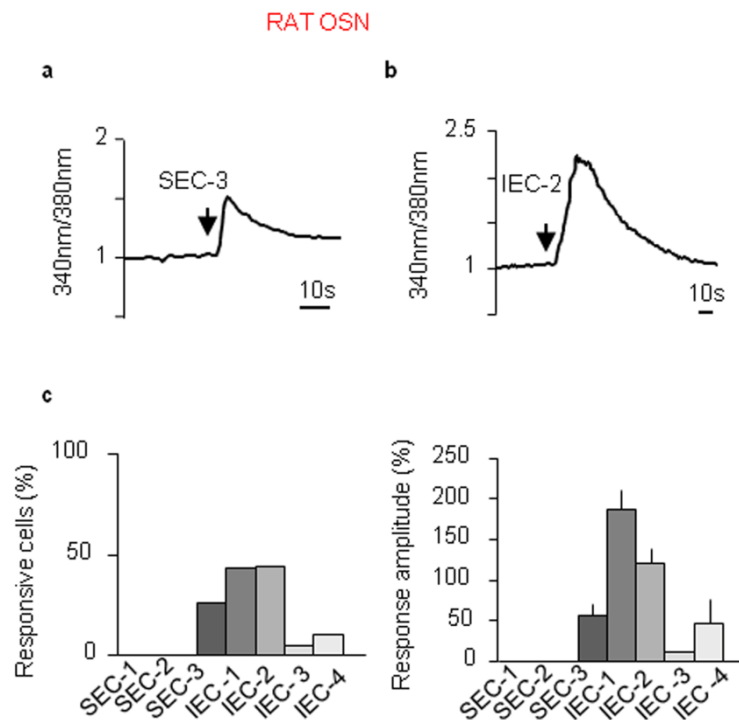


Figure.1.32. Ca^{2+} dynamics in olfactory sensory neuron (OSN) axon terminals in response to molecules from the olfactory bulb. Fura-2 Ca^{2+} imaging **a-b**) Embryonic rat OSN axon terminals exhibit a prompt Ca^{2+} rise upon stimulation with the third peak of size- exclusion-chromatography (SEC-3, **a**) and with the second peak of ionic-exchange-chromatography (IEC-2, **b**). **c**) Summary of results (SEC-1 n= 21, SEC-2 n = 20, SEC-3 n = 31; IEC-1 n= 92, IEC-2 n = 97, IEC-3 n = 20; IEC- 4 n = 20). Bars = SEM

To ascertain that Ca^{2+} rise observed in OSN in response to IEC-2 (**Figure 1.32 b, c**) was due to OR activation, they transfected HEK293T cells with different ORs (OREG, S6, Olfr62).

They found that HEK293T cells not expressing ORs (pCI vector), did not exhibit a rise in Ca^{2+} upon stimulation with IEC-2 nor with odors (**Figure 1.33 a**). However, HEK293T cells expressing distinct ORs (OREG, S6, Olfr62) exhibited a prompt Ca^{2+} rise upon challenge with IEC-2 or with the corresponding-odor ligand of the OR (**Figure 1.33 b, d, e, f**).

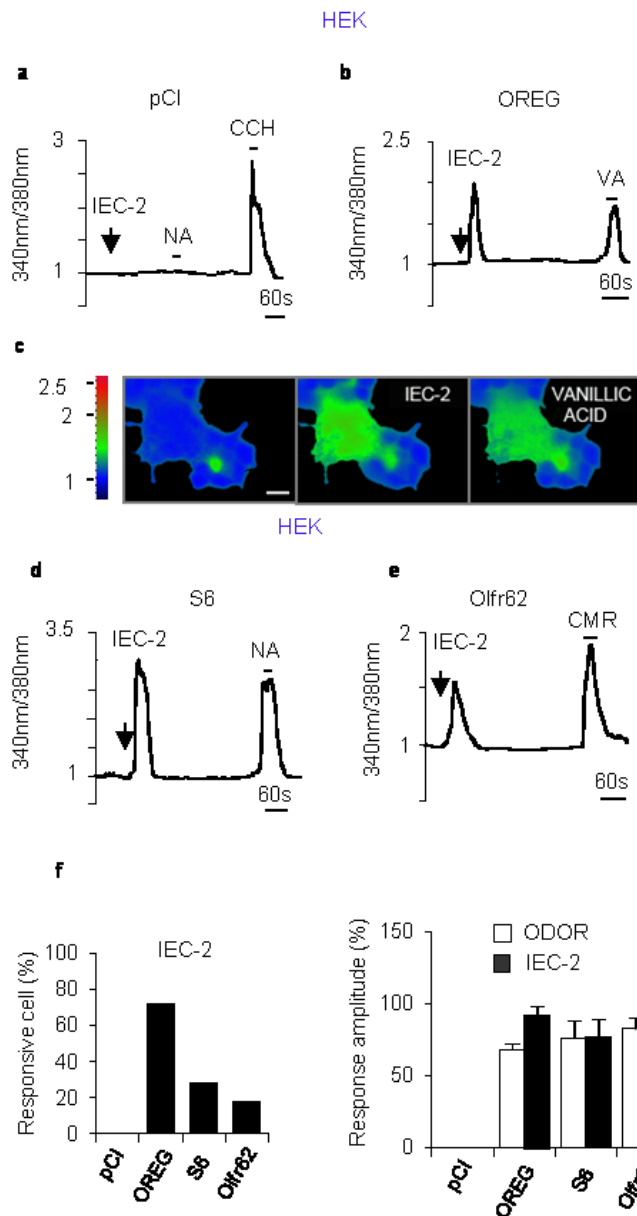


Figure 1.33. Fura-2 Ca^{2+} imaging in HEK293T cells transfected with specific OR in response to olfactory bulb (OB) molecules. a) HEK293T cells not expressing odorant receptor, (pCI= empty vector, $n = 76$), do not exhibit Ca^{2+} response to IEC-2 nor to odors (nonanedioic acid, NA). A prompt Ca^{2+} rise is present in response to carbachol (CCH, used as control). **b, d, e)** HEK293T cells expressing odorant receptors (OR) exhibit Ca^{2+} rise in response to IEC-2 and the corresponding-odor. OREG-vanillic acid (VA, e) ($n = 72$), S6-nonanedioic acid (NA, g), ($n= 63$), Olfr62-2-coumaranone (CMR, h) ($n= 122$). **c)** Sequence of pseudocolor images of HEK293T cells expressing OREG, showing the changes in $[\text{Ca}^{2+}]_i$ before and upon stimulation with IEC-2 and with VA. **f)** Summary of results of Ca^{2+} dynamics in HEK cells ($n = 18$).

IEC-2 was also able to elicit Ca^{2+} response when applied to mouse olfactory sensory neuron axon terminals (**Figure 1.34 a-c**).

All these results demonstrated that molecules isolated from the OB were capable of eliciting Ca^{2+} responses via activation of specific OR.

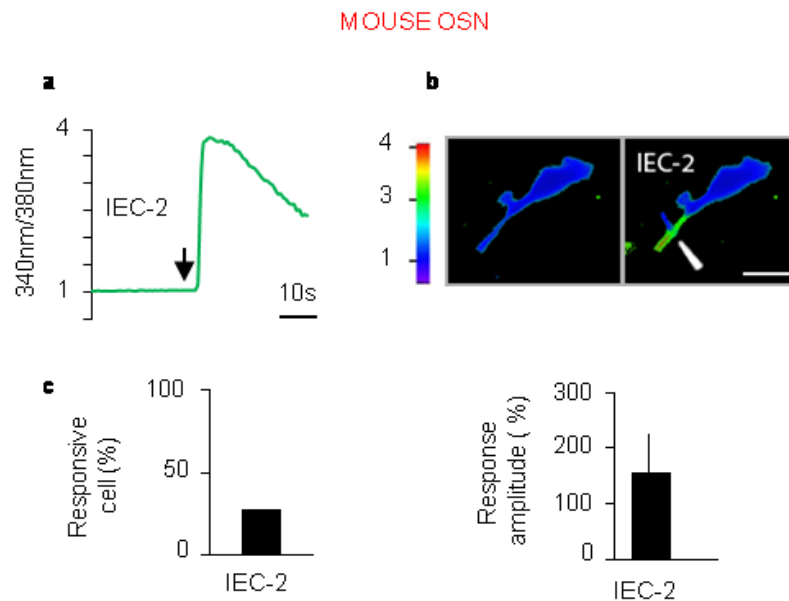


Figure 1.34. Molecules from the olfactory bulb (OB) also activate mouse olfactory sensory neuron (OSN) axon terminals. a) Ca^{2+} response to IEC-2 in a mouse OSN axon terminal. **b)** Pseudocolor images of the mouse OSN, showing changes in $[\text{Ca}^{2+}]_i$ before and after the local IEC-2 stimulation (arrowhead). Bars = SEM. Scale bars, 20 μm .

Upon odor binding, OR triggers an increase in cAMP and Ca^{2+} via cyclic nucleotide gated channel opening (CNG channel) (Pifferi *et al.*, 2006).

Lodovichi's group demonstrated that Ca^{2+} rise observed in response to OR activation by molecules extracted in the olfactory bulb was dependent on cyclic nucleotide gated channel activation (**Figure 1.35**).

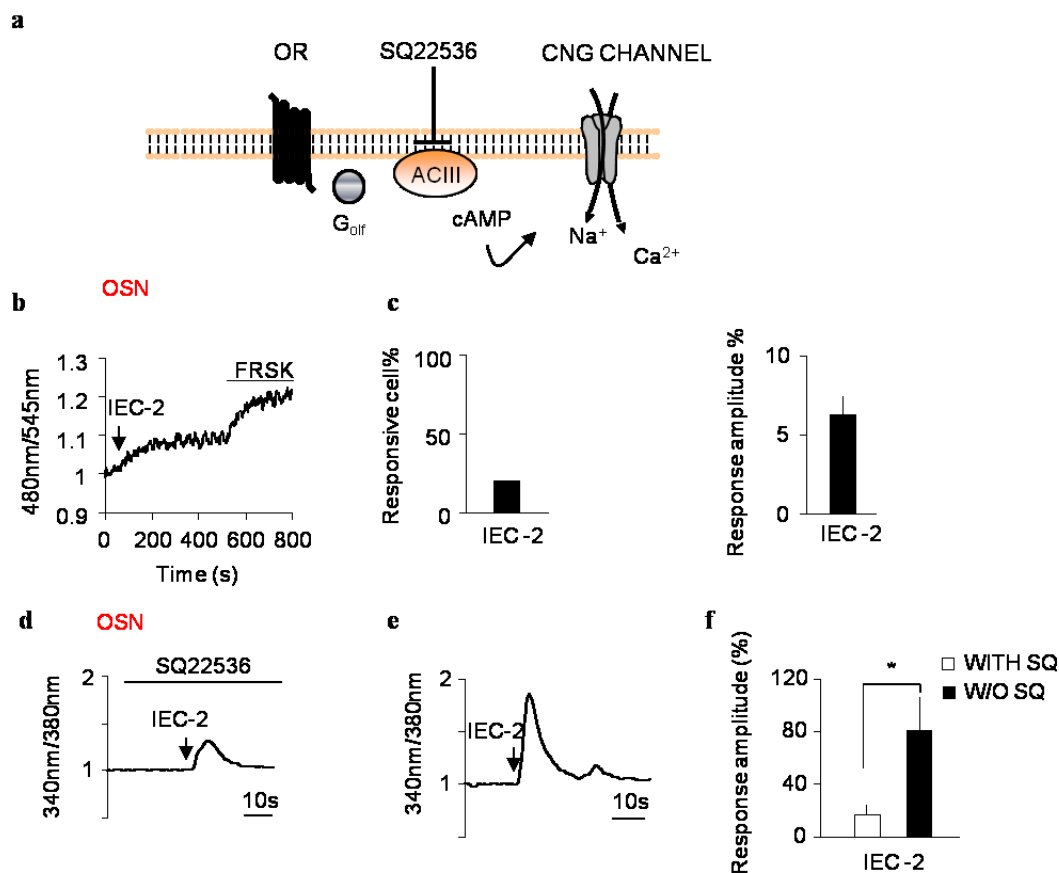


Figure 1.35. Ca^{2+} influx in olfactory sensory neuron (OSN) axon terminals is due to cyclic nucleotide gated (CNG) channel activation. **a)** Schematic of the signal transduction pathway coupled to the odorant receptor (OR). ACIII= adenylyl cyclase III. SQ22536 = generic inhibitor of ACIII. CNG channel= cyclic nucleotide gated channel. **b)** Example of cAMP dynamics at the axon terminal of OSN in response to ionic exchange chromatography peak 2 (IEC-2) focally applied and to subsequent bath application of forskolin (FRSK, 25 μ M). **c)** Summary of results. **d)** Ca^{2+} response in OSN axon terminal challenged with IEC-2 is significantly reduced in presence of SQ22536 n=12. **e)** A prompt Ca^{2+} rise is observed in the same OSN axon terminal, after washing out the inhibitor, in response to IEC-2 (n=12). **f)** Summary of results. * $P < 0.05$. Bars = SEM.

To identify possible ligand candidate (s) of the axonal OR, the active pools of molecules isolated from rat embryonic olfactory bulb (OB) dialysate, was further fractionated by chromatographic procedures (Reverse phase chromatography, RCP) (see Appendix, **supplementary Figure S2**) and then processed by mass spectrometry (see Appendix, **supplementary Table S1** and **supplementary Table S2**).

By mass spectrometry, among the active pool of molecules isolated from the OB, a small protein of ~21 kDa, named phosphatidyletanolamine-binding-protein-1 (PEBP1) was identified as a putative ligand of the odorant receptor expressed at the axon terminal of olfactory sensory neurons. Its low molecular weight, the ability to be secreted although via a non-canonical pathway, the fact that mice carrying a null mutation for PEBP1 exhibit olfactory deficit, make PEBP1 a suitable ligand for the axonal OR.

1.6 Phosphatidylethanolamine binding-protein family (PEBP)

Phosphatidylethanolamine binding protein-1 (PEBP1) first isolated from the bovine brain belong to the phosphatidylethanolamine binding protein superfamily, an evolutionary conserved family of proteins . In humans PEBP1 is a protein of ~21Da composed by 186 aa. Humans and rat PEBP proteins have more than 87% of similarity (*Al-Mulla et al., 2013*).

According to X-ray analysis, PEBP1 is formed by 4 α - helices and 9 – stranded β -sheets folded together to give stability to the protein (*Simister et al., 2002; Skinner & Rosner, 2014*). The binding pocket of PEBP1 is composed by 16 amino acids residues and is able to bind different substrates/ligands such as nucleotides, ATP, GTP and GDP, Raf-1, not lipid-organic compound (i.e. locostatin) (*Shemon et al., 2009; Skinner & Rosner, 2014*). It is shown that this pocket exerts different functions in different species and/or at different pH.

In the mouse genome, 5 sequences of PEBP1 were found. PEBP1 and PEBP2 are active, while PEBP3-5 are pseudogenes. PEBP2 is expressed only in the testis, while PEBP1 is widely expressed in several types of tissues such as adrenal gland, stomach, kidney, spleen, intestine, heart, liver, testis and neuronal cells (*Frayne et al., 1999; Al-Mulla et al., 2013*).

Initially, PEBP1 immunoreactivity was identified in the cytoplasm and in the plasma membrane of Schwann cells, oligodendrocytes and it was observed in testis suggesting a possible role in the membrane biogenesis and lipid transfer (*Frayne et al., 1999*).

PEBP1 is also known as Raf-kinase inhibitory protein-1 (RKIP-1) involved, intracellularly, in the Raf/MEK/ERK pathway (*Al-Mulla et al., 2013; Lorenz et al., 2014; Hahm et al., 2016*). PEBP1 interacts and binds Raf-1 exerting an inhibitory effect, preventing the activation of MEK. In contrast, the phosphorylation of PEBP1 by PKC at the residues S153 lead to activate kinase belong to MAPK pathway. PEBP1 is also involved in the G-protein coupled receptor (GPCRs)

signaling regulation. In particular, G-protein coupled kinase 2 (GRK-2) that represents the primary negative feedback inhibitor of GPCRs, was inhibited by PEBP1. The phosphorylation of PEBP1 by PKC at the residues S153 determines the dissociation of Raf-1 from PEBP1 and the consequentially block of the inhibitory activity of GRK-2. Then, PEBP1 forms dimers with GRK-2 instead of Raf-1 (*Deiss et al., 2012*).

PEBP1, apart from being involved in intracellular signaling (see above) and present in the matrix as a soluble protein, it can also be secreted (*Goumon et al., 2004*). By immunocytochemistry coupled with confocal laser and immunoelectron microscopy, Goumon and colleagues reported that PEBP1 is present in different compartments of bovine adrenal medullary chromaffin cells indicating that it could be secreted. For the lack of a consensus signal peptide, PEBP1 is secreted via a non-canonical pathway with catecholamines in the circulation. PEBP1 and hippocampal cholinergic neurostimulating peptide (HCNP) (see below), secreted with catecholamines, exert a inotropic negative effect on the heart, likely acting on β -adrenergic receptor (GPCR) (*Goumon et al., 2004*).

In this PhD thesis we will investigate its role in the olfactory system as a secreted protein.

1.6.1 PEBP1 role in the brain

The pattern of expression of PEBP1 in the nervous system was investigated by Frayne and colleagues and then by Theroux and coauthors in 2007. PEBP1 is localized in several brain areas (*Frayne et al., 1999*). PEBP1 is expressed widely in the brain, although its function remains largely obscure. Its receptor has not been identified yet.

Theroux and colleagues (*Theroux et al., 2007*) generated, by insertional mutagenesis, a transgenic mice carrying a null mutation of PEBP1 (RKIP^{-/-} mice, or PEBP1^{-/-} mice). PEBP1^{-/-} mice carry a β -geo reporter (see methods sections) that allows to follow PEBP1 expression by immunostaining with X-gal, that reveal the β -galactosidase activity in all tissues, including the brain. This approach was useful to analyze the expression of PEBP1. Theroux and colleagues observed that PEBP1 is expressed in several brain areas, including the hippocampus, mostly in pyramidal cell and in the granular layer of dentate gyrus together with the CA fields. Moreover, PEBP1 expression was observed in amygdala, and in hypothalamic nuclei. PEBP1 expression is high also in piriform cortex and connected areas.

Due to PEBP1 expression in the olfactory bulb and cortex, PEBP1 mutant mice (PEBP1^{-/-} mice) exhibit an olfactory deficit in an odor (cheddar cheese) recognition test and in olfactory discriminations task (*Theroux et al., 2007*).

1.6.2 Hypocampal cholinergic neurostimulating peptide (HCNP)

PEBP1 is the precursor of an undecapeptide named hippocampal cholinergic neurostimulating peptide (HCNP) located at its N-terminal (*Tohdoh et al., 1997; Ojika et al., 1998; Ojika et al., 2000*). HCNP was isolated from rat hippocampus and is expressed in different regions of the central nervous system. HCNP immunoreactivity was detected principally in neurons of the cerebral cortex, hippocampus, olfactory system, nucleus accumbens, caudate putamen, and in arcuate hypothalamic, mesencephalic trigeminal, spinal trigeminal and amygdaloid nuclei (*Mitake et al., 1996; Tohdoh et al., 1997*).

HCNP is involved in the differentiation of cholinergic neurons in the medial septal nuclei both *in vitro* and *in vivo*, hence its name, hippocampal cholinergic neurostimulating peptide (*Ojika et al., 1998; Kato et al., 2012*). The over-expression of HCNP induces the increase of choline acetyltransferase (ChAT) in the medial septal cholinergic nucleus, suggesting its role in the synthesis of acetylcholine *in vivo* (*Uematsu et al., 2009*). Recently, it was demonstrated that HCNPpp co-localize with the collapsing response mediator protein-2 (CRMP-2) at the presynaptic terminals suggesting a possible role in the presynaptic function in the hippocampus (*Kanamori et al., 2010; Kato et al., 2012*).

2 AIM

It is known for more than 20 years that the odorant receptor (OR) not only detects odorant molecules (odors) but it plays also an instructive role in the convergence of sensory neuron axons to form glomeruli in specific loci of each olfactory bulb, giving rise to the sensory map. The sensory map has a critical role in encoding odors, that are represented by a spatial pattern of activated glomeruli.

The odorant receptor (OR) is expressed specifically and exclusively in two locations of the olfactory sensory neurons (OSN): at the cilia, where it detects odors, and at the axon terminal. Why odorant receptors are expressed at the axon terminal of olfactory sensory neurons (OSN)? The expression of the OR in this location corroborates its role as a putative axon guidance molecule. However, the mechanism of activation and function of the OR expressed at the axon terminal has remained elusive for all these years.

The open critical questions that remained to be address are :

1. What are the mechanisms of activation of the axonal OR?
2. What are the natural ligands of the odorant receptor expressed at the axon terminal of olfactory sensory neurons?
3. What is the function of the axonal OR?

A few molecules expressed in the olfactory bulb could bind and activate the odorant receptor expressed at the axon terminal of olfactory sensory neurons.

To ascertain this hypothesis, Lodovichi and colleagues obtained a dialysate from embryonic rat olfactory bulb that was then processed by different chromatographic techniques. The active pool of molecules where analyzed by mass spectrometry for the identification of natural ligands of the axonal OR. Among these molecules, phoshatydylethanolamine protein-1 (PEBP1) was identified as a ligand of the axonal OR.

The goal of this PhD project was to investigate the role of PEBP1, by addressing the following specific aims (SA):

- ✓ SA1. To ascertain that PEBP1 could activate the axonal OR, Ca^{2+} imaging was performed in rat and mouse olfactory sensory neuron (OSN) and in HEK293T cells expressing specific OR, loaded with the calcium indicator (fura-2).
- ✓ SA2. Axon guidance molecules steer axon turning. To explore the ability of PEBP1 to regulate axon behaviour, time-lapse imaging of single OSN axons in response to gradients of pharmacological agents and to molecules from the OB, including PEBP1, was performed.
- ✓ SA3. If PEBP1 could act as an axon guidance molecule, acting on the axonal OR, mice carrying a null mutation in PEBP1 should exhibit an altered sensory map. The convergence of subsets of OSN to form glomeruli in specific locations in the olfactory bulb was analyzed in mice carrying a null mutation for PEBP1 (PEBP1^{-/-}) mice and controls.
- ✓ SA 4. The sensory map has a key role in odor coding. Altered topography in the OB results in altered odor discrimination. To analyze the functional outcome of an altered sensory map, olfactory behaviour was tested in PEBP1^{-/-} mice and controls.

3 MATERIAL AND METHODS

3.1 Animal Models

All experimental and animal care procedures were approved by Italian Ministero della Salute (authorization number 818/2016-PR).

Experiments were performed on embryonic rat E18-19, on postnatal rats (P0-P4, (Sprague Dawley, Charles River), and on mice at age P0-P4 or P40-P50, according to the type of experiment, specified in the main text. The following lines of genetically modified mice were employed: P2-IRES-GFP (P2-GFP), generously provided by J.A. Gogos (Columbia University, New York, NY), and described in detail previously (*Gogos et al., 2000*). M72-ChR2-YFP (M72-YFP, Charles River), PEBP1^{-/-} (also known as RKIP-1^{-/-}) was generously provided by Evan Keller, University of Michigan, and described in *Theroux et al., 2007*. We used C57BL/6 wild type (WT) mice (Charles River) and C57BL/6-Tyr^{c-Brd} (Charles River) as controls for PEBP1^{-/-} mice.

3.1.1 PEBP1^{-/-} mice (RKIP1^{Gt(pGT01xrBetageo) 1Jkl})

PEBP1^{-/-} mice (also known as RKIP-1^{-/-}) were generated (*Theroux et al., 2007*) by injecting 12-20 ES cells in E3.5 blastocysts derived from C57BL/6-Tyr^{c-Brd} female mice. The ES cells line carries a pGT01xr vector that was used for the insertional mutagenesis (**Figure 3.1**). The injected blastocysts were implanted into the uteri of female to generate chimeras, which were mated with C57BL/6-Tyr^{c-Brd} females to obtain F1 progeny (RKIP1^{Gt(pGT01xrBetageo) 1Jkl}).

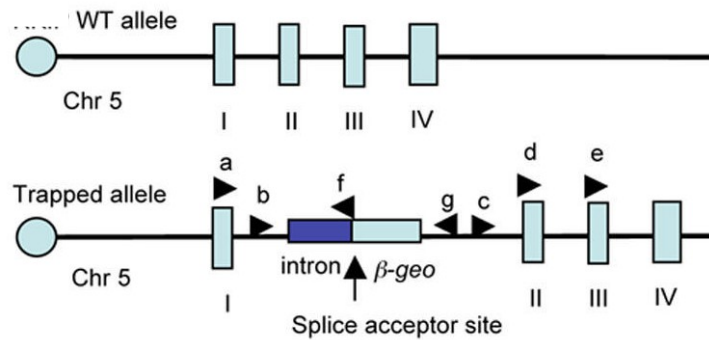


Figure 3.1. Genomic structure of $RKIP^{-/-}$ gene and the gene trapped allele. pGT01xr vector carries the β -geo selectable marker. β -geo is a recombinant chimeric protein that at its N-terminal contains β -galactosidase while at C-terminal a neomycin phosphotransferase. After the insertional mutagenesis the cassette was placed under the control of the gene promoter target. The expression of the targeted gene could be followed by immunostaining with X-gal, that reveal the β -galactosidase activity (Theroux *et al.*, 2007).

PEBP1^{-/-} mice carrying a null mutation for PEBP1 (Theroux *et al.*, 2007) were crossed with homozygous lines of mice co-expressing different odorant receptors with GFP, such as P2 and M72. We obtained then P2-GFP ; PEBP1^{+/-} and P2-GFP ; PEBP1^{-/-}, M72-YFP ; PEBP1^{+/-} and M72-YFP ; PEBP1^{-/-} that were used to investigate the sensory map organization in absence of PEBP1 (see paragraph 4.5).

3.2 Isolation of olfactory bulb products

Olfactory bulbs (OB) (~300) were collected from rat embryos (E18 – E19) and frozen in liquid nitrogen. Frozen rat olfactory bulbs were powdered by pestle and mortar and lysed in a buffer containing 20 mM HEPES pH 7.4, 140 mM NaCl, 5 mM KCl, 5 mM NaHCO₃, 1.2 mM Na₂HPO₄, 1 mM MgCl₂, 20 mM HEPES pH 7.4, 10 mM dextrose, 1.8 mM CaCl₂, Roche Complete Protease Inhibitor Cocktail, 1 mM PMSF, 1 mM NaVO₃, 5 mM NaF and 3 mM β -glycerophosphate. The lysate was centrifuged to remove cell debris and membranes at 4°C for 30 minutes at 13000 rpm. Then the supernatant was purified with a slide-A-lyzer dialysis cassette (cut off 350MW, Thermo Scientific) in 20mM HEPES and 100mM NaCl.

The dialyzed olfactory bulb extract was applied onto a HiTrap Desalting column (GE Healthcare), equilibrated with the elution buffer (20mM Tris pH=7.4 and 100mM NaCl). The proteins were eluted in a single peak and concentrated. They were purified by a Superdex 200 prep-grade 300/10 column (GE Healthcare), equilibrated with the elution buffer, and the resulting three peaks were separately collected (Size Exclusion Chromatography, SEC). The third peak (SEC-3), which elicited Ca²⁺ rises at the axon terminal in OSN, was adjusted to the composition of buffer A (20mM Tris, pH 8) and was loaded onto a HiTrap Capto Q column (GE Healthcare), equilibrated with buffer A (ionic exchange chromatography, IEC). The proteins that did not bind to the column were collected in fraction 1 (IEC-1). After washing the column with 10ml buffer A, a linear gradient (0-30%) of buffer B (20mM Tris, 1M NaCl, pH 8) was applied and three peaks were collected (IEC- 2, - 3 and -4). These chromatographic runs were performed with an AKTA Fast Protein Liquid Chromatography (FPLC) system (GE Healthcare).

Further HPLC analyses of the active fraction IEC-2 were conducted using reversed phase chromatography (RPC) using a Jupiter C4 column (4.6 mm x 150 mm; Phenomenex, CA, USA). Elution was done with a gradient of acetonitrile/0.085% TFA vs water/0.1% TFA from 5% to 38% in 5 minutes, from 38% to 43% in 15 minutes. The effluent was monitored by recording the absorbance at 226 nm. The products obtained in every step were concentrated and tested functionally as described above, peaks 23 and 35 were active.

Proteins were quantified using the Bradford assay. IEC-2 was heated at 99⁰ C for 30 minutes to denature proteins in the sample (heated-IEC-2).

3.3 Identification of the eluted material from HPLC

The identity of active peaks 23 and 35 was assessed by mass spectrometry. Mass determinations were carried out with an electrospray ionization (ESI) mass spectrometer with a Q-ToF analyzer (Micro) from Waters (Manchester, UK). The measurements were conducted at a capillary voltage of 2.5 kV and a cone voltage

of 30-35 V. The molecular masses of protein samples were estimated using the Mass-Lynx software 4.1 (Waters).

To identify the protein species, a fingerprinting analysis by trypsin was performed. Proteolysis with trypsin was conducted using an E/S ratio of 1:25 (by weight), in ammonium bicarbonate, pH=8, after reduction of disulfide bridges and carbamidomethylation of cysteine residues and the reaction was quenched by acidification with TFA in water (4%, v/v). The tryptic digest mixture was analyzed by LC-MS/MS on a 6520 Q-TOF mass spectrometer (Agilent Technologies, Santa Clara, CA, USA) coupled to a chip-based chromatographic interface. A Large Capacity Chip (C18, 150 μm \times 75 μm) with an enrichment column (C18, 9 mm, 160nl volume) was used to separate peptides at a flow rate of 0.3 $\mu\text{l}/\text{min}$. Water/formic acid 0.1% and acetonitrile/formic acid 0.1% were used as eluents A and B, respectively. The chromatographic separation was achieved with a gradient of B from 5% to 50% in 20 minutes. Raw data files were converted into Mascot Generic Format (MGF) with MassHunter Qualitative Analysis Software version B.03.01 (Agilent Technologies) and analyzed with Mascot Search Engine version 2.2.4 (Matrix Science). MS/MS spectra were searched against the SwissProt database (version 2011-05, 528048 sequences). Enzyme specificity was set to trypsin/P with 1 missed cleavage, using a mass tolerance window of 1.2 Da for peptides and 0.6 Da for fragment ion matches. Carbamidomethylation of cysteine was set as fixed modification and methionine oxidation as variable modification. Proteins were considered as positive hits if at least 2 peptides per protein were identified with high confidence ($p < 0.05$).

3.4 Primary culture of rat and mouse olfactory sensory neurons

The olfactory epithelium was harvested from embryonic rats (E18 - E19) in ice-cold Hank's balanced salt solution (HBSS) (Invitrogen) and then the tissue was enzymatically dissociated (*Maritan et al., 2009; Pietrobon et al., 2011*).

After 3 centrifugation at 3000rpm for 4min at room temperature, the cell suspension was plated onto 24mm cover slips coated with poly-L lysine (Sigma Aldrich) and maintained for 24 hours in culture medium (D-Val MEM, 10% fetal bovine serum (FBS), 5% Nu Serum, Penstrep L-glutamine, 100 U/ml (Invitrogen), 10 μ M Cytosine β -D-arabinofuranoside (Ara C) (Sigma Aldrich), 25 ng/ml nerve growth factor (NGF) (Corning) before calcium imaging experiment or transfection with Epac-1 based sensor for cAMP (*Ponsioen et al., 2004*).

3.5 HEK 293T cell culture

HEK293T cells were maintained in MEM (Invitrogen) containing 10% FBS and 1% Penstrep (Invitrogen) in a 37° C incubator with 5 % CO₂. The cells were seeded on a 24 mm cover slip (Falcon) coated with poly-L-lysine (Sigma Aldrich) 24 hours prior to transfection. Lipofectamine 2000 (Invitrogen) was used for the transfection of 0.8 μ g plasmid driving Rho-tagged odorant receptor expression, i.e. OREG, P2, S6, Olfr62, M72 and 0.4 μ g of RTP1S, 0.4 μ g of RTP2 and 0.8 μ g of G $_{\alpha 15}$ or pCI. (The Rho-tagged OR and all the accessory plasmid DNA were generously provided by H. Matsunami, Duke University, Durham, NC, and describe in details in (Zhuang & Matsunami, 2007; 2008) mKate fluorescent protein (0.3 μ g) (Thermo Fisher) was used as a control for transfection efficiency.

3.6 Ca²⁺ imaging in olfactory sensory neurons (OSN) and HEK293T cells

Ca²⁺ imaging was performed on embryonic (E18-E19) rat olfactory sensory neurons (OSN), on OSN of postnatal day (P) P0-P4 mice and on HEK293T cells. The day of experiment (~10 -12 hours after plating), neurons or HEK293T cells were loaded with 5 μ M Fura 2-AM (Life Technologies), 500 μ M sulphinyl pyrazone (Sigma Aldrich) and 0.01% pluronic acid (Life Technologies) in medium

at 37° C for 30 minutes. Cover slips were mounted in a thermostatic chamber at 37°C (Warner Instruments) and maintained in Ringer's solution (140mM NaCl, 5mM KCl, 1mM CaCl₂ *2H₂O, 1mM MgCl₂, 10mM HEPES, 10mM glucose, 1mM sodium pyruvate, pH 7.2). OSN and HEK293T cells were continuously perfused with the Ringer's Solution (3 ml/min) except during stimulus presentation. Experiments on OSN were performed in the presence of 4µM TTX (Latoxan) in order to avoid action potential contribution to the measured Ca²⁺ signal. The Ca²⁺ imaging experiments were performed on an inverted microscope IX 81 (Olympus) equipped with a UPlanFL 60X NA 1.25 oil immersion objective (Olympus), a xenon light source (150 W) for epifluorescence illumination, a 12-bit CCD camera (SIS F-View) and an illumination system MT20 (Olympus). Images were acquired every second (s) (for OSN) and every 3 second (for HEK293T cells) using 380/15 nm and 340/15 nm excitation filters and collected through a 510/40 nm emission filter (Olympus). Data were acquired with a Cell[^]R software and analyzed offline with the ImageJ software (NIH). Changes in fluorescence (340nm/380nm) were expressed as R/R₀ where R is the ratio at time t and R₀ is the ratio at time = 0 second. Amplitude of response was computed as $\Delta R/R_{\min}$ (%), where $\Delta R = R_{\max} - R_{\min}$. Calcium responses with amplitude < 10 % were excluded from the analysis. Percentage of responsive HEK293T cells was calculated as: number of HEK293T cells responsive to the corresponding-odor and to molecules from the OB/ tot number of HEK293T cells responsive to the corresponding-odor X 100. In case of P2 odorant receptor, carbachol (CCH) instead of corresponding odor (still unknown) was employed. For HEK293T cells transfected with empty vector pCI, i.e. not expressing any OR, only cells responsive to carbachol, used as cell vitality test, were considered for statistics. Percentage of responsive OSN was calculated as: number of OSN responsive to molecules from the OB/ tot number of OSN tested X 100.

3.7 Cyclic AMP imaging in olfactory sensory neurons

Cells were transiently transfected with the Epac – based sensor for cAMP (Ponsioen et al., 2004), using Transfectin transfection reagent (Biorad). After transfection, neurons were maintained in culture for an additional 10 - 12 h before FRET imaging experiments to allow the genetically encoded sensor to be expressed. Imaging experiments were performed on an inverted microscope Olympus IX 70 with PlanApo 60X NA 1.4 oil-immersion objective. Excitation at 430 nm was performed with a Polychrome IV monochromator (Till Photonics GmbH, Germany) equipped with a 150 W xenon lamp. Images were captured every 3 seconds with a 16-bit sCMOS pco.edge camera (pco imaging) and the emission wavelengths were separated with a dual-emission beam splitter (Multispec Microimager; Optical Insights) with a 505 nm dichroic filter and 480 ± 15 and 545 ± 20 nm emission filters for CFP and YFP, respectively. All filters and dichroics were from Chroma Technology. The system is controlled by a custom made software. Exposure time was set to 200-300 ms. Data were processed off-line with ImageJ software (National Institutes of Health).

FRET changes were measured as changes in the background - subtracted 480/545 nm fluorescence emission intensities on excitation at 430 nm and expressed as R/R_0 , where R is the ratio at time t and R_0 is the ratio at time = 0 s.

3.8 Stimuli

Olfactory bulb products, size exclusion chromatography (SEC) peaks 1-3, ionic exchange chromatography (IEC) peaks 1-4, 0.6-0.8 $\mu\text{g} / \mu\text{l}$, reverse phase chromatography (RPC) peaks, 0.1-0.3 $\mu\text{g} / \mu\text{l}$, were focally applied to the growth cone of OSNs in culture and on HEK293T cells by a single-puff pressure ejection (Pneumatic pico-pump, WPI) with a glass micropipette (3–5 μm tip diameter, puff

duration= 1s, amplitude = 5 psi). The micropipette was positioned at 5–10 μm from the growth cone. To exclude contaminants in the purification protocol of PEBP1, HEK293T cells transfected with specific OR are challenged with cyclin-dependent kinase 2 (CDK2) (0.02 $\mu\text{g}/\mu\text{l}$). CDK2 was used as a negative control of PEBP1 purification since they were purified with the same procedure. For HEK293T cells, PEBP1 was diluted to a final concentration of 0.02 $\mu\text{g}/\mu\text{l}$ in the bath solution. Odors were prepared as 1mM stock in Ringer's solution and diluted to a final concentration of 100 μM in the bath solution. Odors: vanillic acid (VA), nonanedioic acid (NA), 2-coumaranone (CMR), methyl salicylate (MS). Other stimuli: Carbachol (CCH) 100 μM . Forskolin (FRSK) 25 μM . All chemicals were from Sigma Aldrich. Stimuli, i.e. odors and molecules from the bulb, were presented in random order.

PEBP1 was heated at 99°C for 30 minutes to be denatured (heated-PEBP1) and also digested with proteinase K 10mg/ml (PEBP1+Prot.K) for 1hour and 30 minutes at 57°C with Tris-HCl 1M pH=7.5

3.9 Time-lapse imaging of axon turning of olfactory sensory neurons

The day after plating, embryonic rat olfactory sensory neurons (see methods for primary culture above) were stimulated with microscopic gradients of chemicals, produced as described in *Lohof et al., 1992*. Briefly, repetitive pressure injection of picoliter volumes of solutions containing the chemical was applied through a micropipette (tip diameter = 1 μm). The pressure was applied with an electrically gated pressure application system (PV820 pneumatic PicoPump, WPI). A standard pressure pulse of 4 psi in amplitude was applied for 20 ms to the pipette at a frequency of 2 Hz using a pulse generator (A310 Accupulser, WPI). The micropipette was placed at a distance of about 100 μm from the center of the growth cone and an angle of 45-95° from the direction of axon extension.

The images were acquired every 10 s on an inverted microscope Olympus IX 70 equipped with a 16-bit sCMOS PCO.edge camera (PCO imaging) and a modified LWD NeoSPlan 50X/0.60 air objective (Olympus). The objective was modified applying a ring of led in order to produce a source of light below the sample to increase the resolution of the growth cone contours. To quantify the turning response, the angle between the position of the center of the growth cone at the onset and the position of the center of the growth cone at the end of the stimulation period (~1 h) period was computed in polar coordinates.

Stimulus concentrations in the glass pipette were: forskolin 5mM, odor mixture (citralva, citronellal, menthone, carvone, eugenol, geraniol, acetophenone, hexanal, benzyl alcohol, heptanoic acid, propionic acid, benzaldehyde, and IBMP (all from Sigma) 1mM in Ringer's solution, ionic exchange chromatography fraction 2 (IEC-2) 5µg/µl, PEBP1 1 µg/µl. Ringer's solution was used as control.

3.10 Expression and purification of pGEX-RKIP-1 fusion protein

pGEX2T-rat-RKIPcDNA (Raf Kinase Inhibitor protein, RKIP also known as Phosphatidylethanolamine-binding protein 1, PEBP1) was kindly provided by MR Rosner, Department of Biol. Science, University of Chicago. The purification of RKIP-GST fusion protein was performed following the standard procedures according to (*Harper & Speicher, 2011*).

The purification of the glutathione S-transferase (GST)-tagged protein (pGEX-RKIP-1) was performed by Glutathione Affinity purification. *E. coli* BL21(DE3) cells were transformed with a pGEX-2T vector enclosing the RKIP-1 coding sequence. Cells were grown for 2–3 hours at 37°C, then the temperature was decreased to 20 °C prior to induction. Expression was induced with 1 mM IPTG at OD600 = 0.6 over-night at 20°C. Cells were harvested by centrifugation for 20 min at 4000 g at 4°C. Bacteria were suspended in 50 mM Tris-HCl pH 8.0, 500 mM

NaCl, and 1 mM DTT (buffer A) supplemented with EDTA-free Complete Mini Protease Inhibitor Cocktail (Roche) and were lysed using a French pressure cell press. The lysate was centrifuged for 45 min at 12000 rpm (15500 g, on a Beckman Coulter TA-14-50 rotor) at 4°C, and the supernatant was filtered and applied to a GST-affinity column (GE Healthcare) equilibrated with buffer A. GST-RKIP1 was eluted using buffer A supplemented with 10 mM reduced glutathione. The fusion protein was cut over-night with thrombin (Sigma Aldrich), then the cleaved GST tag was removed by a second GST-affinity chromatography. Finally, thrombin was removed from the purified RKIP1 exploiting a HiTrap Benzamidine FF (GE healthcare) column. The final protein was concentrated at ~2 mg/mL, aliquoted, flash frozen in liquid nitrogen, and stored at -80 °C. In each step samples were collected for 12 % sodium dodecyl sulfate polyacrylamide gel electrophoresis (SDS-PAGE) to test the GST-tagged protein expression. In each step samples were collected for 12% sodium dodecyl sulfate polyacrylamide gel electrophoresis (SDS-PAGE) to test the GST-tagged protein expression.

3.11 RT-PCR

Total RNA was extracted with Trizol reagent (Invitrogen) and isolated from OSNs (Embryonic and postnatal rat and postnatal mice OSNs) , and from OB of WT and PEBP1^{-/-} mice. Expression of PEBP1 was analyzed by reverse transcription polymerase chain reaction (RT-PCR). Total RNA was reverse-transcribed into single-stranded cDNA using the transcriptor high capacity cDNA Reverse Transcription kits (Applied Biosystem).

1µg of total RNA was retrotranscribed in a 25 µl reaction volume following the manufactures's instructions. β-actin was used as a control. The following primers were used: PEBP1: 5'-TCATGAATAGACCAAGCAGCAT-3'; 5'-CATGCTTTATACGACTTGACTG -3'; β-actin: 5'-CCCTGTGCTGCTCACC-3' and 5'-GCACGATTTCCCTCTCAG-3'.

3.12 Western blot

Proteins from olfactory bulb (embryonic and postnatal rat, wild type and PEBP1^{-/-} mice), heart and skin (wild type and PEBP1^{-/-} mice) were dissected and solubilized in RIPA lysis buffer (Invitrogen) + protease inhibitor cocktail (Sigma Aldrich) and fractionated by tissues Lyzer II (Qiagen) for 2 cycles of 30 seconds. Then, a centrifugation at 14000rpm at 4°C for 30 minutes was performed. Protein concentration was determined using BCA protein concentration assay kit (catalog #23225 Thermo Scientific) as manufacturer's instructions. Primary antibodies used were: rabbit anti-RKIP (1:800, Millipore) and mouse anti-β-Actin (1:5000, Sigma Aldrich). Secondary antibodies used were: horseradish peroxidase-conjugated anti-rabbit IgG (1:5000, GE Healthcare), horseradish peroxidase-conjugated anti-mouse IgG (1:5000, GE Healthcare) in PBS Tween-20 0.05% + 5% non-fat dry milk (Sigma Aldrich) for 1.5 hours at RT. Then, the filter (Amersham™Hybond™ P.045 PVDF, GE healthcare) was incubated with a chemiluminescent substrate (Thermo Scientific) and detected by ImageQuant LAS 4000mini (GE healthcare). Protein levels were normalized with β-actin (Sigma Aldrich).

3.13 Immunohistochemistry

Immunohistochemistry was performed on olfactory bulb (OB) sections (horizontal and coronal) of: wild type mice (WT, used as control), PEBP1^{-/-} mice, P2-GFP mice, M72-YFP mice, PEBP1^{-/-} X M72-YFP mice and PEBP1^{-/-} X P2-GFP mice, at postnatal day (P) > 40. Immunohistochemistry was performed also on horizontal OB sections of rat embryos (E18) and of postnatal rats, postnatal day P0-P4. Animals were euthanized and then perfused with 0.9% saline followed by 4% paraformaldehyde in 1X PBS. Brains were dissected and olfactory bulb promptly removed, post fixed overnight in 4% paraformaldehyde. Olfactory bulbs were sectioned at 40μm-60μm at the vibratome (Leica, VT 1000S) or at 25 μm at cryostat (Leica1860). Expression of PEBP1 was analyzed in C57BL/6 mice

(Charles River) and C57BL/6-Tyr^{c-Brd} (Charles River) as a control for PEBP1^{-/-} mice. No differences in PEBP1 expression were observed between C57BL/6 wild type and C57BL/6-Tyr^{c-Brd}, therefore the results were pooled together.

Primary antibodies used were: goat anti OMP (1:500, Wako Chemicals), rabbit anti RKIP, also known as PEBP1 (1:200, Millipore). Primary antibodies were revealed with CY3-conjugated donkey anti-goat (1:500, Jackson ImmunoResearch); Alexa Fluor 488-conjugated donkey anti-goat (1:500, Jackson ImmunoResearch); CY3-conjugated donkey anti-rabbit (1:500, Jackson ImmunoResearch). DAPI (1:50000, Invitrogen) was used as a nuclear counterstaining. Sections were mounted with Aqua-Poly/Mount (Polysciences) and images were acquired at the Zeiss LSM700 or Leica MZ16 microscopes. The signal intensity of PEBP1, background subtracted, were performed on anterior, medial, lateral and posterior side of olfactory bulb sections from embryonic and postnatal rat, WT and PEBP1^{-/-} mice, using Image J software (RRID: nif-000030467).

3.14 Whole mount analysis.

P2-GFP mice, P2-GFP; PEBP1^{+/-} mice, P2-GFP; PEBP1^{-/-} mice, M72-YFP mice, M72-YFP; PEBP1^{+/-} mice and M72-YFP; PEBP1^{-/-} mice were transcidentally perfused with 0.9 % saline followed by 4% paraformaldehyde in 1 X PBS. Brains were promptly removed and whole mount images of olfactory bulbs were taken on Leica MZ 16F stereo microscope. Lateral and medial views of the olfactory bulb, in P2-GFP mice, P2-GFP; PEBP1^{+/-} and P2-GFP; PEBP1^{-/-} mice, and dorsal views of the olfactory bulb of M72-YFP, M72-YFP; PEBP1^{+/-} and M72-YFP; PEBP1^{-/-} mice, were taken to calculate medial, lateral and dorsal surface areas, computed off line using Image J software. The same images were used to measure the position of the main homogeneous glomeruli along the antero-posterior and dorso-ventral axis, in cartesian coordinates. Y axis = a line parallel to the coronal plane that separates the olfactory bulb from the brain. A line perpendicular to the previous line .i.e. the Y axis, corresponds to the X axis. The dorso-ventral position of glomeruli was

calculated along the Y axis, while the antero-posterior position was computed along the X axis. No differences were observed between the position of the main glomeruli in the left and in the right olfactory bulb. Therefore, the data related to the position of glomeruli were pooled together for the right and the left olfactory bulb.

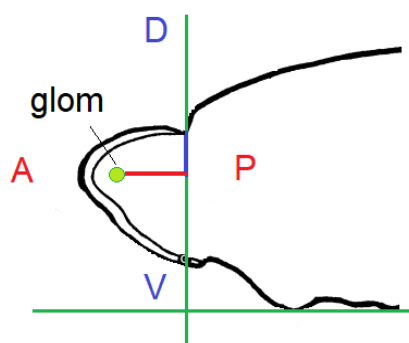


Figure 3.2: Example of whole bulbs analysis along A-P and D-V axis. Schematic view of the olfactory bulb. The position of a glomerulus (Glom), shown in green, is calculated by drawing a line parallel to the coronal plane that separates the olfactory bulb from the brain, that represents the Y axis (D/V position). The line perpendicular to the previous one, i.e. Y axis

correspond to the X axis (A/P position). The measurement were performed within these cartesian coordinates. A=Anterior; P=Posterior; D=Dorsal; V=Ventral. The dorso-ventral position of glomeruli was calculated along the Y axis, while the anterior-posterior position was computed along the X axis.

3.15 Habituation and dishabituation test in mice

Wild type (C57BL/6 wild type mice and C57BL/6-Tyr^{c-Brd} (Charles River) and PEBP1^{-/-} mice (Theroux et al., 2007) were habituated to the cage (35 X 20 X 14 cm) for 3 minutes. Then, mice were exposed for 3 minutes to a filter paper (2 x 2 cm) scented with a double-distilled water (ddW) (20 µl) for 3 times (Habituation-trial) with 1 minute inter-trial interval. On the 4th trial (Dishabituation-trial), a filter paper with Eugenol (1mM, Sigma Aldrich) was presented for 3 minutes. The mouse behaviour was recorded with a digital video camera (30 frames per second, 2592 X 1944 pixels) and the sniffing time in which mice nose contact (1mm distance) the filter paper was considered in the analysis as " investigation

time" and evaluated in seconds (s). We performed Student's *t*-test between the investigation time between the 3rd and 4th trail in control and PEBP1^{-/-} mice.

3.16 Statistical analysis

Data are presented as means \pm SEM. Normal distribution of the variables of interest was checked using Shapiro -Wilk test. Statistical comparisons of pooled data were performed using two-tailed Student's *t*-test. For experiments in which more than 2 groups were compared, one-way ANOVA followed by post-hoc Bonferroni correction, was performed using Prism software (GraphPad, San Diego, CA, USA). A *P* value of < 0.05 was considered statistically significant.

3.17 Key resources table

REAGENT or RESOURCE	SOURCE	IDENTIFIER
Antibodies		
rabbit-polyclonal anti RKIP (PEBP1)	Millipore	Cat#07-137
anti-olfactory marker protein (OMP)	Wako Chemicals	Cat#544-10001
donkey anti-goat (H+L), Alexa 488	JacksonImmuno	Cat#705-545-147
donkey anti-rabbit (H+L),Cy3	JacksonImmuno	Cat#711-165-152
mouse anti β -actin	Sigma Aldrich	Cat#MA1-140
ECL TM anti-rabbit HRP-conjugated	GE Healthcare	Cat#NA934V
ECL TM anti-mouse HRP-conjugated	GE Healthcare	Cat#NA931
BCA protein concentration assay kit	Thermo Scientific	Cat #23225
Chemicals, Peptides, and Recombinant Proteins		
(\pm) Citronellal	Sigma Aldrich	Cat#C25-13
(R)-(-) Carvone	Sigma Aldrich	Cat#12,493-1
(S)-(+) Carvone	Sigma Aldrich	Cat#435759
2-coumaranone	Sigma Aldrich	Cat#12,459-1
2-isobutyl-3-Methoxypyrazine (IBMP)	Sigma Aldrich	Cat#297666
3,7-Dimethyl-2,6-Octadienenitrile (Citalva)	Sigma Aldrich	Cat#15,767-8
Acetophenone	Fluka	Cat#00790
Benzaldehyde	Sigma Aldrich	Cat#41,809-9
Benzyl alcohol	Fluka	Cat#13170
Carbamoylcholine chrolide (Carbachol)	Sigma Aldrich	Cat#4382
Cytosine β -D-arabinofuranoside	Sigma Aldrich	Cat# C1768
D-Valine	Sigma Aldrich	Cat#1255
Eugenol	Sigma Aldrich	Cat#E51791

Forskolin	Sigma Aldrich	Cat#F6886
Fura-2,AM	Life technologies	Cat#F1201
Geraniol	Fluka	Cat#48799
High capacity cDNA Reverse Transcription kits	Applied Biosystems	Cat# 4368813
Heptanoic acid	Sigma Aldrich	Cat# 111-14-8
Hexanal	Sigma Aldrich	Cat#11,560-6
L- glutathione reduced	Sigma Aldrich	Cat#G4251
Lipofectamine 2000	Thermo Fisher	Cat#11668027
Menthone	Fluka	Cat#63680
Methyl salicylate	Sigma Aldrich	Cat#M6752
Nerve growth factor (NGF)	Corning	Cat#354009
Nonanedioci acid	Sigma Aldrich	Cat# 246379
Pluronic acid	Life technologies	Cat# P2443
Poly-L-Lysine	Sigma Aldrich	Cat#P2636
Propionic acid	Fluka	Cat#81912
Sulphinyl pyrazine	Sigma Aldrich	Cat# P56003
Tetrodotoxin (TTX)	Latoxan	Cat#L8503
Thrombin	Sigma Aldrich	Cat#T6884
TransFectin™ Lipid Reagent	Biorad	Cat#170-3350
Trizol	Invitrogen	
Vanillic acid	Sigma Aldrich	Cat#94770
Experimental Models: cell lines		
human:HEK293T cells	ATCC	ATCC® CRL-3216™
Experimental Models: Organisms/Strains		
mouse: wild type C57BL/6J	Jackson Lab	Stocknum#000664
mouse: wild type C57BL/6-Tyr ^{c-Brd}	Charles River	Strain code 493

mouse: RKIP1 ^{Gt(pGT01xrBetageo)1Jkl} (PEBP1 ^{-/-})	Evan Keller	Michigan University
mouse:P2-IRES-GFP (P2-GFP)	J.A Gogos	Columbia University
mouse:Olf160 ^{tm1.1(COP4*/EYFP)1boz} /J (M72-ChR2-YFP)(M72-YFP)	Charles River	Cat#021206
rat:sprague Dawley	Charles River	Strain code 001
Recombinant DNA		
pCI	H. Matsunami	Duke University
OREG (MOR174-9)	H. Matsunami	Duke University
P2 (MOR171-3)	H. Matsunami	Duke University
S6 (MOR42-3)	H. Matsunami	Duke University
Olf162 (MOR 258-5)	H. Matsunami	Duke University
M72 (MOR263-5)	H. Matsunami	Duke University
G _{α15}	H. Matsunami	Duke University
RTP1S	H. Matsunami	Duke University
RTP2	H. Matsunami	Duke University
pGEX2T-rat-RKIPcDNA	MR Rosner	Chicago University
mKate	Thermo Fisher	
Epac-based sensor for cAMP	Ponsioen et al.,2004	
Software and Algorithms		
MassLynx 4.1	Waters Corporation	
MassHunter Qualitative Analysis Software B.03.01	Agilent Technologies	
Mascot Search Engine 2.2.4	Matrix Science	
Image J	NIH Software	RRID:nif-000030467
Prism 7.0	GraphPad Software	RRID:SCR_002798

Cell R	Olympus BioSystems	
Other		
Slide-A-Lyzer Dialysis cassette	Thermo Scientific	Cat#66330
HiTrap™ Benzamidine FF (High Sub)	GE Healthcare	Cat#17-5143-01
Glutathione Agarose	Jena Bioscience	Cat#AC-210-10
Superdex 200-prep-grade 300/10 column	GE Healthcare	Cat#S6782
HiTrap Capto Q column	GE Healthcare	Cat#11-0013-02
ImageQuant LAS 4000mini	GE healthcare	
AKTA Fast protein Liquid Chromatography System	GE Healthcare	
Jupiter C4 Column	Phenomenex	
Electrospray ionization mass spectrometry with Q-TOF analyzer	Waters Corporation	
Q-TOF mass spectrometer	Agilent Technologies	
PV80 pneumatic PicoPump	WPI	Cat#SYS-PV820
Single Channel Pulse Generator (A310 Accupulser)	WPI	Cat#SYS-A310
Thermostatic chamber	Warner Instruments	
Tissues lyzer II	Quiagen	

4 RESULTS

4.1 Identification of a ligand of axonal odorant receptor: a phosphatidyletanolamine-binding-protein-1 (PEBP1)

In a previous work, Lodovichi's group by performing Ca^{2+} imaging experiments demonstrated that a pool of cues extracted from embryonic rat olfactory bulb, was able to elicit Ca^{2+} response at the axon terminal of olfactory sensory neurons (OSNs) and in HEK293T cells transfected with a specific odorant receptor (OR) (see paragraph 1.5).

By mass spectrometry, among the active pool of molecules isolated from the OB, they identified a small protein of 21kDa, named phosphatidyletanolamine-binding-protein-1 (PEBP1) as a putative ligand of the odorant receptor expressed at the axon terminal of olfactory sensory neurons. PEBP1, also known as Raf-kinase inhibitory protein-1(RKIP-1), belongs to a highly conserved protein family (see paragraph 1.6), widely expressed in non-neuronal and neural cells (*Frayne et al., 1999; Al-Mulla et al., 2013*).

Its small molecular weight, its ability to be secreted, although in non-canonical way and the presence of olfactory deficits in mice carrying a null mutation for PEBP1 (*Goumon et al., 2004; Theroux et al., 2007*), make PEBP1 a suitable candidate to be a putative ligand of the odorant receptor (OR). Noteworthy, the receptor of PEBP1 is still unknown and its function in the brain remains elusive.

4.2 PEBP1 activates odorant receptors expressed at the axon terminal of olfactory sensory neurons.

To ascertain whether PEBP1 can activate the OR at axon terminal of olfactory sensory neurons, we performed calcium imaging experiments in rat and mouse olfactory sensory neurons (OSNs) in response to PEBP1, isolated from embryonic rat olfactory bulb (OB) (**Figure 4.1 a, c**). Embryonic rat olfactory neurons, loaded with Ca^{2+} indicator fura-2, exhibited a prompt Ca^{2+} rise at the axon terminal in response to PEBP1 locally applied with a glass pipette (**Figure 4.1 a, c - d**). Noteworthy, PEBP1 extracted from rat bulb elicited a prompt Ca^{2+} rise also at axon terminal of mouse olfactory sensory neurons, corroborating the role of this molecule as ligand of the odorant receptor (**Figure 4.1 b, d**).

To assess whether the calcium rise observed in OSNs was due to OR activation, we studied Ca^{2+} dynamics in HEK293T cells transfected with specific OR (OREG, P2, S6, Olfr62, M72), loaded with fura-2 and challenged with PEBP1 and with the corresponding odor of the transfected odorant receptor: vanillic acid (VA) for the receptor EG, nonanedioic acid (NA) for the receptor S6, 2-coumaranone (CMR) for the receptor Olfr62, methylsalicylate (MS) for the receptor M72 (**Figure 4.1 f, i**). Carbachol (CCH) was used for the receptor P2, whose corresponding-odor is still unknown (**Figure 4.1 g, i**).

No rise in Ca^{2+} was observed in HEK293T cells transfected only with the empty vector (not expressing any OR, pCI) (**Figure 4.1 e, i**), used as controls. A prompt Ca^{2+} rise was observed in response to CCH used as a test of cell vitality.

A prompt Ca^{2+} rise was observed in HEK293T cells transfected with the odorant receptor OREG, P2, S6 and olfr62 in response to PEBP1, and to the corresponding odor (**Figure 4.1 f, i**). However, we found that M72 was not responsive to PEBP1 but only to M72-corresponding odor methylsalicylate (MS) (**Figure 4.1 h-i**) suggesting the presence of other molecules elaborated in the olfactory bulb that could activate other odorant receptors, such as M72-OR.

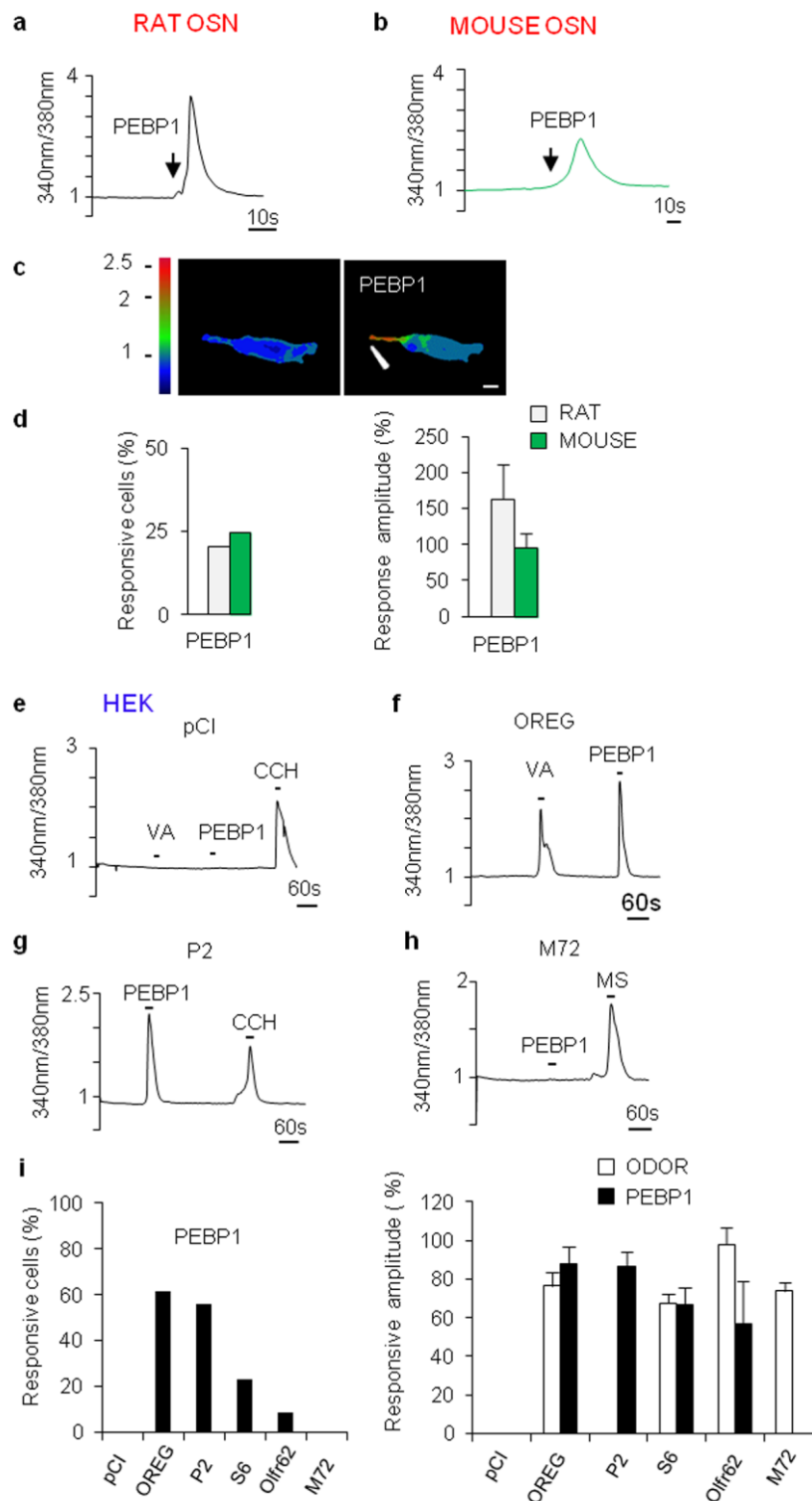


Figure 4.1. Ca^{2+} dynamics in olfactory sensory neuron (OSN) axon terminals and HEK293T cells in response to phosphatidylethanolamine-binding protein-1 (PEBP1). Fura-2 Ca^{2+} imaging. **a-b)** Normalized fluorescence ratio changes (340 nm / 380 nm) at the OSN axon terminals of rat (a) and mouse (b), upon stimulation with PEBP1. **c)**

Pseudocolor images of the rat OSN, showing changes in $[Ca^{2+}]_i$ at the axon terminal (arrowhead) before and upon application of PEBP1. Scale bar, 20 μ m. **d)** Summary of results (Embryonic rat OSNs: $\Delta R/R0\% = 162.70 \pm 49.05$, PEBP1-responsive cells = 20.55%, cell n = 15; Mouse OSNs: $\Delta R/R0\% = 95.42 \pm 20.42$, PEBP1-responsive cells = 24.56%, cell n = 14). **e)** HEK293T 7 cells not expressing odorant receptors, (pCI= empty vector, n = 112) do not exhibit Ca^{2+} response to PEBP1 nor to odor, i.e. vanillic acid (VA). A prompt Ca^{2+} rise is observed in response to carbachol (CCH), used as control. **f-h)** Examples of Ca^{2+} dynamics in HEK 293T cells transfected with distinct odorant receptors (OREG, P2, M72) and stimulated with the corresponding odor (vanillic acid, VA; methyl salicylate, MS) or carbachol (CCH) and with PEBP1. **i)** Summary of results (PEBP1: pCI responsive cells = 0%; CCH: $\Delta R/R0\% = 74 \pm 0.4$; OREG-responsive cells n = 70, (61.70%); $\Delta R/R0\% = 87.9 \pm 9.05$; P2-responsive cells n = 39 (55.71%); $\Delta R/R0\% = 86.4 \pm 7.14$; S6-responsive cells n = 112 (23.2%); $\Delta R/R0\% = 66.8 \pm 8.8$; Olfr62-responsive cells n = 45 (7%); $\Delta R/R0\% = 14.5 \pm 4.1$; M72 responsive cells = 0%; MS: M72 responsive cells n = 110 $\Delta R/R0\% = 73.8 \pm 4.20$). Bars = SEM

Then, to verify the specificity of PEBP1 activity we performed several controls. We studied Ca^{2+} dynamics in HEK293T cells transfected with specific OR, in response to PEBP1 denatured by higher temperature (PEBP1 Heated), or by proteinase K (PEBP1+proteinase K) (see methods for details).

To exclude that contaminants, rather than PEBP1 itself, elicited Ca^{2+} rise, HEK cells expressing specific OR were challenged with another protein, named cyclin-dependent kinase 2 (CDK2), that was purified with the same protocol than the one used to purify PEBP1 (**Figure 4.2.**). No Ca^{2+} rise was observed in response to PEBP1 denatured (heated PEBP1 and PEBP1+proteinase K, ProtK) nor in response to CDK2.

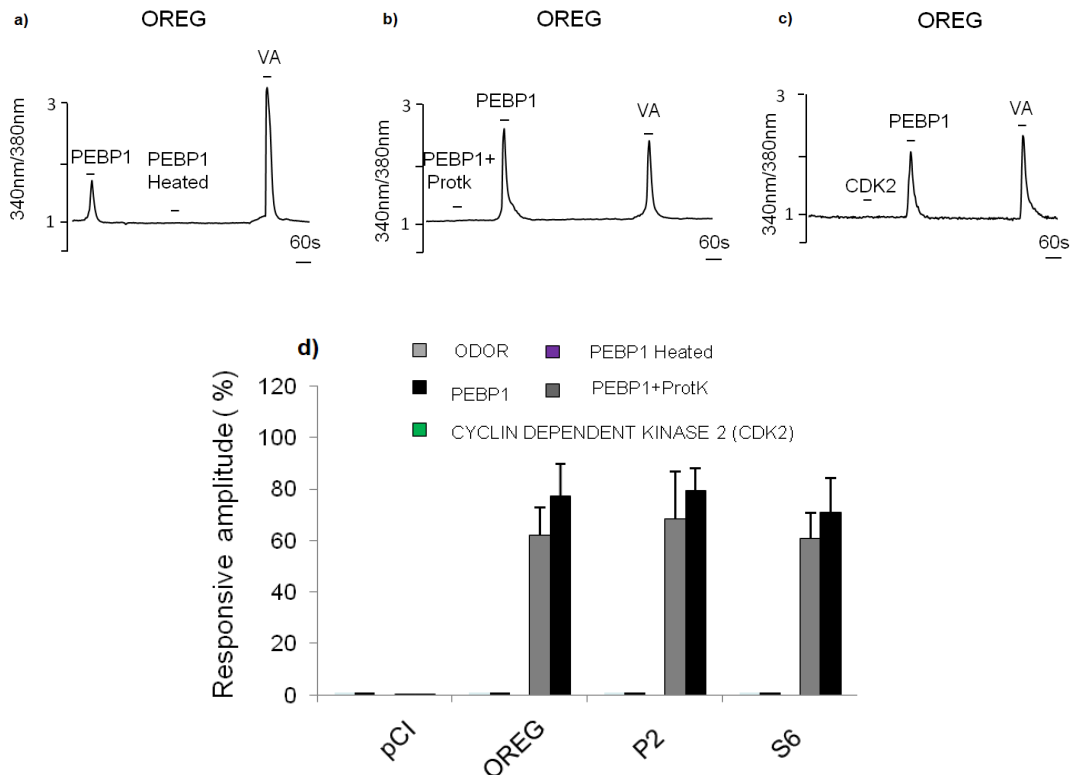


Figure 4.2. Ca^{2+} dynamics in HEK 293T expressing specific OR in response to PEBP1 denatured and to cyclin-dependent kinase 2 (CDK2). Fura-2 Ca^{2+} imaging. **a-c)** Examples of Ca^{2+} dynamics in HEK 293T cells transfected with the odorant receptors OREG challenged with PEBP1, the corresponding odors and PEBP1 denatured with higher temperature (PEBP1 Heated) in a, or with Proteinase K (PEBP1+ProtK) in b, or challenged with cyclin-dependent kinase 2 (CDK2) used as a control of the purification procedures. For the receptors OREG and S6 Vanillic acid (VA) and nonanedioic acid were used as corresponding odors. For the P2 odorant receptors we used Carbachol (CCH) since P2 corresponding odor is still unknown. **d)** Summary of results. Bars = SEM. (PEBP1 heated: OREG n = 26; PEBP1+ProtK: OREG n=9; P2 n=29; S6 n=14; CDK2: OREG n = 14; P2 n=8; S6 n=27).

4.3 PEBP1 modulates axon turning behavior of olfactory sensory neurons

Axon guidance molecules play an important role in the axon elongation and turning behavior. To ascertain whether the identified ligand of the axonal OR can affect the growth cone behaviour of the OSN, real time imaging of single olfactory neuron axon turning was performed in response to a gradient of PEBP1 (**Figure 4.3**).

To study the turning behavior of the growth-cone of OSN, we generated microscopic gradients by pulsatile ejections of molecules able to modulate cAMP and/or Ca^{2+} levels at the axon terminal, such as forskolin (FRSK) (a generic activator of adenylyl cyclase, AC), a mix of odors, the active pool of molecules (IEC-2) elaborated in the OB and the putative ligand of axonal OR, PEBP1.

To analyze the turning behaviour of the axon, we evaluated the turning angle between the position of the axon at the beginning ($t=0$), and the position of the axon at the end of the stimulation period (**Figure 4.3 f-g**).

We found, that not only pharmacological agent such as forskolin, and odors, but also the active pool of molecules (IEC-2) and, most importantly, PEBP1 were able to modulate the axon turning behaviour (**Figure 4.3**). All together our results indicate that PEBP1 can trigger Ca^{2+} rise at the axon terminal via OR activation and direct neurite turning.

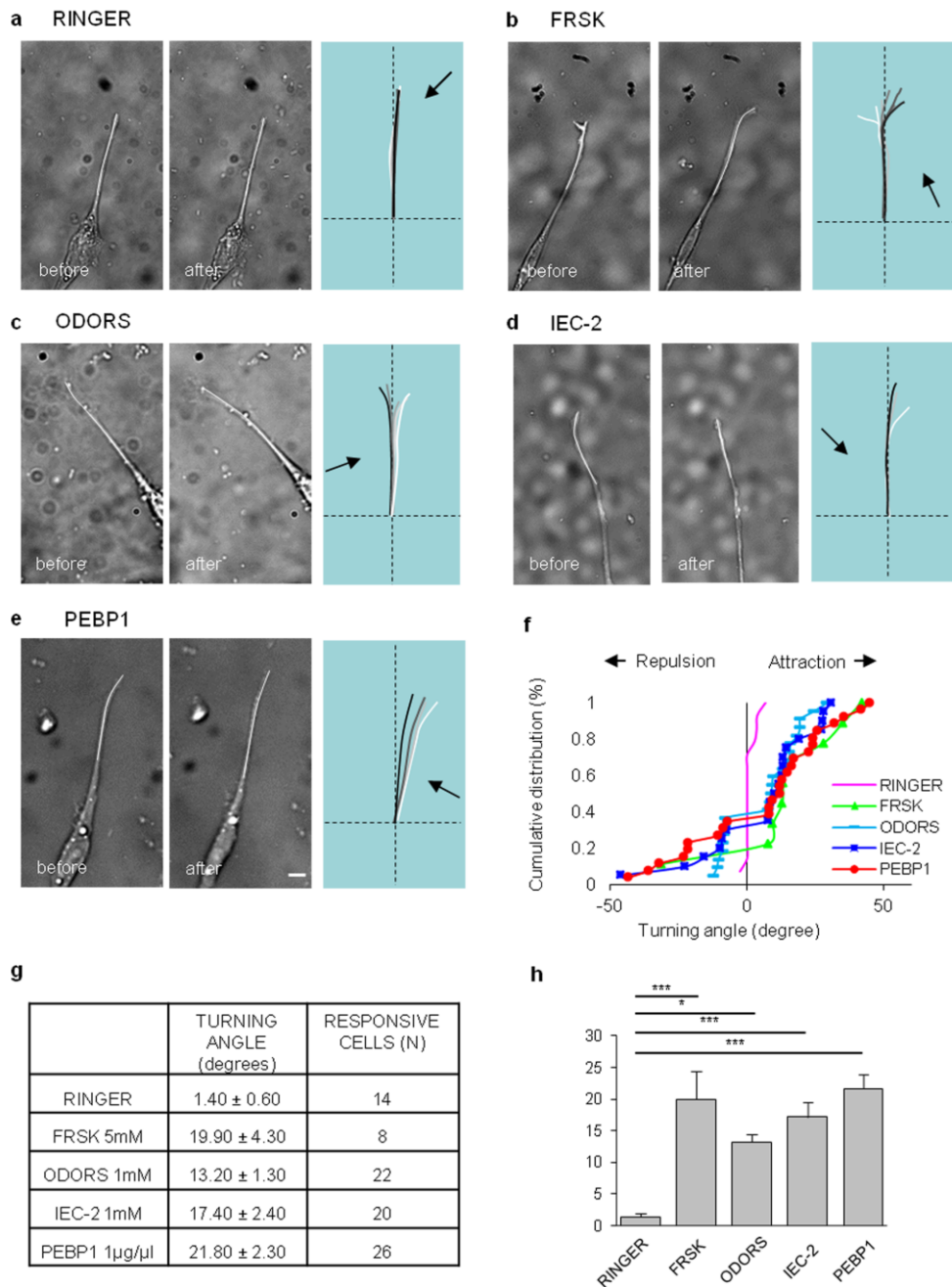


Figure 4.3. Turning response of olfactory sensory neuron (OSN) axon terminal in presence of chemical gradients. a-e) Examples of stop-frames of isolated embryonic rat OSN axon terminals at the beginning (left panel) and at the end (central panel) of pulsatile application of chemicals from a glass pipette. Axon terminals are highlighted with a white line. Composite drawings (right panel) of the turning responses of neurites during the stimulation period were made superimposing traces to the video records of the microscopic images. White traces depict the position of the axon terminal at the beginning, while black

traces indicate the trajectory of the neurites at the end of the stimulation period (1h). Trajectories of the axon terminal at intermediate time points during the stimulation period are indicated by traces in shades of gray. Black arrows indicate the pipette position. OSNs were stimulated with pulsatile application of: **a)** Ringer's solution, **b)** forskolin (FRSK), **c)** odors mixture, **d)** ionic exchange chromatography peak 2 (IEC-2) and **e)** phosphatidylethanolamine-binding protein 1 (PEBP1). Scale bar, 20 μ m. **f)** Distribution of turning angles for all neurons in response to the chemicals tested. **g-h)** Summary of results, reported as mean \pm SEM. One-way ANOVA, Bonferroni corrected, * $p < 0.05$; ** $p < 0.01$; *** $p < 0.001$.

4.4 PEBP1 expression in the rat and mouse olfactory bulb

To analyze the expression pattern of PEBP1, we performed detailed immunofluorescence assays both in embryonic, postnatal rat and postnatal mouse olfactory bulb sections (**Figure 4.4 -Figure 4.6**). Mice carrying a null mutant for PEBP1 (PEBP1^{-/-} mice, see methods) were used as a negative control (**Figure 4.6 i**).

First, we performed immunofluorescence in embryonic and postnatal rat olfactory bulb sections with antibody against PEBP1 (**Figure 4.4; Figure 4.5**). We found that PEBP1 was highly expressed in periglomerular cells, the cells that surround the glomeruli, a suitable location for the expression of a molecule that was supposed to act on the incoming olfactory sensory neuron axons.

We found that in both developmental stages, high expression of PEBP1 was detected in periglomerular cells in the anterior (A), medial (M) and lateral (L) side of the OB (**Figure 4.4 a-d; Figure 4.5 a-e**) while low expression was present in the posterior (P) side (**Figure 4.4 a, e; Figure 4.5 b, f**). PEBP1 expression was distributed in a patchy pattern, with no a clear gradient.

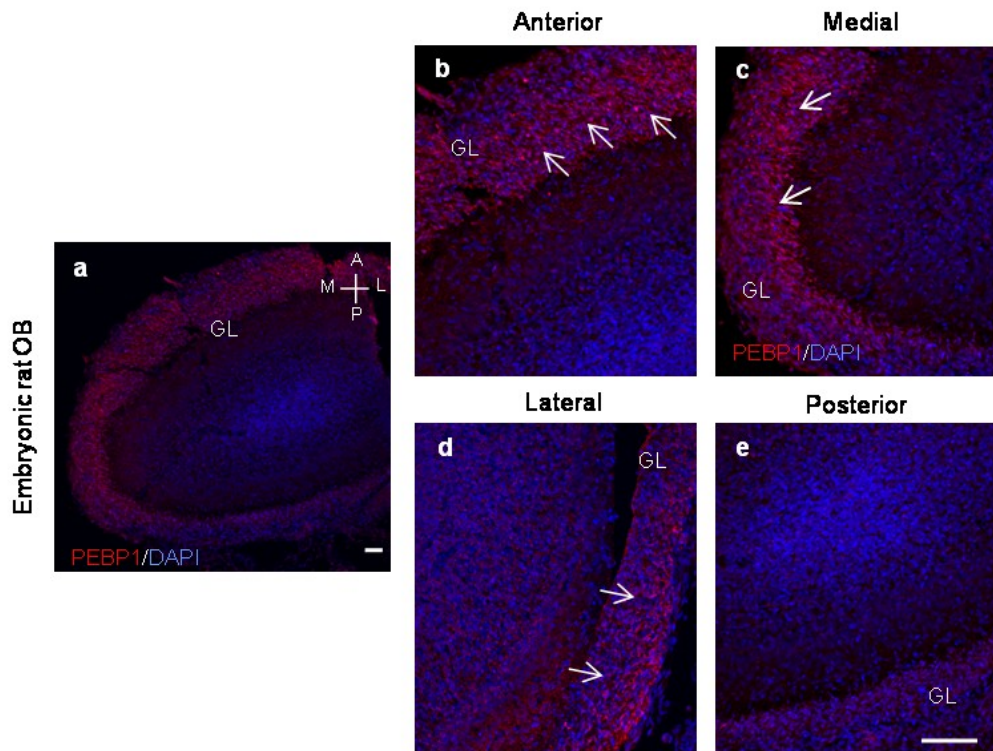


Figure 4.4. Expression of phosphatidylethanolamine-binding protein 1 (PEBP1) in embryonic rat olfactory bulb (OB). **a**) Horizontal sections of rat OB labelled for PEBP1 (red). Nuclear marker DAPI (blue). **b-e**) Higher magnification of the anterior (**b**), medial (**c**), lateral (**d**) and posterior (**e**) side of the embryonic rat olfactory bulb shown in **a**. **b-c**) High expression of PEBP1 is detected in periglomerular cells in the anterior (**a**), medial (**b**) and lateral (**c**) side of embryonic rat OB. Low expression is present in the posterior (**e**) side of the bulb. A=anterior; M=medial; L=lateral; P=posterior side of the olfactory bulb (Rat embryos $n = 5$, from 4 pregnant rats; Postnatal rat pups, P0-P4, $n = 5$, from 5 litters; Wild type (WT) mice $n=8$; PEBP1^{-/-} mice (mice $n = 4$). Scale bar, 50 μ m in **a**). Scale bar, 100 μ m in **b-c**, **d-e**).

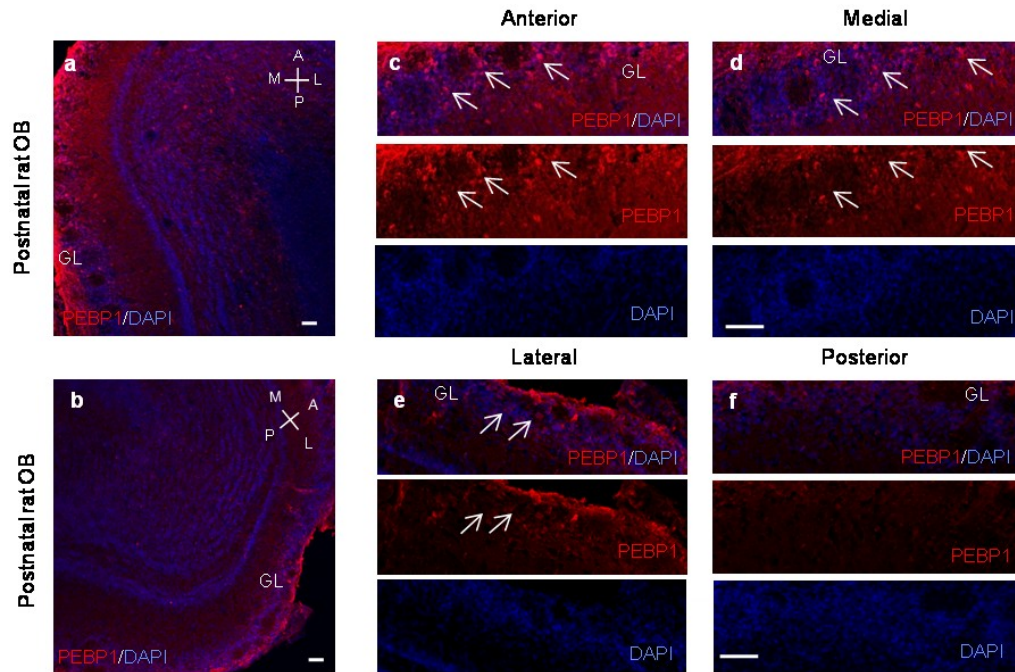


Figure 4.5. Expression of phosphatidylethanolamine-binding protein 1 (PEBP1) in olfactory bulb (OB) of postnatal day 2, (P2) mice. Horizontal sections of postnatal rat OB with antibody against PEBP1 (red). Nuclear marker DAPI (blue). **a)** Anterior and medial side of the olfactory bulb. **c-d)** higher magnification of the anterior and medial sides of the section shown in a, where high expression of PEBP1 is detected in periglomerular cells. **b)** lateral and posterior side of the olfactory bulb labeled for PEBP1 (red) and DAPI (blue). **e-f)** Higher magnification of the lateral, posterior side of postnatal day 2 olfactory bulb shown in b. PEBP1 positive cells are observed around the glomeruli, in the periglomerular cells, in the lateral aspect of the OB in j. Low expression of PEBP1 is detected in the posterior side, in f. (Postnatal rat pups, P0-P4, n = 5, from 5 litters). scale bar, 50 μm in a-b). scale bar, 100 μm in c-d) and e-f). Arrows indicate PEBP1 positive cells. GL = glomerular layer. A= anterior, M = medial, P = posterior, L = lateral.

To further investigate the expression pattern of PEBP1, we performed immunostaining with antibody against PEBP1 also in mouse olfactory bulb sections (**Figure 4.6**).

Again, we found that PEBP1 was mostly expressed in the periglomerular cell in the anterior (A), medial (M) and lateral (L) side of the olfactory bulb, with a patchy distribution (**Figure 4.6 a-c, e-g**).

PEBP1 was hardly detected in the posterior (P) side of the olfactory bulb (**Figure 4.6 d, h**). No expression of PEBP1 around the glomeruli was detected in PEBP1^{-/-} mice (**Figure 4.6 i**).

Noteworthy, in zones of highly expression, PEBP1 is expressed in a patchy manner, without a clear gradient (see also **Figure 4.10**).

We performed a detailed quantification analysis of PEBP1 expression for each areas of rat bulb, (Anterior, medial, lateral and posterior side of OB) in both developmental stages, (**Figure 4.7 a**) and of mouse OB (**Figure 4.7 b**).

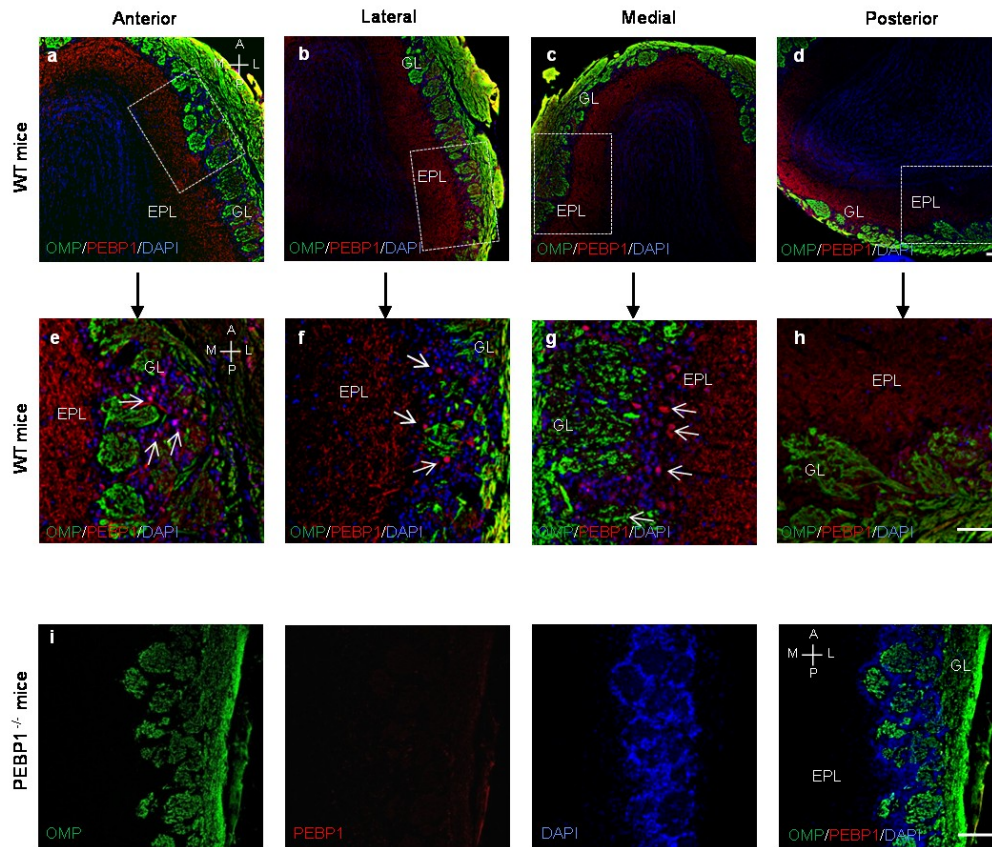


Figure 4.6. Expression of phosphatidylethanolamine-binding protein 1 (PEBP1) in mouse olfactory bulb (OB). Coronal sections of the mouse OB (> P40) labeled for PEBP1 (red), for olfactory marker protein (OMP) (green) and nuclear marker DAPI (blue). **a-d)** PEBP1 is highly expressed in periglomerular cells along the anterior (a), lateral (b) and medial (c) side of the OB. Low PEBP1 expression is detected along the posterior, d) side. Scale bar, 50 μ m. **e-h)** Higher magnification of the areas in dashed rectangles in a-d), respectively. Scale bar, 100 μ m. White arrows indicate PEBP1 positive cells. (wild type (WT) mice n = 8). **i)** Staining for PEBP1 in coronal sections of the OB of PEBP1^{-/-} mice. PEBP1 positive cells are not present in the OB of PEBP1^{-/-} mice (mice n = 4). Scale bar, 100 μ m. GL = glomerular layer. EPL = external plexiform layer. A= anterior, M = medial, P = posterior, L = lateral.

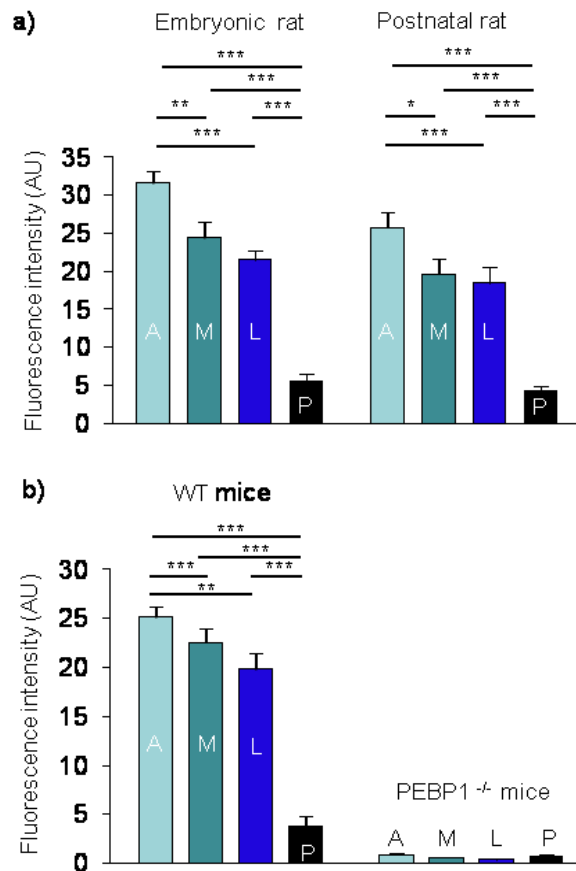


Figure 4.7. Quantification of PEBP1 expression in rat and mouse olfactory bulb (OB). Quantification of PEBP1 in OB coronal sections of embryonic and postnatal rat in a), and of wild type (WT) and PEBP1^{-/-} mice in b). Data are presented as mean ± SEM. One-way ANOVA, Bonferroni corrected, * p < 0.05; ** p < 0.01; *** p < 0.001. (Rat embryos n = 5, from 4 pregnant rats; Postnatal rat pups, P0-P4, n = 5, from 5 litters ; Wild type ,WT mice n = 8; PEBP1^{-/-} mice n = 4). Fluorescence intensity (AU) for each areas of the bulb: A=anterior; M=medial; L=lateral; P=posterior. (Rat embryos: Anterior=31.6±1.6, Medial=24.4±2.15, Lateral=21.5±1.3; Posterior=5.6±0.94; Rat postnatal P0-P4: Anterior=25.8±1.98; Medial=19.6±1.92; Lateral=18.47±2.02; Posterior=4.3±0.5; WT mice: Anterior=25.7±1.2, Medial=18.7±1.5, Lateral=20.3±1.4, Posterior=4.4±1.07).

We observed that PEBP1 is not expressed in the core of glomeruli, occupied by the axonal projections of olfactory sensory neurons, but only in periglomerular cells (Postnatal rat (n=3), and WT mice (n= 4) (**Figure 4.8**).

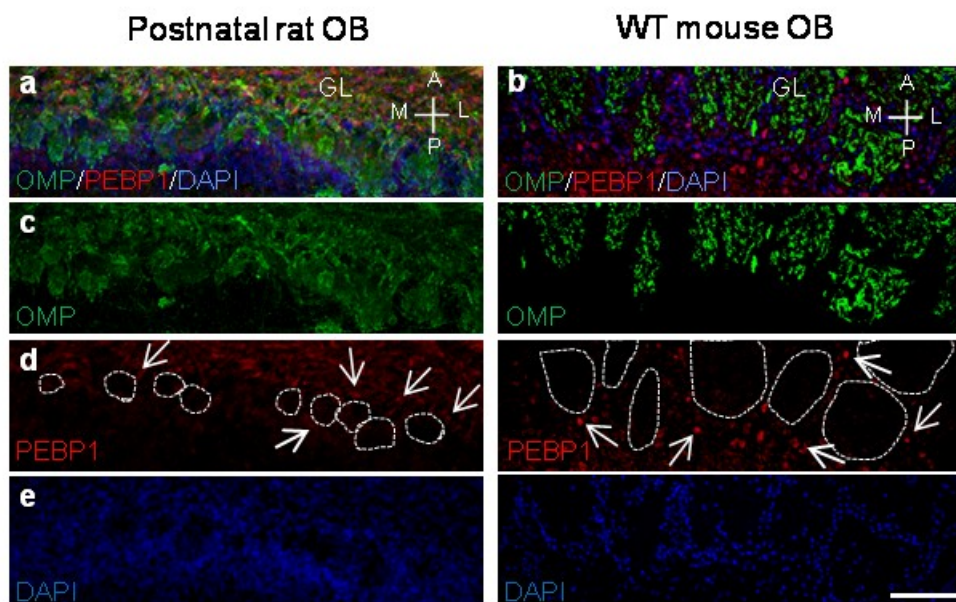


Figure 4.8. PEBP1 is not expressed in olfactory sensory neuron axon terminal located in the glomeruli. **a-b)** Horizontal sections of olfactory bulb (OB) of postnatal rat (n=3), **a** and mice (n= 4), **b**) olfactory bulb (OB). Immunofluorescence with olfactory marker protein, OMP (green), PEBP1 (red) and DAPI (blue). **c)** Immunostaining for OMP in rat (left) and mouse (right) OB. **d)** Immunostaining for PEBP1 in rat (left) and mouse (right) OB. PEBP1 is not expressed in olfactory sensory neuron axon terminals, at the glomerular level, but is expressed in periglomerular cells (indicated by arrows). Dashed circles indicate the boundaries of glomeruli. **e)** DAPI immunostaining in rat (left) and mouse (right) OB. Scale bar = 100 μ m. GL = glomerular layer. A = anterior, P = posterior, M = medial, L = lateral.

To confirm that PEBP1 is not expressed in OSNs, (see above) we performed immunofluorescence assay and RT-PCR in the MOE in embryonic, and postnatal rat, in postnatal mouse, in controls and in a PEBP1^{-/-} mice (**Figure 4.9**). By

immunofluorescence (Figure 4.9 a-t) and RT-PCR (Figure 4.9 u), we found that the olfactory sensory neurons did not express PEBP1. Western blot performed on the OB tissues confirmed the expression of PEBP1 in the OB (Figure 4.9v).

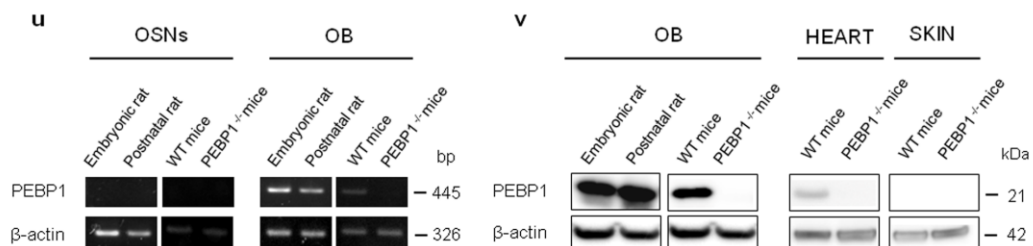
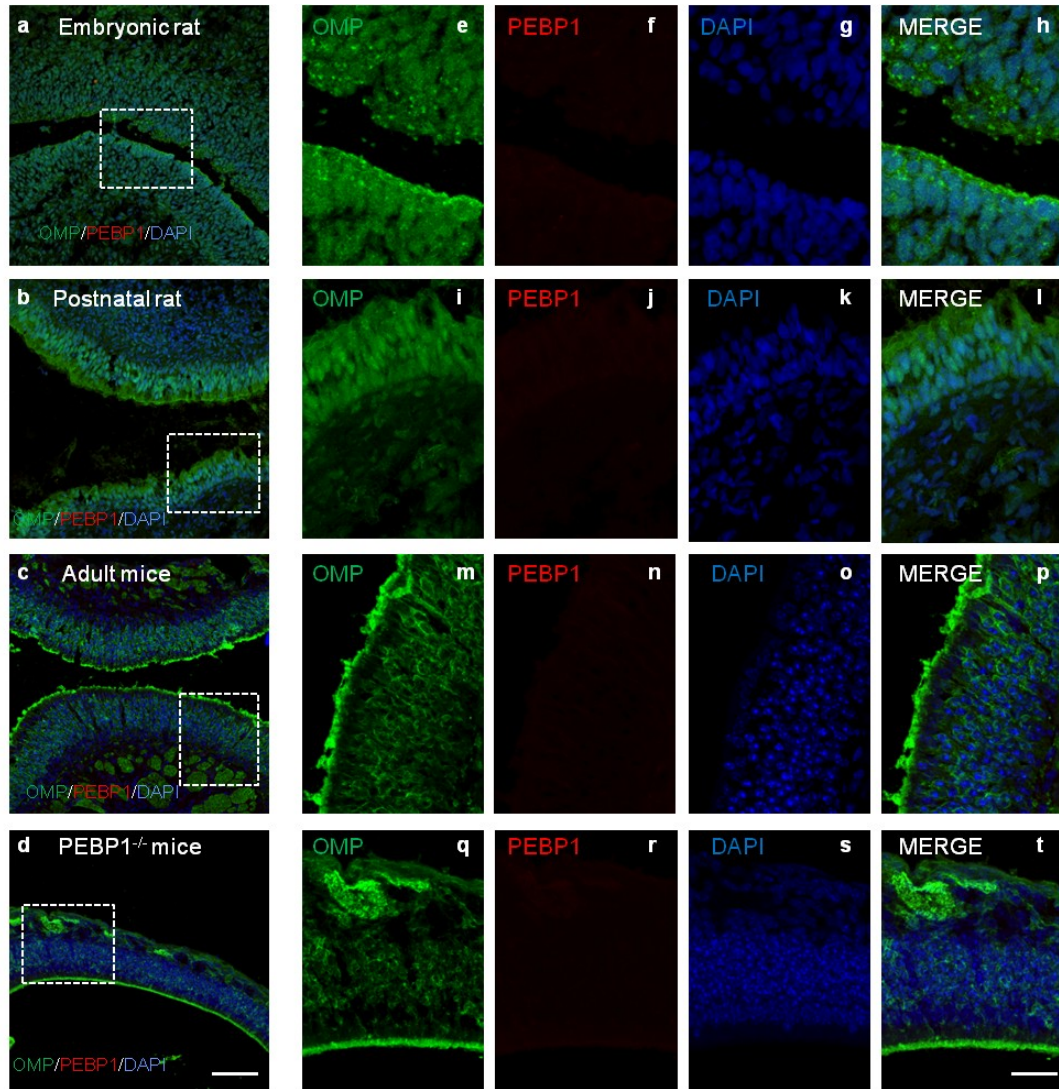


Figure 4.9. PEBP1 is not expressed in olfactory sensory neurons (OSNs) in the main olfactory epithelium (MOE) of rat and mouse. a-d) coronal sections of olfactory epithelium of a embryonic rat (n=3), **b)** postnatal rat (n=3), **c)** Adult mice (n=3), **d)** PEBP1^{-/-} mice (n=3), labelled for: olfactory marker protein (OMP) in green, PEBP1 in red, DAPI, in blue. Scale bar = 100 μm. In **e-t)** higher magnifications of the dashed rectangular areas in a- d, respectively, labeled for OMP, in green, PEBP1 in red, DAPI in blue. Merged images in the right column. Scale bar = 100 μm. **u)** RT-PCR for PEBP1 in olfactory sensory neurons (OSNs) and olfactory bulb (OB) of rat, WT and PEBP1^{-/-} mice. **v)** western blot analysis of protein extracts (30μg) from OB tissue of rat, WT and PEBP1^{-/-} mice with PEBP1 antibody. Heart and skin are used as positive and negative controls, respectively. β-actin is used as house-keeping gene. WT=wild-type.

All together these data indicate that PEBP1 is expressed in the periglomerular cell in the rat and mouse olfactory bulb (**Figure 4.4-4.7**) but not in olfactory sensory neurons (**Figure 4.8-4.9**).

Then, we analyzed PEBP1 expression around P2 and M72 glomeruli. We performed immunofluorescence experiments with antibody against PEBP1 in two different transgenic line of mice: P2-GFP and M72-YFP mice, in which the odorant receptor P2 and M72, are co-expressed with green fluorescent proteins (GFP or YFP, respectively). As a result of these genetic manipulations the axon of a specific odorant receptors (P2 and M72) and the corresponding glomeruli (P2-glomeruli and M72 glomeruli) are labeled in green and easily to identify. We choose the odorant receptors P2 because exhibited a prompt calcium response to PEBP1 in our *in vitro* Ca²⁺ imaging experiments, while M72 did not response to PEBP1, and therefore was used as a negative control (**Figure 4.1 g-i**). Noteworthy, P2 and M72 glomeruli are located in distinct areas of the olfactory bulb (**Figure 4.10 a-c, f-g**) that exhibited high expression (medial and lateral side) and low expression (posterior side) of PEBP1 (**Figure 4.4-4.7**) respectively.

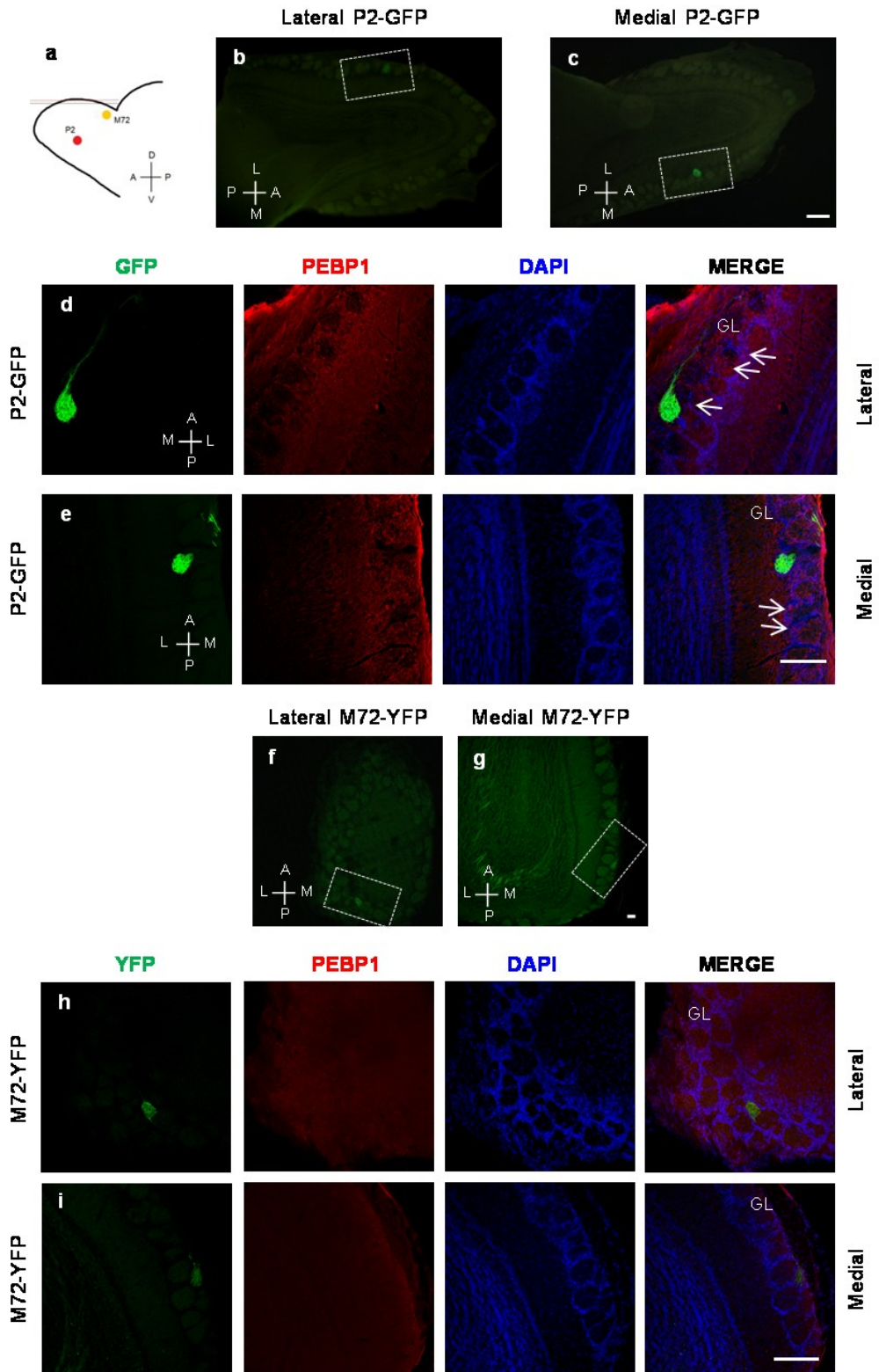


Figure 4.10. Expression of phosphatidylethanolamine-binding protein 1 (PEBP1) near P2-GFP and M72-YFP glomeruli. a) Schematic view of the P2 and M72 glomeruli

position, in the olfactory bulb (OB). **b–c**) Horizontal sections of the OB of P2-GFP mice, with the lateral, b and the medial, c P2-GFP glomeruli, in dashed rectangular areas. Scale bar, 500 μm . **d–e**) Horizontal sections of the same OB in b and c, stained for PEBP1 (red). GFP-expressing axons and corresponding glomeruli (green). Nuclei stained with DAPI (blue). Expression of PEBP1 is high in periglomerular cells around the medial and the lateral P2-GFP glomeruli (mice $n = 4$). Scale bar, 100 μm . Arrows indicate periglomerular cells expressing PEBP1. **f–g**) Horizontal sections of the OB of M72-YFP mice, with the lateral, f and the medial, g M72-YFP glomeruli, in dashed rectangular areas. Scale bar, 50 μm . **h–i**) Horizontal sections of the same OB in f and g stained for PEBP1 (red). YFP–M72 expressing axons and corresponding glomeruli (green). Nuclei stained with DAPI (blue). Almost none PEBP1 expressing cells are present in the area occupied by M72-YFP glomeruli (mice $n = 3$). Scale bar, 100 μm . GL = glomerular layer. A= anterior, M = medial, P = posterior, L = lateral

4.5 PEBP1^{-/-} mice show a deeply perturbed sensory map organization

To investigate the role of the OR ligand in the sensory map formation, we analyze the glomeruli organization in PEBP1^{-/-} mice. A hallmark of mature glomeruli is that they are formed exclusively by axons of OSN expressing the same odorant receptor, indicated as homogeneous glomerulus (i.e. formed by OSN axons expressing the same odorant receptor)(*Mombaerts et al., 1996*).

If PEBP1 directs the axonal convergence to form glomeruli in specific locations in the olfactory bulb, then mice carrying a null mutation for PEBP1 (PEBP1^{-/-} mice) should exhibit an altered segregation of sensory afferents and a disrupted sensory map.

To verify this hypothesis we analyzed the convergence of olfactory sensory axons to form glomeruli in PEBP1^{-/-} mice, crossed with P2-GFP and M72-YFP mice. GFP-YFP expression in OSNs, allows to identify olfactory sensory neuron axons and their corresponding glomeruli.

The choice of these two ORs was dictated by fact that P2 exhibited a prompt Ca²⁺ rise in response to PEBP1, while M72 was not responsive to PEBP1, in our in vitro experiments (**Figure 4.1 g-i**). Furthermore, P2 and M72 glomeruli are located in areas of the OB with different level of PEBP1 expression. Namely, P2 is in an area of high PEBP1 expression (medial side) while M72 is located on the posterior side of the bulb, where PEBP1 is hardly detected. (**Figure 4.4-4.7**) (**Figure 4.10**).

We studied the convergence of olfactory sensory axons in PEBP1^{-/-} crossed with P2-GFP (P2-GFP ; PEBP1^{-/-}) and M72-YFP mice (M72-YFP ; PEBP1^{-/-}) and their relative controls. We stained OB sections with antibodies against olfactory marker protein (OMP), a cytosolic protein of unknown function expressed by all mature OSNs.

Analysis of the organization of glomeruli was conducted both in heterozygous (P2-GFP ; PEBP1^{+/-} and M72-YFP ; PEBP1^{+/-}) and in homozygous mice (P2-GFP ; PEBP1^{-/-} and M72-YFP ; PEBP1^{-/-}).

We found that in P2-GFP control mice, P2-expressing fibers converge to form a main P2-homogeneous glomerulus, that is formed exclusively by fibers positive for OMP and GFP, i.e. expressing the same odorant receptor P2 (**Figure 4.11 a, g, h**). On the contrary, we found that in homozygous mice for PEBP1 crossed with P2-GFP (P2-GFP ; PEBP1^{-/-}), P2-GFP expressing fibers converge to form the main homogeneous glomerulus, but also target several additional glomeruli, formed by axons both positive for GFP and OMP (i.e. expressing P2), but also positive only for OMP, i.e. expressing different ORs from P2 (heterogeneous glomeruli) (**Figure 4.11 c, g, h**). The phenotype was even more deeply perturbed, with higher number of additional heterogeneous glomeruli in homozygous in respect to heterozygous PEBP1 mutant mice.

We calculated the number of heterogeneous glomeruli per each bulb in PEBP1 mutant mice (both heterozygous and homozygous mice) and in the control P2-GFP mice. We observed a significant increase number of heterogeneous glomeruli in heterozygous mice (P2-GFP ; PEBP1^{+/-}) in respect to controls. The homozygous PEBP1 mutant mice (P2-GFP ; PEBP1^{-/-}) showed a more deeply perturbed sensory map caused by higher number of additional heterogeneous glomeruli in respect to heterozygous mice and to P2-GFP control mice (**Figure 4.11 a-c, g, h**).

All these results provide compelling evidences that the sensory map was deeply perturbed by the presence of additional heterogeneous glomeruli (i.e. formed by fibers expressing different odorant receptor) in PEBP1^{-/-} mice .

To further explore the impact of PEBP1 on the spatial segregation of sensory afferents, we measured the diameter of the glomeruli and we found that it was similar in PEBP1^{-/-} and control mice (**Figure 4.12 z**).

By analyzing the extension of the OB area targeted by sensory projections in P2-GFP; control mice we found that axon fibers target a confined area of the bulb, strictly adjacent to the corresponding main glomerulus, in controls. Indeed, we could detect GFP-labeled fibers only in limited area closed to the main glomerulus in controls.

In P2-GFP; PEBP1^{-/-} mice the fibers targeted a very extended regions, significantly bigger than in controls. Furthermore, sensory fibers not only coalesce to form a main glomerulus, but targeted also several additional heterogeneous glomeruli, in respect to controls (**Figure 4.12 a-x,y**). A similar targeting defect, although milder, was observed also in heterozygous PEBP1 mutant mice.

We then analyzed the M72-GFP axonal convergence in PEBP1^{-/-} mice.

We found that in control M72-YFP mice and in PEBP1 mutant mice crossed with M72-YFP (M72-YFP ; PEBP1^{+/-} and M72-YFP ; PEBP1^{-/-}), M72-YFP axons converge exclusively to form M72 homogeneous glomeruli, composed by YFP-fibers both positive for OMP and GFP, meaning expressing the same odorant receptor M72 (**Figure 4.11 d-h**).

We did not observed any differences both in the diameter of the main M72-homogeneous glomerulus and in the M72-targeting fibers in PEBP1^{-/-} mice compared to controls (**Figure 4.13 h**).

All this data indicate that the sensory map in PEBP1^{-/-} crossed with P2-GFP mice is deeply disrupted by the presence of several additional heterogeneous glomeruli in respect to controls (**Figure 3.11**). The convergence of M72 fibers was not affected in M72-YFP ; PEBP1^{-/-} mice. These evidences suggest that PEBP1 regulates

olfactory sensory neuron axonal convergence for the receptor P2-OR and likely for other odorant receptors responsive to PEBP1, but not for the not responsive M72-OR. This data is in according to our *in vitro* calcium imaging experiments (**Figure 4.1 g, h, i**).

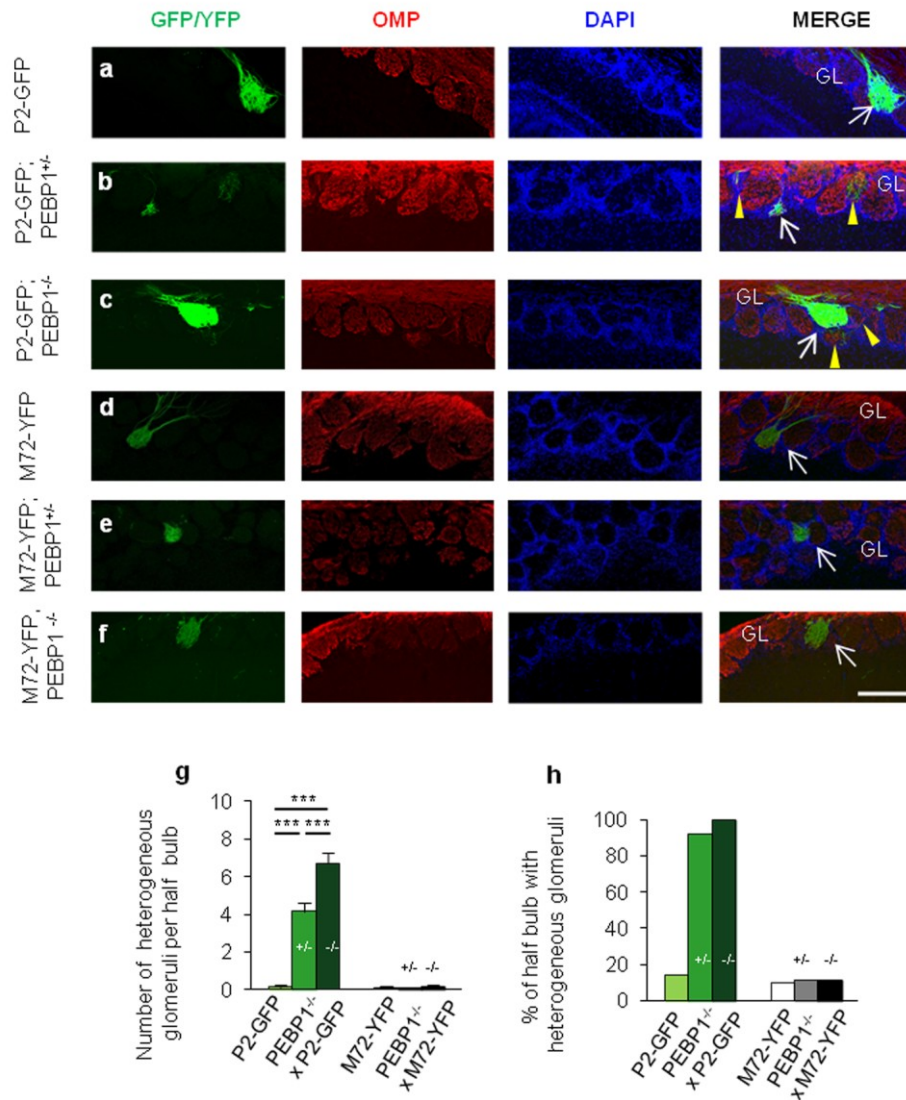


Figure 4.11. Alteration of the sensory map in phosphatidylethanolamine-binding protein 1 (PEBP1) mutant mice. Organization of P2 and M72 glomeruli revealed by immunolabeling sections of the olfactory bulb (OB) with antibodies against OMP (red). GFP and YFP-expressing P2 and M72 axons and corresponding glomeruli (green). Nuclei stained by nuclear marker, DAPI (blue). **a-c**) P2-axons positive for GFP and OMP coalesce

to form a main homogeneous glomerulus in control P2-GFP (mice n = 5) **a**), in P2-GFP ; PEBP1^{+/-} (mice n = 3). **b**), and in P2-GFP ; PEBP1^{-/-} mice (n = 4) **c**). P2 axons innervate also adjacent glomeruli, that result to be formed by fibers positive for GFP and OMP (i.e. expressing P2) but also by fibers positive only for OMP (i.e. expressing a different OR, heterogeneous glomeruli) in P2-GFP ; PEBP1^{+/-} (**b**) and in P2-GFP ; PEBP1^{-/-} mice (**c**). **d-f**) M72 glomeruli are formed by OSN axons expressing YFP and positive for OMP (i.e. homogeneous glomeruli) in control M72- YFP (n = 5). **d**), and also in M72-YFP ; PEBP1^{+/-} (n = 6), **e**) and in M72-YFP ; PEBP1^{-/-} mice (n=6). **f**) Scale bar, 100 μm. **g-h**) Summary of results. Bars = SEM. One-way ANOVA, Bonferroni corrected, ***P < 0.001. White arrows indicate homogeneous glomeruli. Yellow arrowheads indicate heterogeneous glomeruli. GL= glomerular layer. (P2-GFP control mice n=5, heterogeneous glomeruli n=0,14±0.10; P2-GFP ; PEBP1^{+/-}: n= 3 mice, heterogeneous glomeruli n=4,16±0.47,***p<0.001. One-way ANOVA Bonferroni corrected; P2-GFP ; PEBP1^{-/-}: n=4 mice, heterogeneous glomeruli n=6.7±0.58,***p<0.001 One-way ANOVA Bonferroni corrected). (M72-YFP: n=5 mice, heterogeneous glomeruli n= 0,10±0,10; M72-YFP ; PEBP1^{+/-} n=6 mice, heterogeneous glomeruli=0.07±0.07; M72-YFP ; PEBP1^{-/-}: n=6 mice, heterogeneous glomeruli n=0,17±0.11)

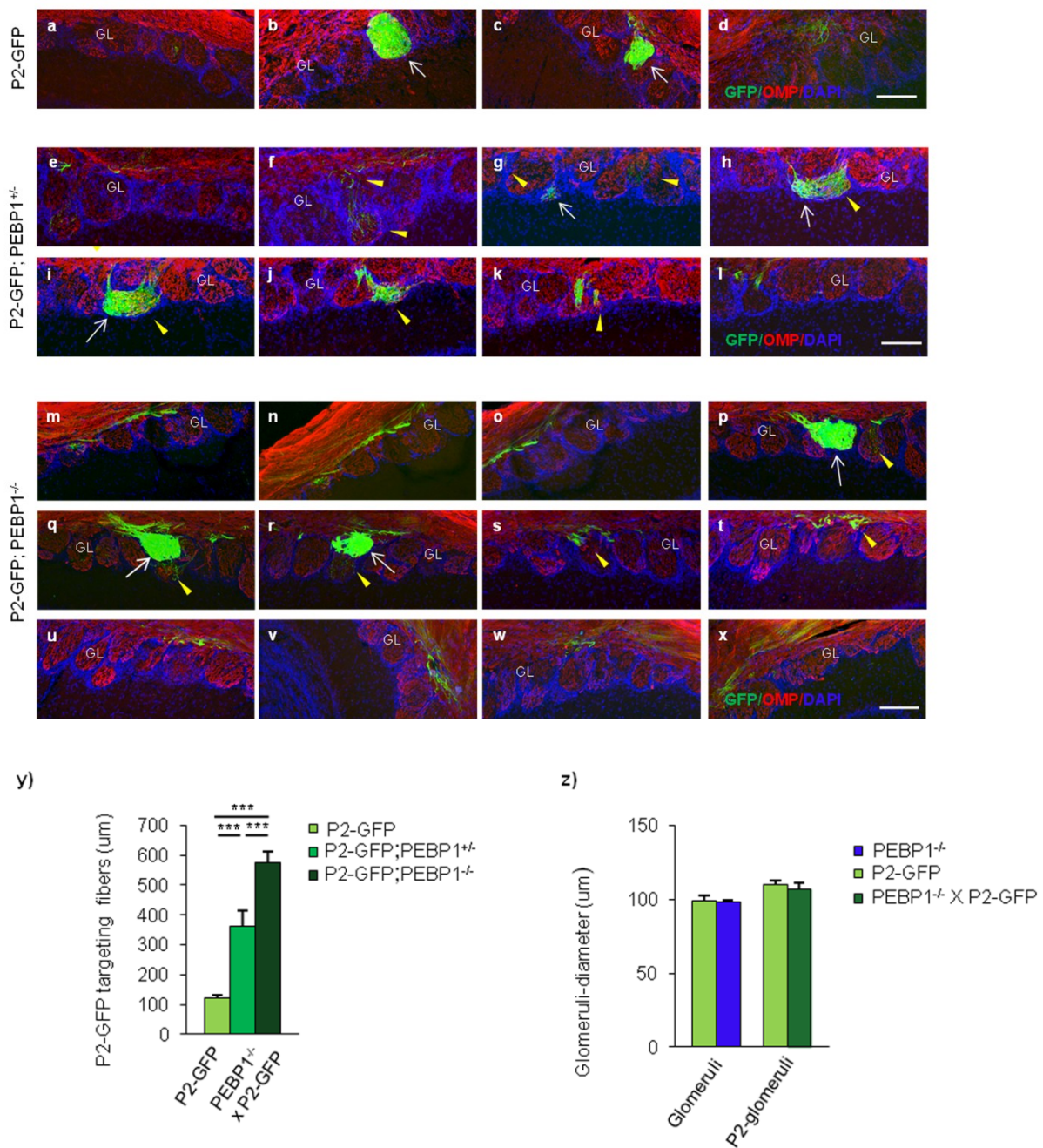


Figure 4.12. P2-GFP targeting fibers in PEBP1 mutant mice and in controls.a-z) Organization of P2-GFP fibers revealed by immunostaining of olfactory bulb horizontal sections (40µm) with antibody against OMP (red) and counterstaining DAPI (blue) in PEBP1 mutant mice crossed with P2-GFP mice (P2-GFP ; PEBP1^{+/-} , P2-GFP ; PEBP1^{-/-}) and in controls. P2-GFP -expressing axons and corresponding P2-glomeruli are shown in green. **a-y)** Targeting of P2-fibers around the main P2-homogeneous glomerulus in control P2-GFP (mice n = 5) (a-d), in P2-GFP ; PEBP1^{+/-} (mice n = 3) (e-l), and in P2-GFP ;

PEBP1^{-/-} (n = 4) (m-x). White arrows indicate P2-homogeneous glomeruli while yellow arrowheads indicate the additional P2-heterogeneous glomeruli. White arrows indicate homogeneous glomeruli. Yellow arrowheads indicate heterogeneous glomeruli. GL= glomerular layer. Scale bar, 100 μ m. **y)** Quantification of targeting fibers in P2-GFP mice and in PEBP1 mutant mice. (P2-GFP expansion fibers=121.4 \pm 8.4 μ m; P2-GFP ; PEBP1^{+/-} targeting fibers:360 \pm 54.4 μ m; P2-GFP ; PEBP1^{-/-} mice targeting fibers: 574.3 \pm 38.6 μ m ***p<0.001). Since we did not observe any differences between the expansion of P2-GFP fiber around the lateral and medial P2-glomeruli the data was pooled together. Bars = \pm SEM. *** p < 0.001. **z)** Quantification of the diameter of P2-homogeneous glomeruli in P2-GFP; PEBP1^{+/-} and P2-GFP; PEBP1^{-/-} mice in respect to controls. Since we did not observed any differences between diameter of P2-homogeneous glomerulus in P2-GFP ; PEBP1^{+/-} and P2-GFP ; PEBP1^{-/-}, we pooled data together. Bars = \pm SEM. *** p < 0.001. (P2-GFP: diameter=109 \pm 2.9 μ m; P2-GFP ; PEBP1^{+/-} mice diameter=111.3 \pm 6.4 μ m; P2-GFP ; PEBP1^{-/-} mice diameter=102.35 \pm 6.7 μ m) (P2-GFP mice n = 5; P2-GFP ; PEBP1^{+/-} mice n = 3, P2-GFP ; PEBP1^{-/-} mice n = 4)

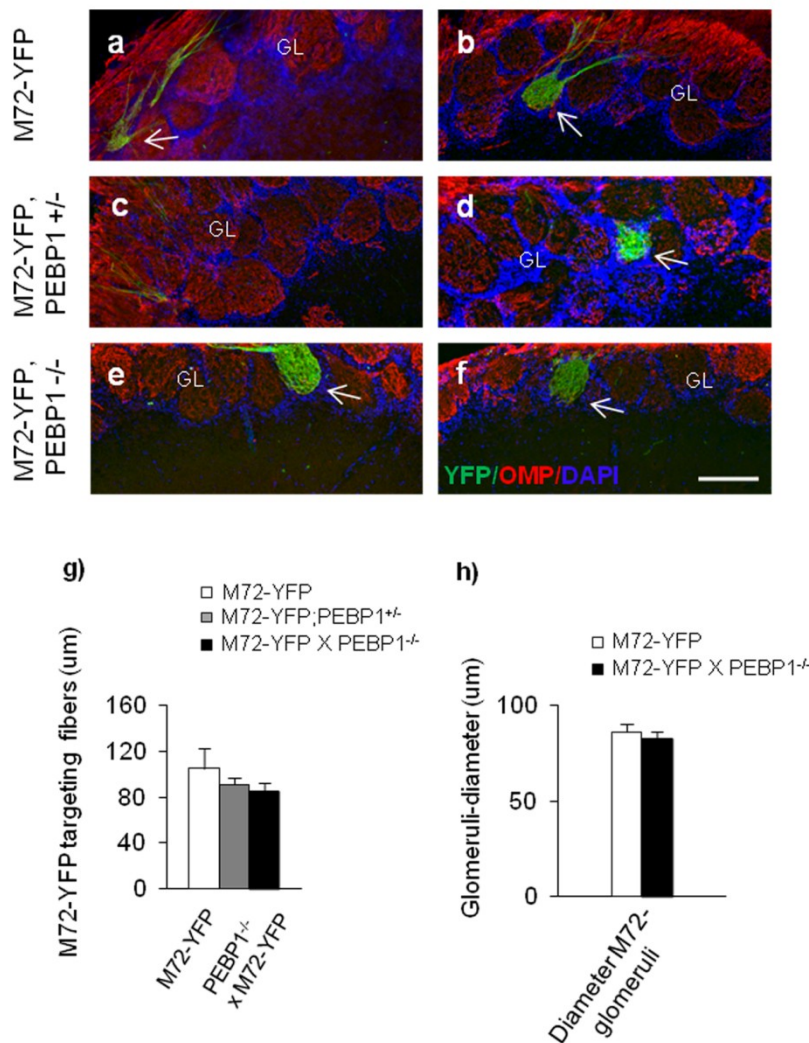


Figure 4.13. M72-YFP targeting fibers in PEBP1 mutant mice and in controls.

Organization of M72-YFP fibers revealed by immunostaining of olfactory bulb horizontal sections (40μm) with antibody against OMP (red) and counterstaining DAPI (blue) in PEBP1 mutant mice (M72-YFP ; PEBP1^{+/-} and M72-YFP ; PEBP1^{-/-}) and in controls. **a-g**) M72-YFP targeting fibers around the main M72-homogeneous glomerulus in M72-YFP control mice n=5 (a-b), M72-YFP ; PEBP1^{+/-} n=8 (c-d) M72-YFP ; PEBP1^{-/-} n=6 (**e-f**). GL= glomerular layer. **g**) Quantification of targeting fibers in P2-GFP mice and in PEBP1 mutant mice. Since we did not observe any differences between the expansion of P2-GFP fiber around the lateral and medial P2-glomeruli the data was pooled together. **h**) Quantification of the diameter of M72-homogeneous glomeruli in M72-YFP ; PEBP1^{+/-} and M72-GFP ; PEBP1^{-/-} mice respect to controls. (M72-YFP: diameter=86±4.3μm; M72-YFP ; PEBP1^{+/-} mice diameter=83.8±5.7μm; M72-YFP ; PEBP1^{-/-} mice diameter=82±3.4μm). Since we did not observed any differences between diameter of

M72-homogeneous glomerulus in M2-YFP ; PEBP1^{+/-} and M72-YFP ; PEBP1^{-/-} ,we pooled data together. Bars = \pm SEM. (M72-YFP control mice n=5, M72-YFP ; PEBP1^{+/-} n=8; M72-YFP ; PEBP1^{+/-} n=6). (M72-YFP targeting fibers=105 \pm 17,9 μ m; M72-YFP ; PEBP1^{+/-} targeting fibers=91 \pm 6.3 μ m; M72-YFP ; PEBP1^{-/-} targeting =85 \pm 7.03 μ m)

4.6 Altered P2-glomeruli position in PEBP1 mutant mice

The key element of topographic map is the spatial distribution of sensory afferents. In the case of the olfactory bulb, the topographic organization is related to the specific location of each glomerulus.

To ascertain whether the absence of PEBP1 could affect the location of convergence of sensory afferents, we computed the position of the main P2 and M72-homogeneous glomeruli (i.e. formed exclusively by sensory axons expressing the same OR) in P2- GFP ; PEBP1^{-/-}, in M72 GFP ; PEBP1^{-/-} mice and in controls mice.

First, we computed the area of the medial and of the lateral aspect of the OB .No variation in the olfactory bulbs areas were observed in PEBP1 mutant mice in respect to controls (**Figure 4.14 b**).

We then computed the position of the main P2-homogeneous glomerulus along the antero-posterior and dorso-ventral axis, on medial and lateral aspects of the bulb, (see methods). The analysis was conducted in heterozygous (P2-GFP ; PEBP1^{+/-}), homozygous (P2-GFP ; PEBP1^{-/-}) and in control mice (**Figure 4.14 a**).

The position of the P2-glomerulus along the dorso-ventral (D-V) axis remains unaffected in PEBP1 mutant mice (heterozygous and homozygous mice) in respect to P2-GFP control mice.

We found that the position of the P2-glomerulus was significantly shifted along the antero-posterior axis (A-P) in PEBP1 mutant mice compared to controls (**Figure 4.14 a, c, d**). We analyzed the position of P2-glomeruli in heterozygous (P2-GFP ; PEBP1^{+/-}) and homozygous (P2-GFP ; PEBP1^{-/-}) mice. We observed that in heterozygous mice (P2-GFP ; PEBP1^{+/-}) the medial P2-glomeruli occupied an ectopic position along the antero-posterior (A-P) axis in respect to controls (**Figure 4.14 a, c**).

In homozygous (P2-GFP ; PEBP1^{-/-}) mice we observed a dramatic shift along the antero-posterior (A-P) axis of both medial and lateral P2-glomeruli compared to the heterozygous and controls (**Figure 4.14 a, c-d**).

All these data indicate that in PEBP1^{-/-} mice the P2-glomerulus occupied an ectopic location along the anterior-posterior axis while no displacement was observed along the dorsal-ventral axis (D-V) in PEBP1 mutant mice compared to controls. Homozygous P2-GFP ; PEBP1^{-/-} mice exhibited a more severe shift in respect to heterozygous mice.

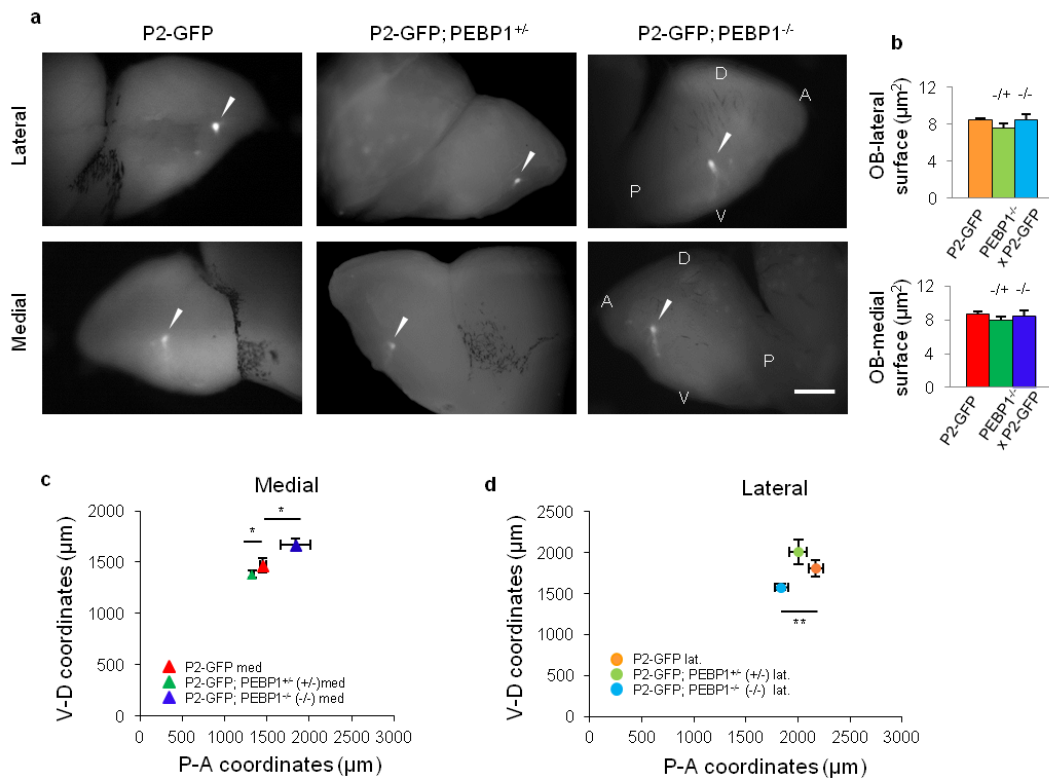


Figure 4.14. Altered location of P2-GFP glomeruli in PEBP1 mutant mice. **a)** Whole mount view of the lateral (top) and medial (bottom) aspect of the olfactory bulb (OB) in control P2-GFP mice (n=5), in P2-GFP ; PEBP1^{+/-} mice (n=5) and in P2-GFP ; PEBP1^{-/-} mice (n=4). P2-GFP fibers converge to form the main glomerulus (indicated by arrowheads) on the lateral and on the medial surface of the OB. Scale bar=1mm. **b)** areas of the lateral and the medial aspects of the OB. **c-d)** localization of P2-GFP medial, (c) and lateral, (d), glomeruli along the ventro-dorsal (V-D) and the antero-posterior (A-P) axis of the OB in P2-GFP control, in P2-GFP ; PEBP1^{+/-} and in P2-GFP ; PEBP1^{-/-} mice, respectively. In PEBP1 mutants, with a more severe phenotype in PEBP1 homozygous, P2 glomeruli location along the A-P axis of the OB is altered in respect to controls. (P2-GFP n=5 mice: medial-P2 glom. D-V=1469.41± 72.68μm; lateral-P2 glom. D-V=1808.44±104.53; medial-P2 glom. A-P=1450.08±37.37; *p<0.05; lateral-P2 glom. A-P=2170.33±67.76) (P2-GFP ; PEBP1^{+/-} n=5 mice: medial-P2 glom. D-V=1382.11±36.5; lateral-P2 glom. D-V=2008.67±144.75; medial-P2 glom. A-P=1322.63±19.85; lateral-P2 glom. A-P=2004.17±83.50)(P2-GFP ; PEBP1^{-/-} n=4 mice: medial-P2 glom D-V=1668.9±58.5; lateral-P2 glom D-V=1578.4±39.22; medial-P2 glom A-P=1839.8±174.17; **p<0.01; lateral-P2 glom A-P=1839.4±63.29;**p<0.01). Bars, ± SEM. One-way ANOVA, * p < 0.05, **p < 0.01, *** p < 0.001. med = medial glomerulus; lat = lateral glomerulus. A= anterior; P = posterior; D = dorsal; V = ventral.

Then we calculated the position of the main M72-homogeneous glomerulus along the antero-posterior (A-P) and medial-lateral (M-L) axis on the dorsal aspect of the olfactory bulb of M72-YFP control mice and PEBP1^{-/-} (**Figure 4.15**).

The olfactory bulbs areas were similar in M72-YFP ; PEBP1^{-/-} and M72 controls (**Figure 4.15 b**).

We found that the position of the M72-glomeruli along the anterior-posterior (A-P) axis and the medial-lateral (M-L) axis remain unaffected in PEBP1^{-/-} mice in respect to controls (**Figure 4.15 a, c-d**).

All together these data indicate that axonal OR activation by PEBP1 is necessary for a correct targeting and coalescence of OSN axon expressing responsive OR to the ligand PEBP1, such as P2-OR. PEBP1 is also required for the proper location of the corresponding glomeruli in the olfactory bulb. In agreement to our *in vitro* data, PEBP1 do not affect the convergence of M72 expressing axon and the position of the M72-glomeruli in the bulb.

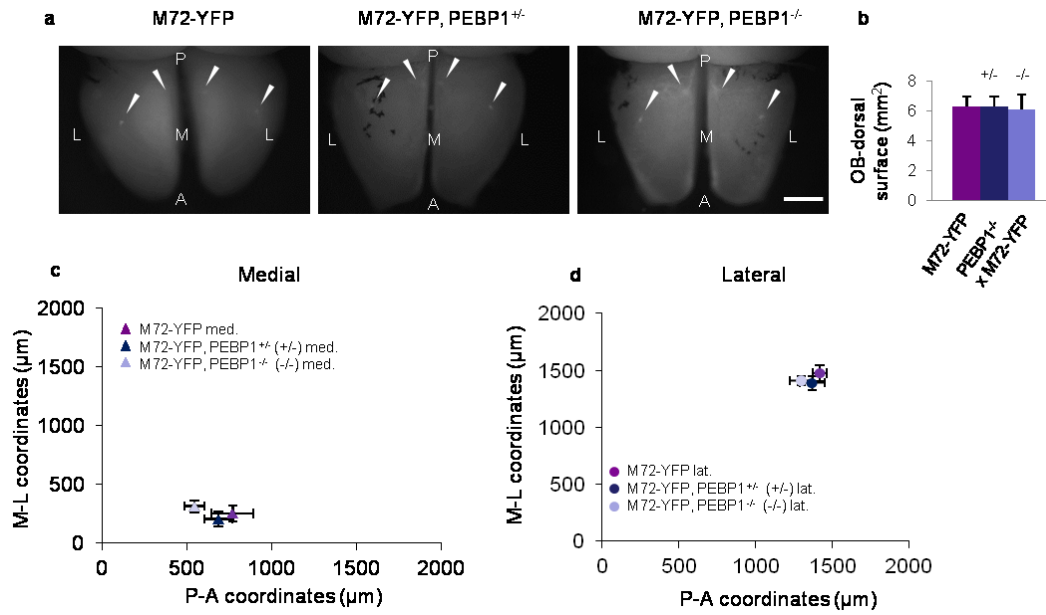


Figure 4.15. M72-YFP glomeruli location is not affected in PEBP1 mutant mice. a) Whole mount view of the dorsal surface of the olfactory bulbs (OB) in control M72-YFP, (left), in M72-YFP; PEBP1^{+/-} mice (center) and in M72-YFP; PEBP1^{-/-} (right). **b)** areas of the dorsal surface of the OB in control M72-YFP (n = 4); in M72-YFP ; PEBP1^{+/-} (n =5) and in M72-YFP ; PEBP1^{-/-} (n=6) mice. **c- d)** localization of M72-YFP medial, c and lateral, d, glomeruli along the medial-lateral (M-L) and the antero-posterior (A-P) axis of the OB is similar in control M72-YFP and in M72-YFP ; PEBP1^{+/-} and in M72-YFP ; PEBP1^{-/-} mice. (M72-YFP n=4 mice: medial-M72 glom. M-L=251± 68.27µm; lateral-M72 glom. M-L=1473.5±72.57; medial-M72 glom. A-P=768.25±122.14; lateral-M72 glom. A-P=1419±44.86) (M72-YFP ; PEBP1^{+/-} n=5 mice: medial-M72 glom. M-L=204.75±43.15; lateral-M72 glom. M-L=1389.25±61.68; medial-M72 glom. A-P=685.25±69.05; lateral-M72 glom. A-P=1372.37±81.02)(M72-YFP ; PEBP1^{-/-} n=6 mice: medial-M72 glom. M-L=314±49.13; lateral-M72 glom. M-L=1410.5±72.57; medial-M72 glom. A-P=544.4±57.45; lateral-M72 glom. A-P=1298±73.34). Bars, ± SEM. med = medial glomerulus; lat = lateral glomerulus. A= anterior; P = posterior; M= medial; L = lateral.

4.7 Olfactory deficit in PEBP1^{-/-} mice

To explore the functional outcome of the altered sensory map, we analyzed the olfactory behaviour in PEBP1^{-/-} mice.

We performed an olfactory habituation-dishabituation test. Briefly, wild-type (WT) and PEBP1^{-/-} mice were exposed to filter paper with double-distilled water, for 3 consecutive times (i.e. 3 habituation-trials). The 4th trial, the dishabituation-trial, mice were exposed to filter paper scented with an odor, eugenol (1mM) (see methods for more details) (**Figure 4.16**).

Control mice (C57BL/6 wild type mice and C57BL/6-Tyr^{c-Brd})(Charles River) exhibited a progressive reduction of sniffing time in the 3rd habituation-trials. A significant increase in sniffing time was observed in the 4th trial, i.e. dishabituation-trial (wild-type mice n= 12,*p <0.01), meaning they were able to recognize and discriminate the new odor (Eugenol) (**Figure 4.16 b**).

PEBP1^{-/-} mice did not exhibit a significant increase in sniffing time between the 3rd and 4th trial, indicating their inability to recognize the new odor compared to controls (PEBP1^{-/-} mice n=6) (**Figure 4.16 c**).

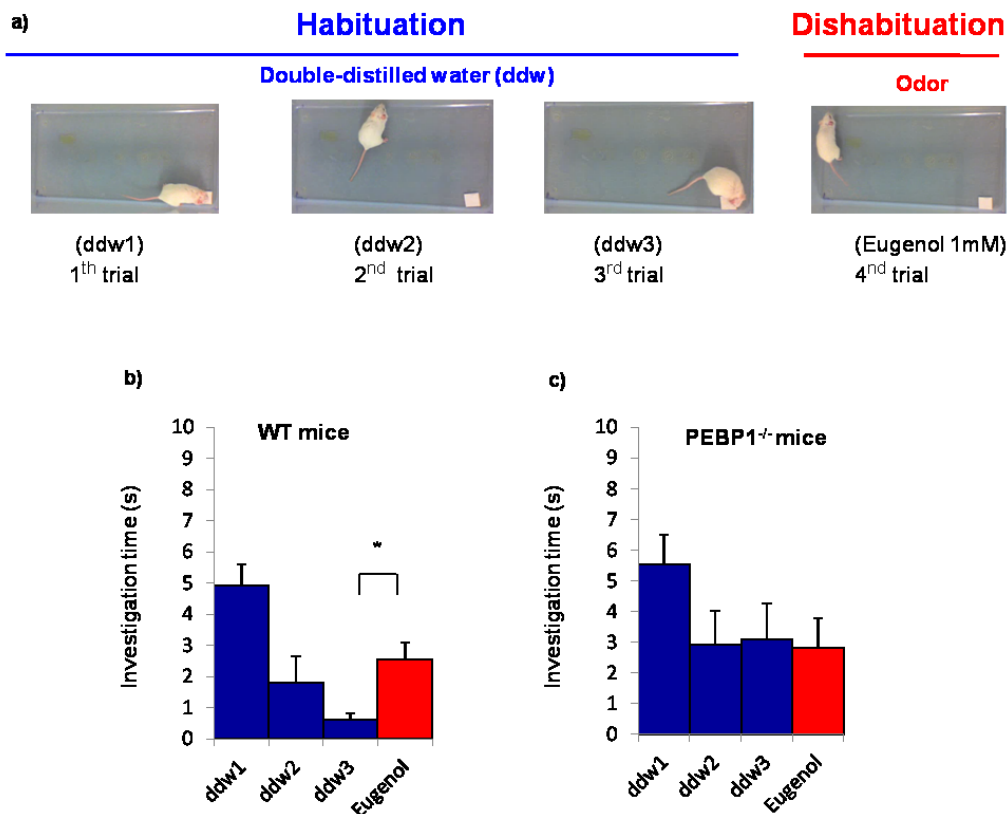


Figure 4.16. Olfactory habituation -dishabituation test in wild-type (WT) and PEBP1^{-/-} mice. Habituation-dishabituation test revealed that PEBP1^{-/-} mice exhibit an olfactory deficit in recognition and discrimination of a new odor. **a)** Olfactory test including the habituation (1st-3rd trials) and dishabituation trail (4th trial) of a PEBP1^{-/-} mouse. During habituation trail, WT mice and PEBP1^{-/-} mice were exposed for 3 times for 3 minutes (with 1 minute inter-trial interval) with double distilled-water (ddW1-3), while during dishabituation trial (4th trial) mice were exposed to an odor (Eugenol, 1mM). In the stop-frame of the video is shown the olfactory test of a PEBP1^{-/-} mouse. **b-c)** Summary of results of wild-type (WT) mice (b) and PEBP1^{-/-} mice (c) during the olfactory test. b) WT mice showed a reduction of sniffing time in the habituation trial (3rd trial) and a significant increase between the 3rd and 4th trials suggesting they recognized the new odor presented. In PEBP1^{-/-} mice no differences in the sniffing time was observed between the habituation and dishabituation trials (3rd and 4th trials) suggesting an olfactory deficit in odor recognition and discrimination. Student *t* test **p*<0.05 (WT mice n=12, PEBP1^{-/-} mice n=6).

5 DISCUSSION

In the present PhD project, we provide compelling evidence that the OR at the axon terminal acts as an axon guidance molecules activated by cues elaborated in the OB. In particular, we identified PEBP1 as a putative ligand of the axonal OR. The small molecular weight, the ability to be secreted although via a non-canonical pathway and the presence of olfactory deficits in mice carrying a null mutation for PEBP1 make this protein a suitable candidate as a ligand for the axonal OR.

We identified this ligand, using Ca^{2+} response as read out of OR activation. A prompt Ca^{2+} rise was observed at the axon terminal of OSN, in response to PEBP1 locally applied.

To ascertain whether PEBP1 calcium response observed in OSN was due to the OR activation, we employed a heterologous system. Namely, HEK293T cells were transfected with specific OR (EG, P2, S6, Olfr62 and M72), loaded with the calcium indicator, fura-2, and challenged with PEBP1 and the corresponding cognate odor. A prompt calcium rise was observed in all the OR tested in response to PEBP1 and to the corresponding ligand with the exception of the M72-OR, that responded only the cognate odor-ligand (Methylsalicylate). The absence of Ca^{2+} response upon M72 stimulation with PEBP1 suggested the presence of other ligands. This is in agreement with our hypothesis that a few ligands elaborate in the bulb can activate the axonal OR and direct sensory axons to their proper target.

HEK293T cells not expressing specific OR, did not exhibit Ca^{2+} response to PEBP1 but only to carbachol, used as a test of cell vitality. Furthermore, the specificity of PEBP1 calcium response was confirmed with several controls (i.e. denatured PEBP1 or another protein, cyclin division kinase-2, to exclude contaminants in the purification protocol).

The physiological importance of our data is corroborated by the fact that PEBP1 is able to modulate the axon behaviour in an *in vitro* assay, a feature proper of axon guidance molecule.

More importantly, for the *in vivo* relevance of our findings, mice carrying a null mutation for PEBP1 exhibit a deeply perturbed sensory map. In the OB, in absence of PEBP1, in homozygous mice, P2-GFP;PEBP1^{-/-}, the convergence of P2 expressing axons and the localization of the corresponding P2-homogeneous glomeruli were deeply altered.

OSN expressing P2 converge to form the main P2-homogeneous glomeruli but they also target several additional heterogeneous glomeruli formed by axons expressing different OR.

The location of P2 glomeruli was also significantly shifted along the antero-posterior axis, in PEBP1 mutant mice in respect to controls. A similar, although milder phenotype was observed in heterozygous PEBP1 mutant mice. Namely, in heterozygous mice, P2-GFP;PEBP1^{+/-}, the sensory map was perturbed by a lower number of additional heterogeneous glomeruli than in homozygous mice, P2-GFP;PEBP1^{-/-}. The shift along the AP axis was smaller, although significant, for the medial P2 glomerulus.

All together these data provide compelling evidence that molecules elaborated in the OB, such as PEBP1, can act as axon guidance molecules, in a gene-dosage dependent manner, and provide olfactory sensory neurons with information to reach the proper target. In contrast, no alterations in the convergence of M72 axons were observed *in vivo*, confirming the absence of responsiveness of M72 to PEBP1, obtained in *in vitro* experiments. The latter suggests that the identity of other ligands for the axonal OR remain to be unraveled.

The different effect of PEBP1 on P2 and M72 glomeruli is reflected by the diverse distribution of PEBP1 expression in the OB.

By performing immunofluorescence in the OB, RT-PCR and western blot we found that PEBP1 is highly expressed along to the lateral, anterior and medial side, where P2 glomeruli are located, while it is hardly detected in the posterior wall, where M72 axons converge to form the glomeruli. Furthermore, within the

zones of the OB where PEBP1 is highly expressed, PEBP1 exhibits a patchy pattern of expression rather than a clear gradient. This patchy pattern of expression of PEBP1 reflects the discrete nature of the olfactory map, whose spatial organization is based on the identity of the OR, and not on the spatial distribution of neighbor sensory neurons in the epithelium. In agreement with our findings, also the expression of Neuropilin 1, a molecule involved in the location of glomeruli along the antero-posterior axis, is expressed in a patchy manner and do not exhibit a clear gradient (*Col et al., 2007; Zapiec & Mombaerts, 2015; Assens et al., 2016*).

The position of P2 and M72 glomeruli, along the dorso-ventral axis, were not affected by PEBP1 mutation. These findings are in agreement with the evidence that the projections of sensory axons along the D-V axis is not regulated by the OR identity, but by other cues, such as the location of sensory neurons in specific zone of the epithelium, or molecular cues such as Slit/Robo and Sema 3F and Neuropilin 2 (*Cloutier et al., 2002; Cloutier et al., 2004; Nguyen-Ba-Charvet et al., 2008; Takeuchi et al., 2010*).

The non-responsiveness of M72 to PEBP1 indicate that other cues, whose identity remains at the moment unknown, are involved in the projection of sensory afferents to the OB. We can envision two possibilities: 1 there are as many cues as glomeruli, therefore more than 1000. 2. A few molecules elaborated in the OB direct sensory axons to their proper location in the OB. The first hypothesis seems unlikely. The data we obtained in the present work indicate that PEBP1 can bind, although with different affinity, different OR, excluding the 1 cue: 1 odorant receptor hypothesis.

The pattern of interaction between PEBP1 and the axonal OR reminds the combinatorial code, that regulates the interaction between cilia- OR and odors (*Malnic et al., 1999*). Therefore, our model favors the existence of a few molecules elaborated in the OB, that interact, with different affinities, with subset of OR. This model implies that specificity of OSN targeting could be achieved by the expression of the axonal OR along with other guidance cues such as Neuropilin and Ephrin. These cues were shown to contribute to dictate the location of glomeruli

along the A-P axis. Furthermore, adhesion molecules, like Kirrel and Big 2 (*Serizawa et al., 2006; Kaneko-Goto et al., 2008*) could further refine the coalescence of fibers to form glomeruli, once they have reached their final destination. Neuronal activity was shown to facilitate this refinement process, too (*Lorenzon et al., 2015*).

In conclusion, in the present PhD project, we provide compelling evidence that PEBP-1 is one of the natural ligand of the axonal OR that act as an axon guidance molecule, providing sensory axons with the information to reach the proper target.

Our finding resolve a long standing riddle in the field. Despite the fact that the topography of the OB hinges on the OR identity, odor evoked activity does not play a significant role in the spatial segregation of sensory afferents (*Belluscio et al., 1998*)(*Zheng et al., 2000*).

However, spontaneous activity was shown to be involved in the refinement and in the maintenance of the sensory map.

Noteworthy, it has been shown that the OR dictates not only the evoked activity but also the spontaneous firing of OSNs (*Connelly et al., 2013*). Namely, OSN expressing different OR exhibit different pattern of basal firing. However, even OSN expressing the same OR exhibit a wide variability in the spontaneous firing rate (*Connelly et al., 2013*). The high variability of basal activity even among OSN expressing the same receptor makes unclear how spontaneous firing could determine specific level of cAMP that would in turn trigger the expression of different levels of other axon guidance molecules, such as Neuropilin, leading to convergence of OSN in glomeruli (*Nakashima et al., 2013*). Furthermore, Nakashima and colleagues' hypothesis is formulated on the possible active state that the β -adrenergic receptor, and not the OR, can assume in absence of specific ligands (i.e. spontaneous activity). The β -adrenergic receptor and OR are both GPCRs. Although the expression of the β -adrenergic receptor leads to the coalescence of OSN to form glomeruli likely because it is able to trigger cAMP production, it is worth noticing that the location of glomeruli formed by fibers expressing the β -adrenergic receptor is deeply perturbed respect to controls. These

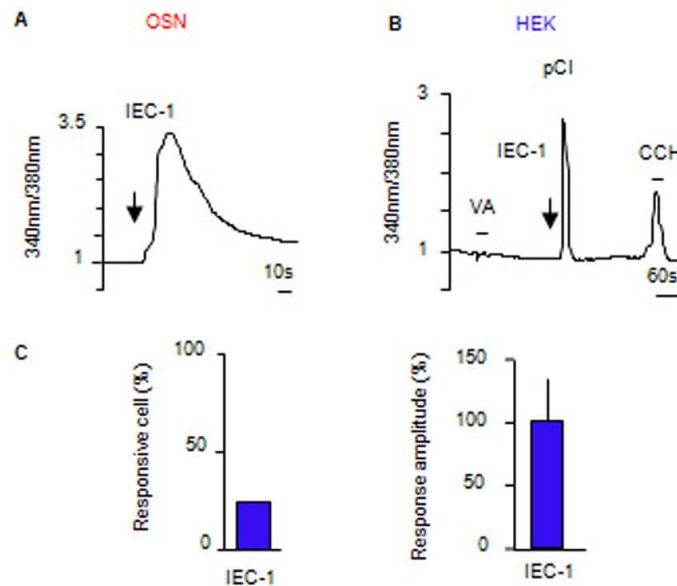
data suggest that the β -adrenergic receptor cannot recapitulate the whole role of the OR in the axon guidance process.

In conclusion, after more than 20 years from the discovery of the role of the OR in the topographic organization of the olfactory bulb, the data obtained in this PhD project unveil the mystery of the mechanism of activation and the function of the axonal OR.

In olfaction, the identity of the OR dictates not only the repertoire of odors detected by a sensory neuron but also its target in the brain.

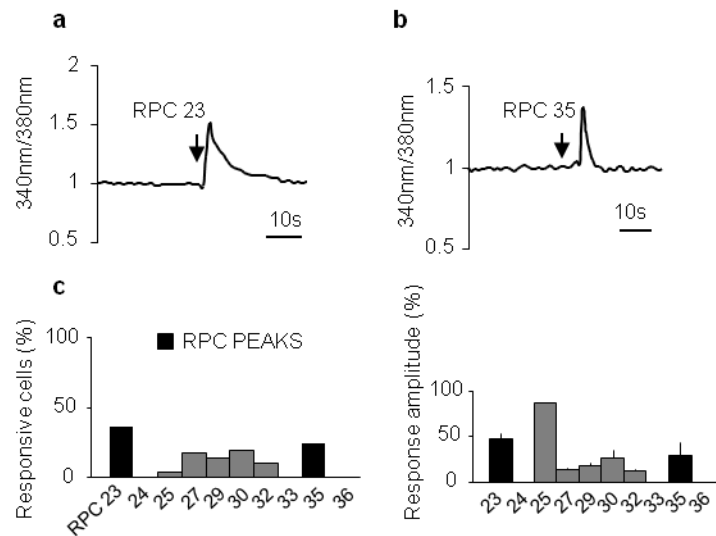
6 APPENDIX

The odorant receptor is activated by molecules expressed in the olfactory bulb

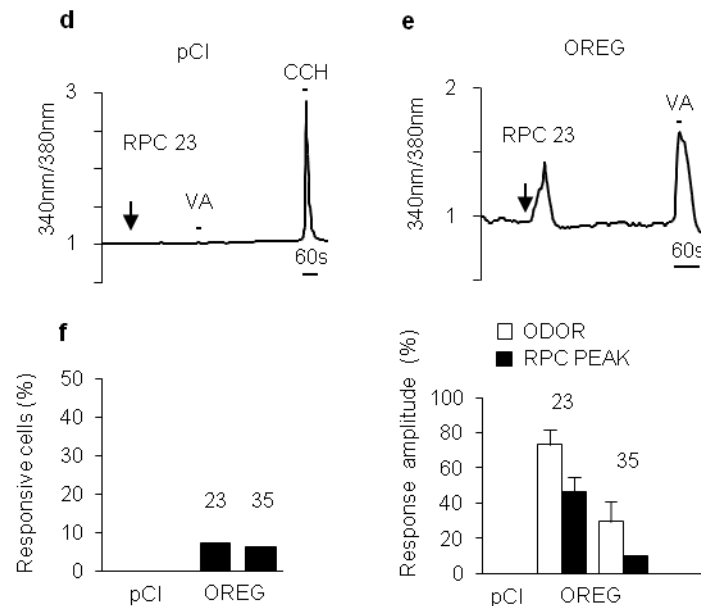


Supplementary Figure S1. Ca^{2+} dynamics in response to IEC-1 in olfactory sensory neuron (OSN) axon terminals and in HEK293T cells. Fura-2 Ca^{2+} imaging. (a) Example of Ca^{2+} response in embryonic rat OSN axon terminal stimulated with ionic exchange chromatography peak 1 (IEC-1) ($n = 92$). Summary of results shown in Figure 3.1c. (b) HEK293T cells not expressing odorant receptors, ($n = 69$) (pCI = empty vector) exhibit a prompt Ca^{2+} rise in response to IEC-1 but not to the odor vanillic acid (VA). Calcium transient is, however, observed upon stimulation with carbachol (CCH), used as control

RAT OSN



HEK



Supplementary Figure S2. Ca^{2+} dynamics in response to pools of molecules of the olfactory bulb obtained by reverse phase chromatography (RPC). Fura-2 Ca^{2+} imaging. **a-b) Normalized fluorescence ratio changes (340nm / 380 nm) in embryonic rat olfactory sensory neuron (OSN) axon terminals in response to RPC peak 23 (n = 22) in a and 35 (n= 25) in b. **c**) Summary of 32 responsive cells (%) and amplitude of response (%) for all the RPC peaks tested. **d**) HEK293T cells 33 not expressing odorant receptors, (n =130) (pCI = empty vector) do not exhibit Ca^{2+} rise in response 34 to RPC peak 23 nor to**

vanillic acid (VA). A prompt Ca^{2+} rise is observed in response to carbachol (CCH), used as control. **e)** HEK293T cells transfected with the odorant receptor (OR) OREG exhibit a timely Ca^{2+} rise in response to RPC peak 23 and to the corresponding odor ligand VA. **f)** Summary of results. (OREG + peak 23 n = 97; OREG + peak 35 n = 32. Bars = SEM.

Mass spectrometry results

Table S1

	Accession	Score	Description
1	gi8393910	3397	Phosphatidylethanolamine-binding protein 1 (<i>Rattus norvegicus</i>)
2	gi290563454	748	SH3 domain binding glutamic acid-rich protein like (<i>Rattus norvegicus</i>)
3	gi6680946	614	Cold-inducible RNA-binding protein (<i>Mus musculus</i>)
4	gi400542	489	Chaperonin 10 (<i>Rattus norvegicus</i>)
5	gi203658	186	Cu-Zn Superoxide dismutase (<i>Rattus norvegicus</i>)
6	gi10946572	179	Fatty Acid-binding protein, brain (<i>Mus musculus</i>)
7	gi12859411	149	Unnamed protein product (<i>Mus musculus</i>)
8	gi3377279	114	AIF-C1 (<i>Rattus norvegicus</i>)
9	gi2555013	101	s-Afadin (<i>Rattus norvegicus</i>)
10	gi1706754	94	Fatty Acid-binding protein

Table S2

	Accession	Score	Description
1	gi3212531	1222	Chain A, Rat Transthyretin
2	gi46485429	1116	Lactoylglutathione lyase (<i>Rattus norvegicus</i>)
3	gi61557414	992	Tubulin-specific chaperone A (<i>Rattus norvegicus</i>)
4	gi8393910	840	Phosphatidylethanolamine binding protein (<i>Rattus norvegicus</i>)
5	gi18017602	813	SH3 domain-binding glutamic acid-rich-like protein 3 (<i>Rattus norvegicus</i>)
6	gi10946572	574	Fatty acid binding protein, brain (<i>Mus musculus</i>)
7	gi13435747	462	RhoGDP dissociation inhibitor (GDI) alfa (<i>Mus musculus</i>)
8	gi61556986	330	Serotransferrin precursors (<i>Rattus norvegicus</i>)
9	gi6981010	261	Hemoglobin subunit alfa-1/2 (<i>Rattus norvegicus</i>)
10	gi4972951	235	Wbscr1 alternative splicing product (<i>Mus musculus</i>)

Supplementary Table S1 and supplementary Table S2. Supplementary Table S1. Mass spectrometry results. List of the most significant proteins in peak 23 of reverse phase chromatography (RCP). Phosphatidylethanolamine-binding protein 1 (PEBP1), is indicated in red. **Supplementary Table S2.** Mass spectrometry results. List of the most significant proteins in peak 35 of reverse phase chromatography (RCP). Phosphatidylethanolamine-binding protein 1, is indicated in red.

7 BIBLIOGRAPHY

- Abaffy, T., Malhotra, A. & Luetje, C.W. (2007) The molecular basis for ligand specificity in a mouse olfactory receptor: a network of functionally important residues. *The Journal of biological chemistry*, **282**, 1216-1224.
- Ahmed, L., Zhang, Y., Block, E., Buehl, M., Corr, M.J., Cormanich, R.A., Gundala, S., Matsunami, H., O'Hagan, D., Ozbil, M., Pan, Y., Sekharan, S., Ten, N., Wang, M., Yang, M., Zhang, Q., Zhang, R., Batista, V.S. & Zhuang, H. (2018) Molecular mechanism of activation of human musk receptors OR5AN1 and OR1A1 by (R)-muscone and diverse other musk-smelling compounds. *Proceedings of the National Academy of Sciences of the United States of America*, **115**, E3950-E3958.
- Al-Mulla, F., Bitar, M.S., Taqi, Z. & Yeung, K.C. (2013) RKIP: much more than Raf kinase inhibitory protein. *Journal of cellular physiology*, **228**, 1688-1702.
- Assens, A., Dal Col, J.A., Njoku, A., Dietschi, Q., Kan, C., Feinstein, P., Carleton, A. & Rodriguez, I. (2016) Alteration of Nrp1 signaling at different stages of olfactory neuron maturation promotes glomerular shifts along distinct axes in the olfactory bulb. *Development*, **143**, 3817-3825.
- Barnea, G., O'Donnell, S., Mancina, F., Sun, X., Nemes, A., Mendelsohn, M. & Axel, R. (2004) Odorant receptors on axon termini in the brain. *Science*, **304**, 1468.
- Barnea, G., Strapps, W., Herrada, G., Berman, Y., Ong, J., Kloss, B., Axel, R. & Lee, K.J. (2008) The genetic design of signaling cascades to record receptor activation. *Proceedings of the National Academy of Sciences of the United States of America*, **105**, 64-69.
- Batista-Brito, R., Close, J., Machold, R. & Fishell, G. (2008) The distinct temporal origins of olfactory bulb interneuron subtypes. *The Journal of neuroscience : the official journal of the Society for Neuroscience*, **28**, 3966-3975.
- Baud, O., Yuan, S., Veya, L., Filipek, S., Vogel, H. & Pick, H. (2015) Exchanging ligand-binding specificity between a pair of mouse olfactory receptor paralogs reveals odorant recognition principles. *Scientific reports*, **5**, 14948.
- Belluscio, L., Gold, G.H., Nemes, A. & Axel, R. (1998) Mice deficient in G(olf) are anosmic. *Neuron*, **20**, 69-81.

- Belluscio, L., Lodovichi, C., Feinstein, P., Mombaerts, P. & Katz, L.C. (2002) Odorant receptors instruct functional circuitry in the mouse olfactory bulb. *Nature*, **419**, 296-300.
- Billig, G.M., Pal, B., Fidzinski, P. & Jentsch, T.J. (2011) Ca²⁺-activated Cl⁻ currents are dispensable for olfaction. *Nature neuroscience*, **14**, 763-769.
- Boekhoff, I., Strotmann, J., Raming, K., Tareilus, E. & Breer, H. (1990) Odorant-sensitive phospholipase C in insect antennae. *Cellular signalling*, **2**, 49-56.
- Bozza, T., Feinstein, P., Zheng, C. & Mombaerts, P. (2002) Odorant receptor expression defines functional units in the mouse olfactory system. *The Journal of neuroscience : the official journal of the Society for Neuroscience*, **22**, 3033-3043.
- Bozza, T., McGann, J.P., Mombaerts, P. & Wachowiak, M. (2004) In vivo imaging of neuronal activity by targeted expression of a genetically encoded probe in the mouse. *Neuron*, **42**, 9-21.
- Bozza, T., Vassalli, A., Fuss, S., Zhang, J.J., Weiland, B., Pacifico, R., Feinstein, P. & Mombaerts, P. (2009) Mapping of class I and class II odorant receptors to glomerular domains by two distinct types of olfactory sensory neurons in the mouse. *Neuron*, **61**, 220-233.
- Bradley, J., Reiser, J. & Frings, S. (2005) Regulation of cyclic nucleotide-gated channels. *Current opinion in neurobiology*, **15**, 343-349.
- Breer, H., Boekhoff, I. & Tareilus, E. (1990) Rapid kinetics of second messenger formation in olfactory transduction. *Nature*, **345**, 65-68.
- Breer, H., Fleischer, J. & Strotmann, J. (2006) The sense of smell: multiple olfactory subsystems. *Cellular and molecular life sciences : CMLS*, **63**, 1465-1475.
- Brennan, P.A. & Zufall, F. (2006) Pheromonal communication in vertebrates. *Nature*, **444**, 308-315.
- Buck, L. & Axel, R. (1991) A novel multigene family may encode odorant receptors: a molecular basis for odor recognition. *Cell*, **65**, 175-187.
- Burton, S.D., LaRocca, G., Liu, A., Cheetham, C.E. & Urban, N.N. (2017) Olfactory Bulb Deep Short-Axon Cells Mediate Widespread Inhibition of Tufted Cell Apical

Dendrites. *The Journal of neuroscience : the official journal of the Society for Neuroscience*, **37**, 1117-1138.

Bushdid, C., de March, C.A., Fiorucci, S., Matsunami, H. & Golebiowski, J. (2018) Agonists of G-Protein-Coupled Odorant Receptors Are Predicted from Chemical Features. *The journal of physical chemistry letters*, **9**, 2235-2240.

Campbell, D.S. & Holt, C.E. (2001) Chemotropic responses of retinal growth cones mediated by rapid local protein synthesis and degradation. *Neuron*, **32**, 1013-1026.

Carter, L.A., MacDonald, J.L. & Roskams, A.J. (2004) Olfactory horizontal basal cells demonstrate a conserved multipotent progenitor phenotype. *The Journal of neuroscience : the official journal of the Society for Neuroscience*, **24**, 5670-5683.

Chesler, A.T., Zou, D.J., Le Pichon, C.E., Peterlin, Z.A., Matthews, G.A., Pei, X., Miller, M.C. & Firestein, S. (2007) A G protein/cAMP signal cascade is required for axonal convergence into olfactory glomeruli. *Proceedings of the National Academy of Sciences of the United States of America*, **104**, 1039-1044.

Chess, A., Simon, I., Cedar, H. & Axel, R. (1994) Allelic inactivation regulates olfactory receptor gene expression. *Cell*, **78**, 823-834.

Chilton, B.S. & Hewetson, A. (2005) Prolactin and growth hormone signaling. *Current topics in developmental biology*, **68**, 1-23.

Cioni, J.M., Koppers, M. & Holt, C.E. (2018) Molecular control of local translation in axon development and maintenance. *Current opinion in neurobiology*, **51**, 86-94.

Cloutier, J.F., Giger, R.J., Koentges, G., Dulac, C., Kolodkin, A.L. & Ginty, D.D. (2002) Neuropilin-2 mediates axonal fasciculation, zonal segregation, but not axonal convergence, of primary accessory olfactory neurons. *Neuron*, **33**, 877-892.

Cloutier, J.F., Sahay, A., Chang, E.C., Tessier-Lavigne, M., Dulac, C., Kolodkin, A.L. & Ginty, D.D. (2004) Differential requirements for semaphorin 3F and Slit-1 in axonal targeting, fasciculation, and segregation of olfactory sensory neuron projections. *The Journal of neuroscience : the official journal of the Society for Neuroscience*, **24**, 9087-9096.

Col, J.A., Matsuo, T., Storm, D.R. & Rodriguez, I. (2007) Adenylyl cyclase-dependent axonal targeting in the olfactory system. *Development*, **134**, 2481-2489.

- Connelly, T., Savigner, A. & Ma, M. (2013) Spontaneous and sensory-evoked activity in mouse olfactory sensory neurons with defined odorant receptors. *Journal of neurophysiology*, **110**, 55-62.
- Cutforth, T., Moring, L., Mendelsohn, M., Nemes, A., Shah, N.M., Kim, M.M., Frisen, J. & Axel, R. (2003) Axonal ephrin-As and odorant receptors: coordinate determination of the olfactory sensory map. *Cell*, **114**, 311-322.
- de Castro, F. (2009) Wiring Olfaction: The Cellular and Molecular Mechanisms that Guide the Development of Synaptic Connections from the Nose to the Cortex. *Frontiers in neuroscience*, **3**, 52.
- de March, C.A., Kim, S.K., Antonczak, S., Goddard, W.A., 3rd & Golebiowski, J. (2015) G protein-coupled odorant receptors: From sequence to structure. *Protein science : a publication of the Protein Society*, **24**, 1543-1548.
- Deiss, K., Kisker, C., Lohse, M.J. & Lorenz, K. (2012) Raf kinase inhibitor protein (RKIP) dimer formation controls its target switch from Raf1 to G protein-coupled receptor kinase (GRK) 2. *The Journal of biological chemistry*, **287**, 23407-23417.
- Dontchev, V.D. & Letourneau, P.C. (2002) Nerve growth factor and semaphorin 3A signaling pathways interact in regulating sensory neuronal growth cone motility. *The Journal of neuroscience : the official journal of the Society for Neuroscience*, **22**, 6659-6669.
- Dubacq, C., Jamet, S. & Trembleau, A. (2009) Evidence for developmentally regulated local translation of odorant receptor mRNAs in the axons of olfactory sensory neurons. *The Journal of neuroscience : the official journal of the Society for Neuroscience*, **29**, 10184-10190.
- Dulac, C. & Torello, A.T. (2003) Molecular detection of pheromone signals in mammals: from genes to behaviour. *Nature reviews. Neuroscience*, **4**, 551-562.
- Eggan, K., Baldwin, K., Tackett, M., Osborne, J., Gogos, J., Chess, A., Axel, R. & Jaenisch, R. (2004) Mice cloned from olfactory sensory neurons. *Nature*, **428**, 44-49.
- Fantana, A.L., Soucy, E.R. & Meister, M. (2008) Rat olfactory bulb mitral cells receive sparse glomerular inputs. *Neuron*, **59**, 802-814.

-
- Feinstein, P., Bozza, T., Rodriguez, I., Vassalli, A. & Mombaerts, P. (2004) Axon guidance of mouse olfactory sensory neurons by odorant receptors and the beta2 adrenergic receptor. *Cell*, **117**, 833-846.
- Feinstein, P. & Mombaerts, P. (2004) A contextual model for axonal sorting into glomeruli in the mouse olfactory system. *Cell*, **117**, 817-831.
- Feldmesser, E., Olender, T., Khen, M., Yanai, I., Ophir, R. & Lancet, D. (2006) Widespread ectopic expression of olfactory receptor genes. *BMC genomics*, **7**, 121.
- Firestein, S. (2001) How the olfactory system makes sense of scents. *Nature*, **413**, 211-218.
- Frayne, J., Ingram, C., Love, S. & Hall, L. (1999) Localisation of phosphatidylethanolamine-binding protein in the brain and other tissues of the rat. *Cell and tissue research*, **298**, 415-423.
- Frostig, R.D., Lieke, E.E., Ts'o, D.Y. & Grinvald, A. (1990) Cortical functional architecture and local coupling between neuronal activity and the microcirculation revealed by in vivo high-resolution optical imaging of intrinsic signals. *Proceedings of the National Academy of Sciences of the United States of America*, **87**, 6082-6086.
- Fuchs, T., Glusman, G., Horn-Saban, S., Lancet, D. & Pilpel, Y. (2001) The human olfactory subgenome: from sequence to structure and evolution. *Human genetics*, **108**, 1-13.
- Fuss, S.H., Omura, M. & Mombaerts, P. (2005) The Grueneberg ganglion of the mouse projects axons to glomeruli in the olfactory bulb. *The European journal of neuroscience*, **22**, 2649-2654.
- Galli, L. & Maffei, L. (1988) Spontaneous impulse activity of rat retinal ganglion cells in prenatal life. *Science*, **242**, 90-91.
- Geithe, C., Protze, J., Kreuchwig, F., Krause, G. & Krautwurst, D. (2017) Structural determinants of a conserved enantiomer-selective carvone binding pocket in the human odorant receptor OR1A1. *Cellular and molecular life sciences : CMLS*, **74**, 4209-4229.
- Glusman, G., Yanai, I., Rubin, I. & Lancet, D. (2001) The complete human olfactory subgenome. *Genome research*, **11**, 685-702.

- Gogos, J.A., Osborne, J., Nemes, A., Mendelsohn, M. & Axel, R. (2000) Genetic ablation and restoration of the olfactory topographic map. *Cell*, **103**, 609-620.
- Goumon, Y., Angelone, T., Schoentgen, F., Chasserot-Golaz, S., Almas, B., Fukami, M.M., Langley, K., Welters, I.D., Tota, B., Aunis, D. & Metz-Boutigue, M.H. (2004) The hippocampal cholinergic neurostimulating peptide, the N-terminal fragment of the secreted phosphatidylethanolamine-binding protein, possesses a new biological activity on cardiac physiology. *The Journal of biological chemistry*, **279**, 13054-13064.
- Hahm, J.R., Ahmed, M. & Kim, D.R. (2016) RKIP phosphorylation-dependent ERK1 activation stimulates adipogenic lipid accumulation in 3T3-L1 preadipocytes overexpressing LC3. *Biochemical and biophysical research communications*, **478**, 12-17.
- Hallem, E.A. & Carlson, J.R. (2006) Coding of odors by a receptor repertoire. *Cell*, **125**, 143-160.
- Hamilton, K.A., Heinbockel, T., Ennis, M., Szabo, G., Erdelyi, F. & Hayar, A. (2005) Properties of external plexiform layer interneurons in mouse olfactory bulb slices. *Neuroscience*, **133**, 819-829.
- Harper, S. & Speicher, D.W. (2011) Purification of proteins fused to glutathione S-transferase. *Methods in molecular biology*, **681**, 259-280.
- Henley, J. & Poo, M.M. (2004) Guiding neuronal growth cones using Ca²⁺ signals. *Trends in cell biology*, **14**, 320-330.
- Huard, J.M. & Schwob, J.E. (1995) Cell cycle of globose basal cells in rat olfactory epithelium. *Developmental dynamics : an official publication of the American Association of Anatomists*, **203**, 17-26.
- Huber, A.B., Kolodkin, A.L., Ginty, D.D. & Cloutier, J.F. (2003) Signaling at the growth cone: ligand-receptor complexes and the control of axon growth and guidance. *Annual review of neuroscience*, **26**, 509-563.
- Imai, T. (2014) Construction of functional neuronal circuitry in the olfactory bulb. *Seminars in cell & developmental biology*, **35**, 180-188.
- Imai, T., Sakano, H. & Vosshall, L.B. (2010) Topographic mapping--the olfactory system. *Cold Spring Harbor perspectives in biology*, **2**, a001776.

-
- Imai, T., Suzuki, M. & Sakano, H. (2006) Odorant receptor-derived cAMP signals direct axonal targeting. *Science*, **314**, 657-661.
- Imai, T., Yamazaki, T., Kobayakawa, R., Kobayakawa, K., Abe, T., Suzuki, M. & Sakano, H. (2009) Pre-target axon sorting establishes the neural map topography. *Science*, **325**, 585-590.
- Kanamori, T., Matsukawa, N., Kobayashi, H., Uematsu, N., Sagisaka, T., Toyoda, T., Kato, D., Oikawa, S. & Ojika, K. (2010) Suppressed phosphorylation of collapsin response mediator protein-2 in the hippocampus of HCNP precursor transgenic mice. *Brain research*, **1355**, 180-188.
- Kaneko-Goto, T., Yoshihara, S., Miyazaki, H. & Yoshihara, Y. (2008) BIG-2 mediates olfactory axon convergence to target glomeruli. *Neuron*, **57**, 834-846.
- Kang, N., Kim, H., Jae, Y., Lee, N., Ku, C.R., Margolis, F., Lee, E.J., Bahk, Y.Y., Kim, M.S. & Koo, J. (2015) Olfactory marker protein expression is an indicator of olfactory receptor-associated events in non-olfactory tissues. *PloS one*, **10**, e0116097.
- Katada, S., Hirokawa, T., Oka, Y., Suwa, M. & Touhara, K. (2005) Structural basis for a broad but selective ligand spectrum of a mouse olfactory receptor: mapping the odorant-binding site. *The Journal of neuroscience : the official journal of the Society for Neuroscience*, **25**, 1806-1815.
- Kato, A., Katada, S. & Touhara, K. (2008) Amino acids involved in conformational dynamics and G protein coupling of an odorant receptor: targeting gain-of-function mutation. *Journal of neurochemistry*, **107**, 1261-1270.
- Kato, A., Reisert, J., Ihara, S., Yoshikawa, K. & Touhara, K. (2014) Evaluation of the role of g protein-coupled receptor kinase 3 in desensitization of mouse odorant receptors in a Mammalian cell line and in olfactory sensory neurons. *Chemical senses*, **39**, 771-780.
- Kato, A. & Touhara, K. (2009) Mammalian olfactory receptors: pharmacology, G protein coupling and desensitization. *Cellular and molecular life sciences : CMLS*, **66**, 3743-3753.
- Kato, D., Mitake, S., Mizuno, M., Kanamori, T., Suzuki, T., Ojika, K. & Matsukawa, N. (2012) Co-localization of hippocampal cholinergic neurostimulating peptide precursor with collapsin response mediator protein-2 at presynaptic terminals in hippocampus. *Neuroscience letters*, **517**, 92-97.

- Kaupp, U.B. (2010) Olfactory signalling in vertebrates and insects: differences and commonalities. *Nature reviews. Neuroscience*, **11**, 188-200.
- Kobilka, B. (2013) The structural basis of G-protein-coupled receptor signaling (Nobel Lecture). *Angewandte Chemie*, **52**, 6380-6388.
- Kosaka, K., Aika, Y., Toida, K. & Kosaka, T. (2001) Structure of intraglomerular dendritic tufts of mitral cells and their contacts with olfactory nerve terminals and calbindin-immunoreactive type 2 periglomerular neurons. *The Journal of comparative neurology*, **440**, 219-235.
- Kosaka, K., Heizmann, C.W. & Kosaka, T. (1994) Calcium-binding protein parvalbumin-immunoreactive neurons in the rat olfactory bulb. 2. Postnatal development. *Experimental brain research*, **99**, 205-213.
- Kosaka, K. & Kosaka, T. (2005) synaptic organization of the glomerulus in the main olfactory bulb: compartments of the glomerulus and heterogeneity of the periglomerular cells. *Anatomical science international*, **80**, 80-90.
- Kosaka, K. & Kosaka, T. (2007) Chemical properties of type 1 and type 2 periglomerular cells in the mouse olfactory bulb are different from those in the rat olfactory bulb. *Brain research*, **1167**, 42-55.
- Kosaka, T. & Kosaka, K. (2016) Neuronal organization of the main olfactory bulb revisited. *Anatomical science international*, **91**, 115-127.
- Leinders-Zufall, T., Cockerham, R.E., Michalakis, S., Biel, M., Garbers, D.L., Reed, R.R., Zufall, F. & Munger, S.D. (2007) Contribution of the receptor guanylyl cyclase GC-D to chemosensory function in the olfactory epithelium. *Proceedings of the National Academy of Sciences of the United States of America*, **104**, 14507-14512.
- Lepousez, G. & Lledo, P.M. (2013) Odor discrimination requires proper olfactory fast oscillations in awake mice. *Neuron*, **80**, 1010-1024.
- Leung, K.M., van Horck, F.P., Lin, A.C., Allison, R., Standart, N. & Holt, C.E. (2006) Asymmetrical beta-actin mRNA translation in growth cones mediates attractive turning to netrin-1. *Nature neuroscience*, **9**, 1247-1256.
- Li, J., Ishii, T., Feinstein, P. & Mombaerts, P. (2004) Odorant receptor gene choice is reset by nuclear transfer from mouse olfactory sensory neurons. *Nature*, **428**, 393-399.

-
- Lin, A.C. & Holt, C.E. (2008) Function and regulation of local axonal translation. *Current opinion in neurobiology*, **18**, 60-68.
- Lledo, P.M., Gheusi, G. & Vincent, J.D. (2005) Information processing in the mammalian olfactory system. *Physiological reviews*, **85**, 281-317.
- Lodovichi, C. & Belluscio, L. (2012) Odorant receptors in the formation of the olfactory bulb circuitry. *Physiology*, **27**, 200-212.
- Lodovichi, C., Belluscio, L. & Katz, L.C. (2003) Functional topography of connections linking mirror-symmetric maps in the mouse olfactory bulb. *Neuron*, **38**, 265-276.
- Lohof, A.M., Quillan, M., Dan, Y. & Poo, M.M. (1992) Asymmetric modulation of cytosolic cAMP activity induces growth cone turning. *The Journal of neuroscience : the official journal of the Society for Neuroscience*, **12**, 1253-1261.
- Lomvardas, S., Barnea, G., Pisapia, D.J., Mendelsohn, M., Kirkland, J. & Axel, R. (2006) Interchromosomal interactions and olfactory receptor choice. *Cell*, **126**, 403-413.
- Lorenz, K., Schmid, E. & Deiss, K. (2014) RKIP: a governor of intracellular signaling. *Critical reviews in oncogenesis*, **19**, 489-496.
- Lorenzon, P., Redolfi, N., Podolsky, M.J., Zamparo, I., Franchi, S.A., Pietra, G., Boccaccio, A., Menini, A., Murthy, V.N. & Lodovichi, C. (2015) Circuit formation and function in the olfactory bulb of mice with reduced spontaneous afferent activity. *The Journal of neuroscience : the official journal of the Society for Neuroscience*, **35**, 146-160.
- Luo, L. & Flanagan, J.G. (2007) Development of continuous and discrete neural maps. *Neuron*, **56**, 284-300.
- Luo, M., Fee, M.S. & Katz, L.C. (2003) Encoding pheromonal signals in the accessory olfactory bulb of behaving mice. *Science*, **299**, 1196-1201.
- Maher, B.J. & Westbrook, G.L. (2008) Co-transmission of dopamine and GABA in periglomerular cells. *Journal of neurophysiology*, **99**, 1559-1564.
- Mainland, J.D., Li, Y.R., Zhou, T., Liu, W.L. & Matsunami, H. (2015) Human olfactory receptor responses to odorants. *Scientific data*, **2**, 150002.

- Malnic, B., Hirono, J., Sato, T. & Buck, L.B. (1999) Combinatorial receptor codes for odors. *Cell*, **96**, 713-723.
- Maritan, M., Monaco, G., Zamparo, I., Zaccolo, M., Pozzan, T. & Lodovichi, C. (2009) Odorant receptors at the growth cone are coupled to localized cAMP and Ca²⁺ increases. *Proceedings of the National Academy of Sciences of the United States of America*, **106**, 3537-3542.
- Masera, A. (1947) [Not Available]. *Bollettino della Societa italiana di biologia sperimentale*, **23**, 209.
- Matthews, R.P., Guthrie, C.R., Wailes, L.M., Zhao, X., Means, A.R. & McKnight, G.S. (1994) Calcium/calmodulin-dependent protein kinase types II and IV differentially regulate CREB-dependent gene expression. *Molecular and cellular biology*, **14**, 6107-6116.
- Menini, A. (1999) Calcium signalling and regulation in olfactory neurons. *Current opinion in neurobiology*, **9**, 419-426.
- Milardi, D., Colussi, C., Grande, G., Vincenzoni, F., Pierconti, F., Mancini, F., Baroni, S., Castagnola, M., Marana, R. & Pontecorvi, A. (2017) Olfactory Receptors in Semen and in the Male Tract: From Proteome to Proteins. *Frontiers in endocrinology*, **8**, 379.
- Mitake, S., Ojika, K., Katada, E., Otsuka, Y., Matsukawa, N. & Fujimori, O. (1996) Distribution of hippocampal cholinergic neurostimulating peptide (HCNP) immunoreactivity in the central nervous system of the rat. *Brain research*, **706**, 57-70.
- Miyamichi, K., Serizawa, S., Kimura, H.M. & Sakano, H. (2005) Continuous and overlapping expression domains of odorant receptor genes in the olfactory epithelium determine the dorsal/ventral positioning of glomeruli in the olfactory bulb. *The Journal of neuroscience : the official journal of the Society for Neuroscience*, **25**, 3586-3592.
- Mombaerts, P. (1996) Targeting olfaction. *Current opinion in neurobiology*, **6**, 481-486.
- Mombaerts, P. (1999a) Molecular biology of odorant receptors in vertebrates. *Annual review of neuroscience*, **22**, 487-509.
- Mombaerts, P. (1999b) Seven-transmembrane proteins as odorant and chemosensory receptors. *Science*, **286**, 707-711.

-
- Mombaerts, P. (2001) How smell develops. *Nature neuroscience*, **4 Suppl**, 1192-1198.
- Mombaerts, P., Wang, F., Dulac, C., Chao, S.K., Nemes, A., Mendelsohn, M., Edmondson, J. & Axel, R. (1996) Visualizing an olfactory sensory map. *Cell*, **87**, 675-686.
- Mori, K., Kishi, K. & Ojima, H. (1983) Distribution of dendrites of mitral, displaced mitral, tufted, and granule cells in the rabbit olfactory bulb. *The Journal of comparative neurology*, **219**, 339-355.
- Mori, K., Nagao, H. & Yoshihara, Y. (1999) The olfactory bulb: coding and processing of odor molecule information. *Science*, **286**, 711-715.
- Mori, K. & Sakano, H. (2011) How is the olfactory map formed and interpreted in the mammalian brain? *Annual review of neuroscience*, **34**, 467-499.
- Munger, S.D., Leinders-Zufall, T. & Zufall, F. (2009) Subsystem organization of the mammalian sense of smell. *Annual review of physiology*, **71**, 115-140.
- Nagayama, S., Homma, R. & Imamura, F. (2014) Neuronal organization of olfactory bulb circuits. *Frontiers in neural circuits*, **8**, 98.
- Nakashima, A., Takeuchi, H., Imai, T., Saito, H., Kiyonari, H., Abe, T., Chen, M., Weinstein, L.S., Yu, C.R., Storm, D.R., Nishizumi, H. & Sakano, H. (2013) Agonist-independent GPCR activity regulates anterior-posterior targeting of olfactory sensory neurons. *Cell*, **154**, 1314-1325.
- Nguyen-Ba-Charvet, K.T., Di Meglio, T., Fouquet, C. & Chedotal, A. (2008) Robos and slits control the pathfinding and targeting of mouse olfactory sensory axons. *The Journal of neuroscience : the official journal of the Society for Neuroscience*, **28**, 4244-4249.
- Niimura, Y. & Nei, M. (2007) Extensive gains and losses of olfactory receptor genes in mammalian evolution. *PloS one*, **2**, e708.
- Nishiyama, M., Hoshino, A., Tsai, L., Henley, J.R., Goshima, Y., Tessier-Lavigne, M., Poo, M.M. & Hong, K. (2003) Cyclic AMP/GMP-dependent modulation of Ca²⁺ channels sets the polarity of nerve growth-cone turning. *Nature*, **423**, 990-995.

- Nissant, A., Bardy, C., Katagiri, H., Murray, K. & Lledo, P.M. (2009) Adult neurogenesis promotes synaptic plasticity in the olfactory bulb. *Nature neuroscience*, **12**, 728-730.
- Oh, S.J. (2018) System-Wide Expression and Function of Olfactory Receptors in Mammals. *Genomics & informatics*, **16**, 2-9.
- Ojika, K., Mitake, S., Tohdoh, N., Appel, S.H., Otsuka, Y., Katada, E. & Matsukawa, N. (2000) Hippocampal cholinergic neurostimulating peptides (HCNP). *Progress in neurobiology*, **60**, 37-83.
- Ojika, K., Tsugu, Y., Mitake, S., Otsuka, Y. & Katada, E. (1998) NMDA receptor activation enhances the release of a cholinergic differentiation peptide (HCNP) from hippocampal neurons in vitro. *Brain research. Developmental brain research*, **106**, 173-180.
- Omura, M., Grosmaître, X., Ma, M. & Mombaerts, P. (2014) The beta2-adrenergic receptor as a surrogate odorant receptor in mouse olfactory sensory neurons. *Molecular and cellular neurosciences*, **58**, 1-10.
- Parrish-Aungst, S., Shipley, M.T., Erdelyi, F., Szabo, G. & Puche, A.C. (2007) Quantitative analysis of neuronal diversity in the mouse olfactory bulb. *The Journal of comparative neurology*, **501**, 825-836.
- Pedemonte, N. & Galietta, L.J. (2014) Structure and function of TMEM16 proteins (anoctamins). *Physiological reviews*, **94**, 419-459.
- Pelosi, P. (1998) Odorant-binding proteins: structural aspects. *Annals of the New York Academy of Sciences*, **855**, 281-293.
- Peng, Z.L., Yang, J.Y. & Chen, X. (2010) An improved classification of G-protein-coupled receptors using sequence-derived features. *BMC bioinformatics*, **11**, 420.
- Pietra, G., Dibattista, M., Menini, A., Reisert, J. & Boccaccio, A. (2016) The Ca²⁺-activated Cl⁻ channel TMEM16B regulates action potential firing and axonal targeting in olfactory sensory neurons. *The Journal of general physiology*, **148**, 293-311.
- Pietrobon, M., Zamparo, I., Maritan, M., Franchi, S.A., Pozzan, T. & Lodovichi, C. (2011) Interplay among cGMP, cAMP, and Ca²⁺ in living olfactory sensory neurons in vitro and in vivo. *The Journal of neuroscience : the official journal of the Society for Neuroscience*, **31**, 8395-8405.

-
- Pifferi, S., Boccaccio, A. & Menini, A. (2006) Cyclic nucleotide-gated ion channels in sensory transduction. *FEBS letters*, **580**, 2853-2859.
- Pifferi, S., Cenedese, V. & Menini, A. (2012) Anoctamin 2/TMEM16B: a calcium-activated chloride channel in olfactory transduction. *Experimental physiology*, **97**, 193-199.
- Pifferi, S., Dibattista, M., Sagheddu, C., Boccaccio, A., Al Qteishat, A., Ghirardi, F., Tirindelli, R. & Menini, A. (2009) Calcium-activated chloride currents in olfactory sensory neurons from mice lacking bestrophin-2. *The Journal of physiology*, **587**, 4265-4279.
- Pifferi, S., Menini, A. & Kurahashi, T. (2010) Signal Transduction in Vertebrate Olfactory Cilia. In Menini, A. (ed) *The Neurobiology of Olfaction*, Boca Raton (FL).
- Ponsioen, B., Zhao, J., Riedl, J., Zwartkuis, F., van der Krogt, G., Zacco, M., Moolenaar, W.H., Bos, J.L. & Jalink, K. (2004) Detecting cAMP-induced Epac activation by fluorescence resonance energy transfer: Epac as a novel cAMP indicator. *EMBO reports*, **5**, 1176-1180.
- Price, J.L. & Powell, T.P. (1970) The synaptology of the granule cells of the olfactory bulb. *Journal of cell science*, **7**, 125-155.
- Ressler, K.J., Sullivan, S.L. & Buck, L.B. (1993) A zonal organization of odorant receptor gene expression in the olfactory epithelium. *Cell*, **73**, 597-609.
- Ressler, K.J., Sullivan, S.L. & Buck, L.B. (1994) Information coding in the olfactory system: evidence for a stereotyped and highly organized epitope map in the olfactory bulb. *Cell*, **79**, 1245-1255.
- Rodolfo-Masera, A. (1943) Sur l'esistenza di un particolare organo olfattivo nel setto nasale della cavia e di altri roditori. *Arch Ital Anat Embryol* **48**, 157-212, 1943.
- Royal, S.J. & Key, B. (1999) Development of P2 olfactory glomeruli in P2-internal ribosome entry site-tau-LacZ transgenic mice. *The Journal of neuroscience : the official journal of the Society for Neuroscience*, **19**, 9856-9864.
- Rubin, B.D. & Katz, L.C. (1999) Optical imaging of odorant representations in the mammalian olfactory bulb. *Neuron*, **23**, 499-511.

- Rydel, R.E. & Greene, L.A. (1988) cAMP analogs promote survival and neurite outgrowth in cultures of rat sympathetic and sensory neurons independently of nerve growth factor. *Proceedings of the National Academy of Sciences of the United States of America*, **85**, 1257-1261.
- Saito, H., Kubota, M., Roberts, R.W., Chi, Q. & Matsunami, H. (2004) RTP family members induce functional expression of mammalian odorant receptors. *Cell*, **119**, 679-691.
- Sakano, H. (2010) Neural map formation in the mouse olfactory system. *Neuron*, **67**, 530-542.
- Salom, D., Padayatti, P.S. & Palczewski, K. (2013) Crystallization of G protein-coupled receptors. *Methods in cell biology*, **117**, 451-468.
- Saraiva, L.R., Kondoh, K., Ye, X., Yoon, K.H., Hernandez, M. & Buck, L.B. (2016) Combinatorial effects of odorants on mouse behavior. *Proceedings of the National Academy of Sciences of the United States of America*, **113**, E3300-3306.
- Schepherd, GM (2004) The synaptic organization of the brain. Oxford University press.
- Schoenfeld, T.A., Marchand, J.E. & Macrides, F. (1985) Topographic organization of tufted cell axonal projections in the hamster main olfactory bulb: an intrabulbar associational system. *The Journal of comparative neurology*, **235**, 503-518.
- Schoppa, N.E. (2006) A novel local circuit in the olfactory bulb involving an old short-axon cell. *Neuron*, **49**, 783-784.
- Scolnick, J.A., Cui, K., Duggan, C.D., Xuan, S., Yuan, X.B., Efstratiadis, A. & Ngai, J. (2008) Role of IGF signaling in olfactory sensory map formation and axon guidance. *Neuron*, **57**, 847-857.
- Serizawa, S., Miyamichi, K. & Sakano, H. (2004) One neuron-one receptor rule in the mouse olfactory system. *Trends in genetics : TIG*, **20**, 648-653.
- Serizawa, S., Miyamichi, K., Takeuchi, H., Yamagishi, Y., Suzuki, M. & Sakano, H. (2006) A neuronal identity code for the odorant receptor-specific and activity-dependent axon sorting. *Cell*, **127**, 1057-1069.
- Shemon, A.N., Eves, E.M., Clark, M.C., Heil, G., Granovsky, A., Zeng, L., Imamoto, A., Koide, S. & Rosner, M.R. (2009) Raf Kinase Inhibitory Protein protects cells against locostatin-mediated inhibition of migration. *PLoS one*, **4**, e6028.

-
- Shigeoka, T., Lu, B. & Holt, C.E. (2013) Cell biology in neuroscience: RNA-based mechanisms underlying axon guidance. *The Journal of cell biology*, **202**, 991-999.
- Shipley, M.T. & Ennis, M. (1996) Functional organization of olfactory system. *Journal of neurobiology*, **30**, 123-176.
- Simister, P.C., Banfield, M.J. & Brady, R.L. (2002) The crystal structure of PEBP-2, a homologue of the PEBP/RKIP family. *Acta crystallographica. Section D, Biological crystallography*, **58**, 1077-1080.
- Skinner, J.J. & Rosner, M.R. (2014) RKIP structure drives its function: a three-state model for regulation of RKIP. *Critical reviews in oncogenesis*, **19**, 483-488.
- Smail, S., Bahga, D., McDole, B. & Guthrie, K. (2016) Increased Olfactory Bulb BDNF Expression Does Not Rescue Deficits in Olfactory Neurogenesis in the Huntington's Disease R6/2 Mouse. *Chemical senses*, **41**, 221-232.
- Song, H.J., Ming, G.L. & Poo, M.M. (1997) cAMP-induced switching in turning direction of nerve growth cones. *Nature*, **388**, 275-279.
- Spehr, M., Gisselmann, G., Poplawski, A., Riffell, J.A., Wetzel, C.H., Zimmer, R.K. & Hatt, H. (2003) Identification of a testicular odorant receptor mediating human sperm chemotaxis. *Science*, **299**, 2054-2058.
- Spehr, M. & Munger, S.D. (2009) Olfactory receptors: G protein-coupled receptors and beyond. *Journal of neurochemistry*, **109**, 1570-1583.
- Spehr, M., Schwane, K., Riffell, J.A., Zimmer, R.K. & Hatt, H. (2006) Odorant receptors and olfactory-like signaling mechanisms in mammalian sperm. *Molecular and cellular endocrinology*, **250**, 128-136.
- Strotmann, J., Levai, O., Fleischer, J., Schwarzenbacher, K. & Breer, H. (2004) Olfactory receptor proteins in axonal processes of chemosensory neurons. *The Journal of neuroscience : the official journal of the Society for Neuroscience*, **24**, 7754-7761.
- Takeuchi, H., Inokuchi, K., Aoki, M., Suto, F., Tsuboi, A., Matsuda, I., Suzuki, M., Aiba, A., Serizawa, S., Yoshihara, Y., Fujisawa, H. & Sakano, H. (2010) Sequential arrival and graded secretion of Sema3F by olfactory neuron axons specify map topography at the bulb. *Cell*, **141**, 1056-1067.

- Theroux, S., Pereira, M., Casten, K.S., Burwell, R.D., Yeung, K.C., Sedivy, J.M. & Klysik, J. (2007) Raf kinase inhibitory protein knockout mice: expression in the brain and olfaction deficit. *Brain research bulletin*, **71**, 559-567.
- Tirindelli, R., Dibattista, M., Pifferi, S. & Menini, A. (2009) From pheromones to behavior. *Physiological reviews*, **89**, 921-956.
- Tohdoh, N., Tojo, S., Kimura, M., Ishii, T. & Ojika, K. (1997) Mechanism of expression of the rat HCNP precursor protein gene. *Brain research. Molecular brain research*, **45**, 24-32.
- Trinh, K. & Storm, D.R. (2003) Vomeronasal organ detects odorants in absence of signaling through main olfactory epithelium. *Nature neuroscience*, **6**, 519-525.
- Tsuboi, A., Miyazaki, T., Imai, T. & Sakano, H. (2006) Olfactory sensory neurons expressing class I odorant receptors converge their axons on an antero-dorsal domain of the olfactory bulb in the mouse. *The European journal of neuroscience*, **23**, 1436-1444.
- Uchida, N., Takahashi, Y.K., Tanifuji, M. & Mori, K. (2000) Odor maps in the mammalian olfactory bulb: domain organization and odorant structural features. *Nature neuroscience*, **3**, 1035-1043.
- Uematsu, N., Matsukawa, N., Kanamori, T., Arai, Y., Sagisaka, T., Toyoda, T., Yoshida, M. & Ojika, K. (2009) Overexpression of hippocampal cholinergic neurostimulating peptide in heterozygous transgenic mice increases the amount of ChAT in the medial septal nucleus. *Brain research*, **1305**, 150-157.
- Valle-Leija, P. (2015) Odorant receptors signaling instructs the development and plasticity of the glomerular map. *Neural plasticity*, **2015**, 975367.
- Vanderhaeghen, P., Schurmans, S., Vassart, G. & Parmentier, M. (1993) Olfactory receptors are displayed on dog mature sperm cells. *The Journal of cell biology*, **123**, 1441-1452.
- Vassar, R., Chao, S.K., Sitcheran, R., Nunez, J.M., Vosshall, L.B. & Axel, R. (1994) Topographic organization of sensory projections to the olfactory bulb. *Cell*, **79**, 981-991.
- Vassar, R., Ngai, J. & Axel, R. (1993) Spatial segregation of odorant receptor expression in the mammalian olfactory epithelium. *Cell*, **74**, 309-318.

-
- Wachowiak, M. & Cohen, L.B. (2001) Representation of odorants by receptor neuron input to the mouse olfactory bulb. *Neuron*, **32**, 723-735.
- Wang, F., Nemes, A., Mendelsohn, M. & Axel, R. (1998) Odorant receptors govern the formation of a precise topographic map. *Cell*, **93**, 47-60.
- Weis, W.I. & Kobilka, B.K. (2018) The Molecular Basis of G Protein-Coupled Receptor Activation. *Annual review of biochemistry*, **87**, 897-919.
- Woo, S. & Gomez, T.M. (2006) Rac1 and RhoA promote neurite outgrowth through formation and stabilization of growth cone point contacts. *The Journal of neuroscience : the official journal of the Society for Neuroscience*, **26**, 1418-1428.
- Yokoi, M., Mori, K. & Nakanishi, S. (1995) Refinement of odor molecule tuning by dendrodendritic synaptic inhibition in the olfactory bulb. *Proceedings of the National Academy of Sciences of the United States of America*, **92**, 3371-3375.
- Zaccolo, M., De Giorgi, F., Cho, C.Y., Feng, L., Knapp, T., Negulescu, P.A., Taylor, S.S., Tsien, R.Y. & Pozzan, T. (2000) A genetically encoded, fluorescent indicator for cyclic AMP in living cells. *Nature cell biology*, **2**, 25-29.
- Zak, J.D., Grimaud, J., Li, R.C., Lin, C.C. & Murthy, V.N. (2018) Calcium-activated chloride channels clamp odor-evoked spike activity in olfactory receptor neurons. *Scientific reports*, **8**, 10600.
- Zapiec, B. & Mombaerts, P. (2015) Multiplex assessment of the positions of odorant receptor-specific glomeruli in the mouse olfactory bulb by serial two-photon tomography. *Proceedings of the National Academy of Sciences of the United States of America*, **112**, E5873-5882.
- Zhang, L.I. & Poo, M.M. (2001) Electrical activity and development of neural circuits. *Nature neuroscience*, **4 Suppl**, 1207-1214.
- Zhang, X. & Firestein, S. (2002) The olfactory receptor gene superfamily of the mouse. *Nature neuroscience*, **5**, 124-133.
- Zhang, X., Rodriguez, I., Mombaerts, P. & Firestein, S. (2004) Odorant and vomeronasal receptor genes in two mouse genome assemblies. *Genomics*, **83**, 802-811.

- Zhang, X., Zhang, X. & Firestein, S. (2007) Comparative genomics of odorant and pheromone receptor genes in rodents. *Genomics*, **89**, 441-450.
- Zheng, C., Feinstein, P., Bozza, T., Rodriguez, I. & Mombaerts, P. (2000) Peripheral olfactory projections are differentially affected in mice deficient in a cyclic nucleotide-gated channel subunit. *Neuron*, **26**, 81-91.
- Zheng, J.Q. & Poo, M.M. (2007) Calcium signaling in neuronal motility. *Annual review of cell and developmental biology*, **23**, 375-404.
- Zhuang, H. & Matsunami, H. (2007) Synergism of accessory factors in functional expression of mammalian odorant receptors. *The Journal of biological chemistry*, **282**, 15284-15293.
- Zhuang, H. & Matsunami, H. (2008) Evaluating cell-surface expression and measuring activation of mammalian odorant receptors in heterologous cells. *Nature protocols*, **3**, 1402-1413.
- Zou, D.J., Feinstein, P., Rivers, A.L., Mathews, G.A., Kim, A., Greer, C.A., Mombaerts, P. & Firestein, S. (2004) Postnatal refinement of peripheral olfactory projections. *Science*, **304**, 1976-1979.
- Zozulya, S., Echeverri, F. & Nguyen, T. (2001) The human olfactory receptor repertoire. *Genome biology*, **2**, RESEARCH0018.
- Zufall, F. & Leinders-Zufall, T. (2007) Mammalian pheromone sensing. *Current opinion in neurobiology*, **17**, 483-489.
- Zufall, F. & Munger, S.D. (2010) Receptor guanylyl cyclases in mammalian olfactory function. *Molecular and cellular biochemistry*, **334**, 191-197.

8 ACKNOWLEDGEMENTS

I would like to Thank my supervisor Dr. Claudia Lodovichi for giving me the possibility to take up my PhD in her laboratory where I can learn new techniques and improve my skills, achieving a professional growth. She gave me a scientific support.

I would like to thank Dr. Ilaria Zamparo, that performed the experiments of the first part of this project. She teach me new techniques and support me to never give up.

Thanks to all my colleagues that in all these years have joined our group.

A special thank to my family, to have always believed in me and support myself during difficulties and to my special friends that share my daily life .

Without all of them I have never reached this important goal.

